Analytical and numerical models of chemical leaching with gypsum precipitation in porous media

Alibek Kuljabekov

Université de Lorraine
Ecole Doctorale 409 : Energies, Mécanique et Matériaux, Nancy-Metz.
Spécialité: Mécanique et Energétique

and

Al-Farabi Kazakh National University,
Faculty of Mechanics and Mathematics
Specialty: Mechanics

Ph. D. Thesis

ANALYTICAL AND NUMERICAL MODELS OF CHEMICAL LEACHING WITH GYPSUM PRECIPITATION IN POROUS MEDIA

Presented by Alibek B. KULJABEKOV

Laboratoire d'Energétique et de Mécanique Théorique et Appliquée, UMR 7563
and
Department of Mechanics, Al-Farabi KazNU

Defended on December 18, 2014

In presence of jury consisting of:

Christophe JOSSERAND, DR, Université Paris-Sorbonne	Examinator
Valeri MOURZENKO, DR, Institut Pprime CNRS	Reviewer
Askar MUNARA, Ph.D., Université Nazarbayev	Reviewer
Michel PANFILOV, Prof., Univerité de Lorraine	Director
Aidarkhan KALTAYEV, Prof., KazNU Al Farabi	Director
Jean-Jacques Royer, Prof., Univerité de Lorraine	Examinator
Antonio PEREIRA, Ph.D., Université de Lorraine	Examinator

To the memory of my father...

ACKNOWLEDGMENTS

I would like to thank and express my sincere gratitude to my advisors, Professor Michel Panfilov and Professor Aidarkhan Kaltayev, whose support, guidance and patience were critical in preparation of this thesis. I value the discussions I had with Dr. Antonio Pereira, Professor Jean-Jacques Royer, Dr. Madina Tungatarova, Professor Altynshash Naimanova and would like to express my gratitude for their collaboration on technical issues of this thesis.

My deepest gratitude to Professor Nargozy Danaev and whole academic staff of the Faculty of Mechanics and Mathematics.

My special thanks to my colleagues and friends from the Faculty of Mechanics and Mathematics of Al-Farabi Kazakh National University and from LEMTA of University of Lorraine.

I would also like to thank the French Embassy in Almaty and Astana and, especially, Noemie Larrouilh, Bernard Paqueteau and Guillaume Giraudet.

Last, but not least, I would like to thank my wife Almira and members of my big family for their understanding and patience through the course of my studies.

This research is sponsored by fellowships of the French Embassy in Kazakhstan, the Scientific Committee of the Ministry of Education and Science of the Republic Kazakhstan, and by proper funds of laboratory LEMTA and Institute of Mathematics and Mechanics.

ABSTRACT

In the present thesis we develop the optimized phenomenological model of in-situ chemical leaching (ISL) of uranium by means of injection of sulfuric acid, with special account for the precipitation of non-soluble species like gypsum, which reduces the uranium recovery. The suggested model describes the mass transport with heterogeneous chemical reactions between liquid and solid rocks, resulting in dissolving uranium oxides and uranium recovery in liquid form. This model is optimized, i.e., it contains the minimum number of chemical reactions, at the same time ensuring the sufficient degree of consistency with the real systems. It includes both useful reactions, describing the dissolution of various kinds of uranium oxides, and detrimental reactions, leading to the precipitation of solid sediments (gypsum), flakes of which cover the surface of porous channels and reduce the efficiency of useful reactions.

We developed the efficient asymptotic method of analysis based on the approximation of the true multicomponent system by a pseudo-binary mixture, which enables us to separate nonlinear and compositional effects: all nonlinear effects are captured in the zero approximation which corresponds to a two-component mixture, whilst all the multi-compositional effects, including the reactions, are kept in the first approximation which is linear. We showed that the real systems perfectly correspond to the pseudo-binary approximation. In 1D case we obtained the analytical solution of the strongly nonlinear problem for the fluid-solid chemically interacting system consisting of 11 chemical components described by 11 nonlinear partial differential equations.

For 3D flow, we developed the numerical code, based on the streamline approach, which enables us to transform any three-dimensional problem into the system of mono-dimensional problems of chemical transport. At the first step we calculate the system of streamlines by solving the simplified 3D problem of flow of a homogeneous fluid. At the second step we solve the 1D problem of species transport along each streamline. The correctness of the simulations was validated by performing several numerical tests and comparing the results obtained with other numerical methods.

Among the qualitative results we revealed the existence of a critical rate of gypsum sedimentation, below which the ultimate uranium recovery is complete. In contrast, it tends to a limit value lower than 100% when sedimentation rate is higher than the critical value. This limit

recovery depends on various parameters of the process.

The theory and methodology developed in this work can be easily extended and applied to other types of ores that are recovered by in-situ leaching method and other types of solvents.

RESUME

Dans cette thèse, nous développons le modèle phénoménologique optimisé de lessivage chimique in situ (ISL) de l'uranium par l'injection d'acide sulfurique, en prenant en compte la précipitation des espèces non-solubles telles que le gypse, qui réduisent la récupération de l'uranium. Le modèle proposé décrit le transport de masse avec des réactions chimiques hétérogènes entre le liquide et les roches solides, qui mènent à la dissolution des oxydes d'uranium et à la récupération de l'uranium sous forme liquide. Ce modèle est optimisé, c'est-à-dire, il contient le nombre minimal de réactions chimiques, en assurant en même temps le degré suffisant d'adéquation avec les systèmes réels. Ce modèle comprend à la fois des réactions utiles, qui décrivent la dissolution de divers types d'oxydes d'uranium, et les réactions néfastesqui conduisent à la précipitation des sédiments solides (gypse), dont les flocons couvrent la surface de canaux poreux et réduisent l'efficacité des réactions utiles.

Nous avons développé la méthode asymptotique efficace d'analyse basée sur l'approximation du système réel multi-composant par un mélange pseudo-binaire, ce qui nous permet de séparer les effets non linéaires et les effets compositionnels : tous les effets non linéaires sont capturés dans l'approximation d'ordre zéro, ce qui correspond à un mélange à deux composants, tandis que tous les effets multi-compositionnels, y compris les réactions chimiques, sont maintenus dans l'approximation d'ordre 1 qui est linéaire. Nous avons montré que les systèmes réels correspondent parfaitement à l'approximation pseudo-binaire. Dans le cas 1D, nous avons obtenu la solution analytique du problème fortement non linéaire pour un système fluide-solide chimiquement actif et composé de 11 espèces chimiques décrites par 11 équations aux dérivées partielles non linéaires.

Pour un écoulement 3D, nous avons développé un code numérique, basée sur l'approche de ligne de courant, ce qui nous permet de transformer tout problème en trois dimensions en un système de problèmes mono-dimensionnels de transport d'espèces chimiques. Lors de la première étape, on calcule le système de lignes de courant en résolvant le problème simplifié 3D de l'écoulement d'un fluide homogène. Lors de la deuxième étape, nous résolvons le problème 1D du transport d'espèces le long de chaque ligne de courant. Les résultats de simulation ont été validés en effectuant plusieurs essais numériques et en les comparant avec ceux obtenus par d'autres méthodes numériques.

Parmi les résultats qualitatifs, nous avons révélé l'existence d'un taux critique de

sédimentation de gypse, en dessous duquel la récupération ultime de l'uranium est complète. En revanche, elle tend à une valeur limite inférieure à 100% lorsque le taux de sédimentation est supérieur à la valeur critique. Ce taux de récupération limite dépend de divers paramètres du processus.

La théorie et la méthodologie développées dans ce travail peuvent être facilement étendues et appliquéesaux autres types de minerais qui sont récupérés par la méthode de lessivage in situ, et autres types de solvant.

CONTENTS

LIST OF FIGURES

LIST OF TABLES

INTRODUCTION

HISTORY

In-situ leaching (ISL) method is a widely used technique in the mining industry for production of metal from the orebody in porous or fractured mineralized zones. It is used in copper mines (porphyry copper deposits), strata form uranium deposits, evaporite type deposits (K, Na, Li) ... This work focuses on the analytical and numerical investigation of dissolution and precipitation process during in-situ leaching of uranium. After presentation of the principle of in-situ leaching, the case of roll-front uranium deposits will be detailed.

In the early 1960s (IAEA, tecdoc, 2001 [10, 42], Brovin and Grabovnikov, 1997;), the former USSR and USA independently developed in-situ leaching (ISL) technology to exploit low grade uranium mines that were not suitable for conventional mining. The method was applied for extracting uranium from roll–front sandstone type deposits located in water saturated permeable rocks. Both countries developed similar engineering and technological approaches. However, the Soviets adopted the acid leach system, while the US specialists used an alkaline one, primarily carbonate based system, in particular because of different geological characteristics of the host formations. Later on in the 1980's, the acid ISL technology was also applied in Bulgaria, Czechoslovakia, German Democratic Republic and China. In 1998 and 1999, new acid leach projects were being developed in Australia.

The interest in ISL has grown significantly during the last 25 years due to its apparent advantages in terms of costs and low environmental impact. The main activity took place in sedimentary deposits located in America, Eastern Europe, and Central Asia. The in-situ leaching was tested for the first time within the Shirley Basin (Wyoming) in United States in 1963 - 1965 by UTAH International under the initiative of Ian Ritchie. In the Eastern Europe, ISL was applied by the USSR in the form of acid leaching. Today this technique is widely used in Central Asia and Australia.

PRINCIPLE OF IN-SITU LEACHING: ADVANTAGES AND DRAWBACKS

Uranium is the main mineral resource for nuclear industry. It is traditionally extracted through application of mining technology such as open pits for out-cropping ore deposits, or by underground works for deeper rich ore deposits. In all these cases the dissolution of the ore leads to formation of significant cavities in the rocks, which consequently may cause significant holes at the surface due to subsidence. *In-situ leaching* (ISL) or *in-situ recovery*(ISR) technology is applied for low grade mineral deposits, for which classical mining techniques are too expensive, or when the mineralized strata are deep (about 600 meters of deep), located in porous rocks of an aquifer.

In-situ leaching belongs to the family of solution mining techniques, applied to extract various solid substances such as salt, sulfur, potassium, etc. The in-situ leaching method consists of circulating an acid leaching solution throughout the ore deposit between injecting and pumping wells drilled from the surface (also referred as injectors and producers). The process is based on a selective transfer of natural uranium ions into the solution by changing its oxidized state (U^{IV} into U^{VI}), the resulting pregnant solution being pumped back to the surface; the uranium is then extracted in a surface processing plant by circulating the solution through selective ionic exchanger, the "clean" solution will be re-injected (Figure 1). In the ISL method the environmental impact is significantly reduced, as it is applied to the deposits with low content of uranium (the similar technique can also be applied to extract copper). In this case, the dissolution of mineral is selective and does not produce significant modifications in the hosting rocks. It produces very few mining wastes, compared to classical underground or open pit mining techniques.

Six steps can be distinguished in the ISL method which consists of: (i) drilling two system of wells: *injectors* and *producers*; (ii) injecting an acid (or alkaline) aqueous solution into the deposit through the injectors with the objective to dissolve solid minerals of uranium; (iii) pumping back the uranium-enriched solution to the surface through producing wells; (iv) extracting uranium from liquid by a selective ion-exchange resin in the processing plant (Figure 1); (v) regenerating the leaching potential of the solution; (iv) recycling[1] (reinjection, ...).

[1]The solution can be recycled many times (up to 50 times).

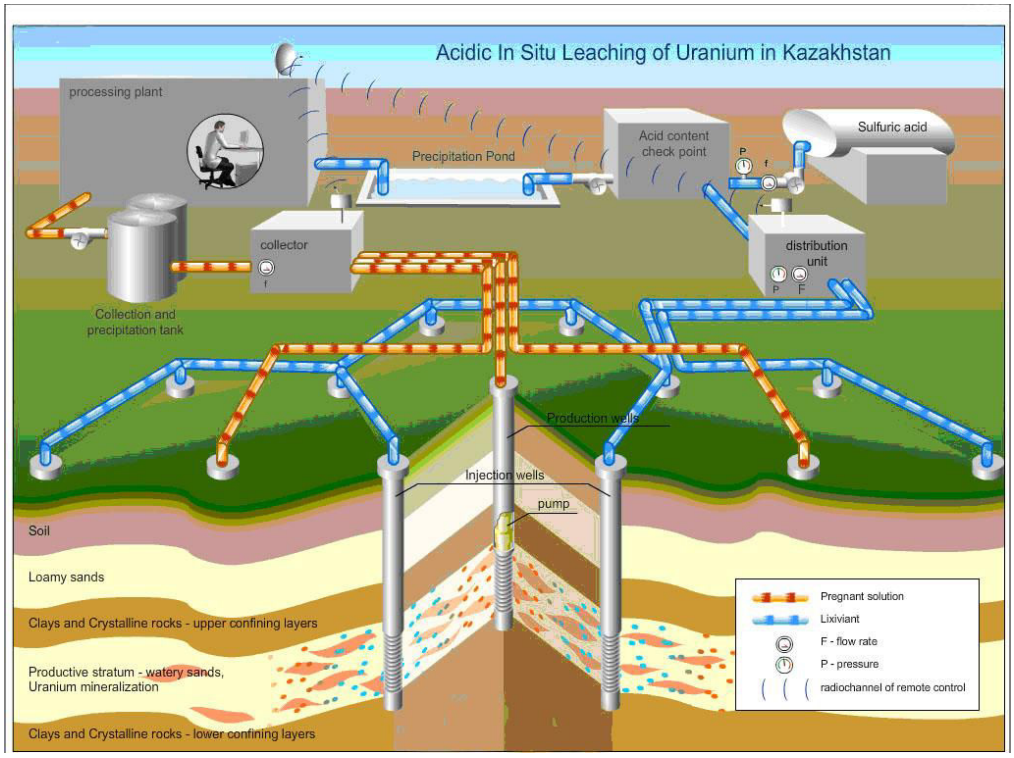

Figure 1 - Schematic representation of the ISL process (after Kazatomprom, 2013 [64])

The injected solution to dissolve uranium can be either:

- acid, essentially sulfuric acid (H_2SO_4);
- or alkaline, usually a sodium carbonate (Na_2CO_3) or bicarbonate solution ($NaHCO_3$).

Alkaline leaching is only used in cases of high carbonate uranium ores for which the acid leaching is not possible, or in order to avoid contamination of aquifers by acid. It had been used in the USA and Uzbekistan. Alkaline leaching is not as effective as acid leaching for uranium recovery. Acid leaching is the most powerful technique for oxidizing uranium constituents, but may have significant environmental impacts at the end of exploitation.

Table 1 - Parity of extraction methods for Uranium production (see World Nuclear Association, 2013 [29])

Method	U (in t)	%
Underground & open pit (except Olympic Dam)*	27,860	47%
In situ leach (ISL)	27,370	46%
By-product*	3,957	7%
Heap leach	186	0%

Table 2 - Advantages of ISL method with respect to conventional mining and domain of applications

Advantages	Disadvantages	Domains of application of acid leaching
• low modifications of underground sites ; • risk of radiological contamination is highly reduced ; • reduced complexity of equipment and maintenance ; • reduced number of personnel, while increased production; • very low production of waste, no issue associated with waste storage; • delay of start of production is minimised; • weak consumption of energy; • financial advantages.	• Recovery degree is sufficiently weak; • The domain of application is limited by several sedimentary ores in line with strict conditions on their permeability; • Risk of possible local contamination of the aquifer ; • Exploitation method is difficult to control due to its high inertia. • Process is sufficiently empirical due to which it is difficult to analyse it; • Several fundamental problems remain non-resolved: problems related to colmatation.	To apply ISL, the ore should satisfy certain physical conditions: • hosting geological formation should be porous and permeable to allow the establishment of a circulating flux of solutions through mineralized zones; • mineral must be soluble under certain oxidizing conditions of pH and Eh easily achievable; • movement of solutions should be controlled and limited to mineralized zones without interaction with upper aquifers; • permeability must be relatively homogeneous to avoid formation of preferential paths for injected liquid; • permeability must be sufficiently high in mineralized zones that will be leached; • mineralization of geological formation should be sufficient to make operation profitable.

Most of uranium deposits in the World are represented as aquifer in usually highly permeable rocks (sandstones), confined in geological strata, sometimes inter-bedded and covered by impermeable rocks (clays). The reservoir rocks contain uranium ores non-uniformly distributed in space that have typical shape of roll-fronts (in red Figure 2). Geological structures that bear uranium strata bound deposits are convenient to be produced using *in-situ* leaching (ISL) methods.

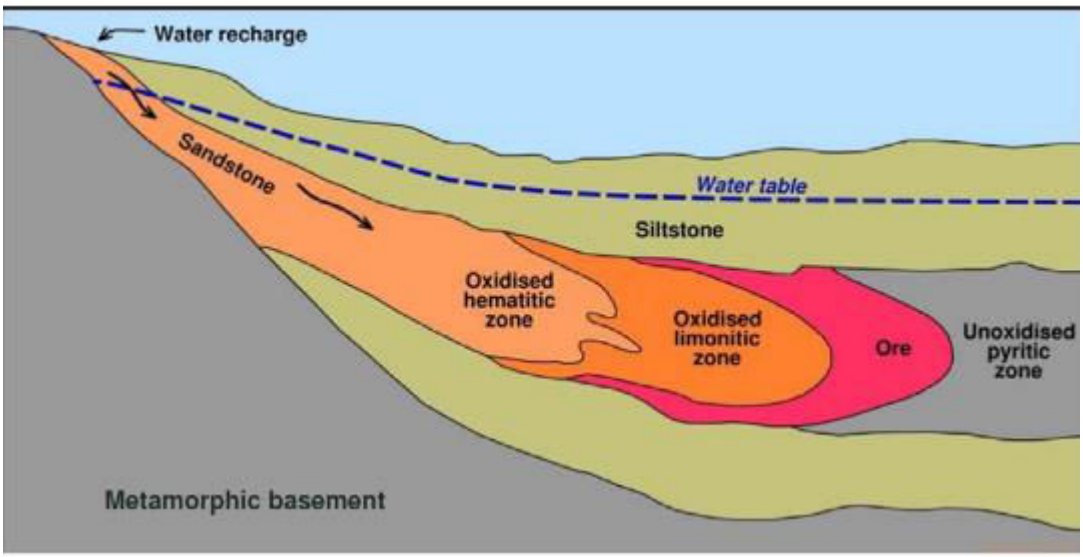

Figure 2 – Uranium deposits formation (after Deffeyes and McGregor, 1980 [20])

The "Roll-fronts" are epigenetic accumulations of uranium, frequently accompanied with sulphur and accessory concentrations or rare elements, such as, vanadium, selenium, molybdenum and the others. The denomination "Roll-front" originates from the shape of mineralization that is similar to a “roll”. The mineralization is located in permeable strata (aquifers), sand of sandstone, limited by clay rocks above and below. The uranium concentrations are localised at the front between the upstream zone, oxidized, and the downstream zone that is reduced. In the USA this kind of mineralization is called "Sandstone-type uranium deposit (IAEA, 1985 [30]), whilst in Kazakhstan one uses the term "Oxidation layer"(Petrov, 1998 [53]).

In the formation of Roll-fronts the uranium has been introduced into the hosting rock after diagenesis, and more exactly by means of oxidizing groundwater. Uranium is more mobile when it is oxidized with the valence +VI, in the form of uranyl ions UO_2^{2+}.

Thus, the uranium deposits in the Roll-fronts have been precipitated at the redox interface of an oxidizing solution, passing through a reduced sandstone containing pyrite and organic matter. The oxidizing solutions are seepage water of meteoric origin coming from the outcrops.

In summary, the formation of a Roll-front generally includes the following steps:

- deposition of sand in continental environment;
- reduction of these sands by diagenetic alteration of plant debris and formation of pyrite;
- dissolution of uranium by subsurface waters to the valence state +VI in the form of uranyl ions (UO_2^{2+});
- flow of oxidizing groundwater containing uranium inside holder sands, thus giving rise to a redox front moving slowly along the hydraulic downstream;

Uranium dissolved in oxidizing water precipitates in the roll-fronts in the valence state +IV, as solubility of U^{iv} is very low in reducing conditions.

IN-SITU LEACHING IN KAZAKHSTAN

Uranium produced through application of ISL methods accounts for about 50% of total amount of uranium produced in the World; the major part being produced in Kazakhstan (about 40% of total amount of uranium in 2013 (Figure 3) and all Kazakh uranium deposits are being mined through application of ISL method (Kazatomprom, 2013 [64]).

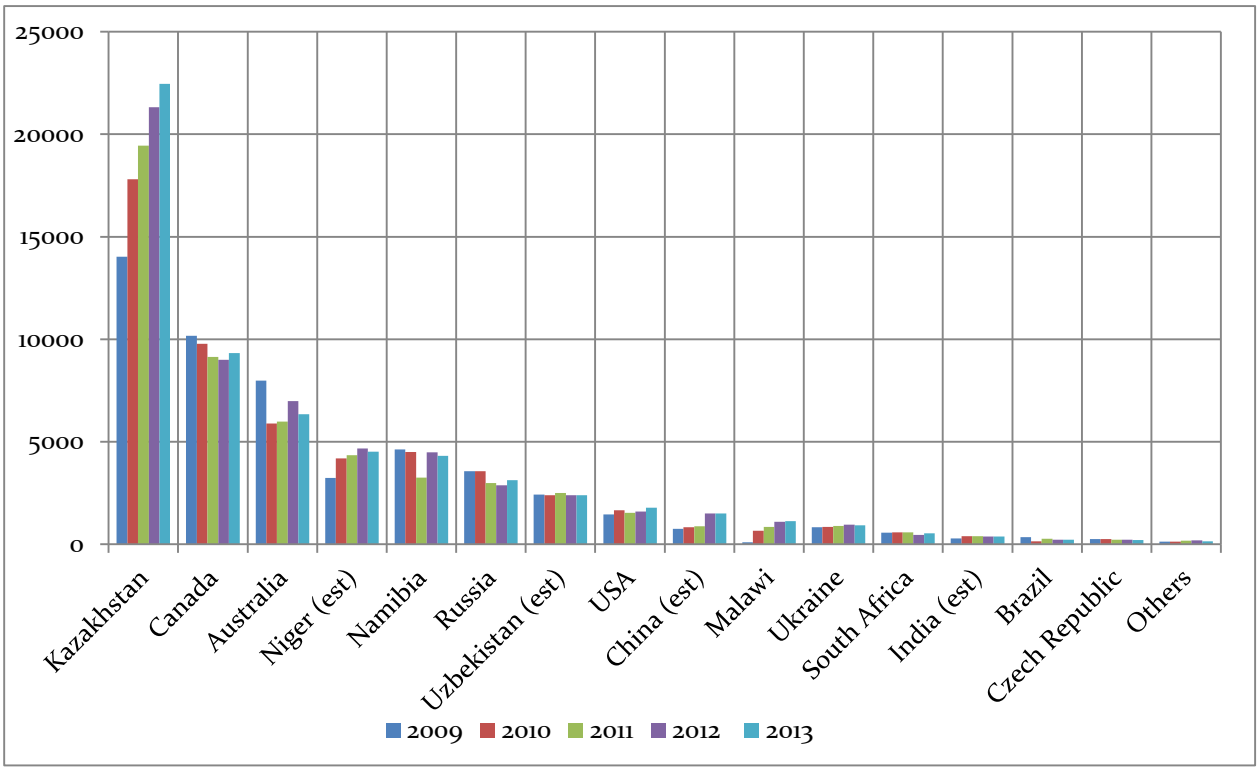

Figure 3 - Activity of uranium mining per country and year in the world (Data after World Nuclear Association, 2013 [29])

In addition to pure scientific reasons, the application of acid or alkaline leaching also frequently depends on economic reasons. For instance, acid leaching is applied practically in all deposits of Kazakhstan, independently of the content of carbonates, as the country possesses high reserves of sulphur, and national industry traditionally produces large amount of sulphuric acid. This is well justified for several areas, such as, Tortkuduk (South Kazakhstan Figure 4), where the content of carbonates is 0.1%, but in other areas this produces some negative effects, such as gypsum precipitation, which reduces leaching efficiency. A typical geological profile of a uranium deposit is shown in Figure 5.

Figure 4 - Potential areas for uranium ores in Kazakhstan (after Sagatov, 2010 [61])

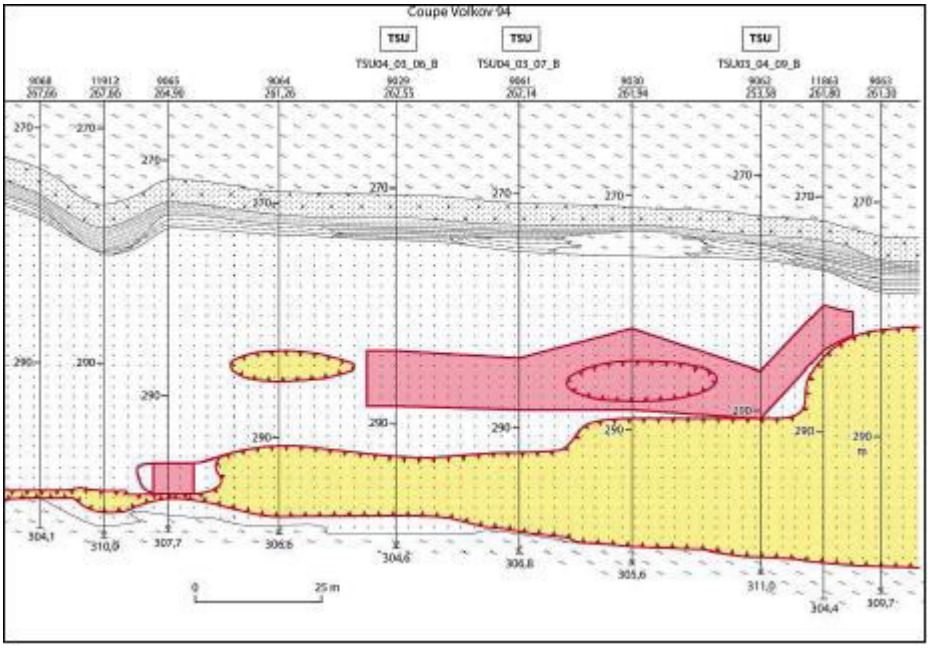

Figure 5 - Geological profile of the roll-front uranium deposit: oxidized areas (yellow) and uranium-enriched area (red)

Amount of sulfuric acid consummated by ISL when extracting uranium depends on: (i) the mineralogical characteristics of the deposit, and (ii) the wells pattern efficiency. Consumption of sulfuric acid in Kazakhstan uranium deposits is about 50-150 tons of H_2SO_4 per ton of U produced (Kazatomprom, 2013 [64]). Optimization of the use of injected leaching fluids (improving the wells

pattern location or adjusting the chemical composition) may have significant effects on the total costs. For instance, a reduction by 5-10% of the consumption of reagent will save about 50,000 to 350,000 tons of sulfuric acid per year at current production volumes. This illustrative example is presented only to demonstrate the potential benefit one can get by reducing the production cost optimizing production.

OBJECTIVES AND SCIENTIFIC NOVELTY OF THE RESEARCH

In-situ recovery (ISR) mining management remains still very empirical. In practice production controlling parameters during ISL are often limited to the data from wells (flow rate, pressures, composition of injected and produced solution). Hence, reactive transport models and use of accurate experimental data on reaction kinetics can help to improve and optimize the economic and environmental efficiency of ISL. However, currently ISL modeling methods that are able to ensure good monitoring and forecast of the composition of produced solution are very few (Lagneau, 2000; Regnault et al., 2014 [38,58]).

Parameters controlling the ISL process include: (i) composition and amount of leaching solution, (ii) flow rate regimes imposed at the well injector, (iii) distances between injectors and producers; (iv) geometrical configuration of injectors and producers [classically 5 or 6 injector wells and a producer at the center of the pentagon (or hexagon)]. Such parameters affect economic and environmental efficiency of the production process (Brovin and Grabovnikov, 1997 [10]) and can be determined by complex mathematical and accurate chemical kinetics modeling of the process.

The main interest of the present thesis is focused on acid leaching. This technology ensures a lower production cost than traditional mining with limited investment and reduced operational costs.

The main reasons for this lack of accuracy and efficiency are related to the fact that the ISL phenomenology is very complex due to chemical reactions involved between the liquid injected in the aquifer, and solids (minerals), to the kinetics reactions, and to the complexity of being able to couple the hydrodynamic transport and chemistry.

The objective of this thesis is triple:

- to develop an optimized conceptual phenomenological model for describing chemical processes involved in the ISL;
- to perform a qualitative analysis of ISL based on mono-dimensional problem;

- to build a numerical code for coupling the hydrodynamics and chemistry based on a streamline technique, one of the most efficient approaches for this kind of problems;

Presently the uranium mining sector in Kazakhstan does not use specific software packages that allow to monitor and manage the process of uranium mining through ISL process. The use of advanced computer codes will allow to reduce the costs at each stage of production, increasing the profitability of uranium mining companies and confirming the practical significance of ISL.

The scientific novelty of the thesis consists of:

- the optimized conceptual phenomenological model of physico-chemical process in porous medium;
- the introduction of gypsum sedimentation assumed to be the reaction slowdown (reaction passivation) factor in the ISL model;
- the asymptotic method of separation nonlinear and compositional effects based on the approximation of almost binary mixtures;
- the analytical solutions for 1D ISL model accounting a complete qualitative analysis of the coupling between hydrodynamic and chemical processes;
- the 3D numerical code for reactive transport based on the streamline technique and its application to some field case studies.

The structure of the thesis is as follows. After the literature review of results obtained previously on ISL, the rest of the thesis is divided into four parts: (i) the general chemical and mathematical model describing reactive transport in ISL; (ii) 1D asymptotic solution obtained by asymptotic method; (iii) implementation of a streamline approach to approximate the 3D reactive transport equations; (iv) discussion on limits and disadvantages of the proposed streamline approach and a conclusion.

LITERATURE REVIEW

ISL TECHNOLOGY

The bases of acid in situ leach uranium mining technology, together with issues of planning and operating of ISL facilities in general, are considered in (Beleckij et al., 1997; IAEA-Tekdoc, 2001 [6, 42], Brovinand Grabovnikov, 1997 [10]). Authors had elucidated important problems of geologic and hydro-geologic conditions for In-Situ leach (ISL) mining, such as classification of deposits amenable to ISL mining, hydro-geological conditions for ISL, influence of composition of ores and rocks on the ISL process. The geology of sandstone type uranium deposits, hydro-geological evaluation of uranium deposits, modeling and laboratory investigation, wellfield leach tests at ISL deposits, wellfield systems for ISL mining of sandstone deposits, processing of solutions and wellfield development for ISL operations, are also elucidated there.

EXPERIMENTAL STUDIES OF CHEMICAL REACTIONS

In order to eliminate mass transport limitations, experimental determination of chemical reaction rates are often measured on crushed minerals in well-mixed laboratory systems, but are not representative of chemical reaction rates observed on pilot sites. This is why Li et al. (2006)[40] recommended not to use directly such rate coefficients in consolidated porous media found in subsurface environments for predicting the reactive transport of chemical species. Such use of lab-measured rate laws may lead to erroneous results in case of heterogeneous porous media and may suggest wrong interpretations of basic mechanisms involved in the interaction of ore contained in porous media with sulfuric acid (Li et al., 2006 [40]). This is confirmed by Grabovnikov (1995) [28] and Golubev et al. (1978) [27] who demonstrated that positive results of laboratory geo-technological tests are not always accompanied by successful pilot works. The results of experimental works on the deposit sites developed by the In-Situ leaching method are reported in Golubev et al. (1978) [27]. They noticed that understanding uranium basic dissolution laws is fundamental to proper leaching model as well as for validation of laboratory and natural experiments. Originally experimental researches of ISL process had been implemented in labs. But the simplicity of how the experiments were carried out makes limited ranges of technological process parameters. Therefore, laboratory experiments had been substituted for the natural (pilot)

ones. Applying these experimental and theoretical results on real case studies, demonstrated the limits of the approach and raised a number of difficulties (Brovin and Grabovnikov, 1997 [10]) connected to: (i) considerable internal heterogeneity of natural ISL systems, (ii) impossibility to control a process directly in the active zone, and (iii) high inertia of such systems. So there is no possibility to connect and explain changes on the input with the target data unequivocally.

Interaction of solid-liquid in porous media is a complicated process. The first theoretical investigation of pore volume changes to find dependence between permeability and porosity during dissolution process was performed by Schechter and Gidley (1969) [62]. They pointed out unstable evolution of the pore radius distribution. Large pores grow faster than the small ones during the dissolution process because the liquid to solid ratio is locally larger for a large pore than for a small one. This phenomenon was studied experimentally by dissolving limestone by hydrochloric acid (Nierode and Williams, 1973 [46]), and theoretically for several regimes: reaction-limited, transport process dominant, diffusion predominant and convection predominant. In the latter case, the dissolution rate increases with the flow rate, and afterward develops dissymmetry. Dissolution is faster at the upstream side of the obstacles.

Gogoleva (2012) [25] and Costine et al. (2013) [17] suggest that precipitation of amorphous TiO_2 species on the contact surface of brannerite (UTi_2O_6), a titano-uranium mineral, may inhibit the leaching process of uranium. Charalambous (2014) [13] has studied this effect experimentally by varying standard leach parameters (total iron content, acid concentration, and temperature) on the dissolution of uranium rate from two naturally occurring brannerite ores using high resolution EPMA mapping. Results indicated that increasing total Fe(III), acid concentration, and temperature increase solubility of uranium from brannerite. The Charalambous' results on high resolution EPMA investigations show evidence of the presence of a thin TiO_2-rich layer, interpreted here as a passivation layer, at the surface of the particles, the remaining U-rich brannerite being protected from the leaching solute. These experimental results confirm thus the hypothesis of Gogoleva (2012) [25]. **Thus the precipitation of secondary mineral that blocks the reaction surface cannot be neglected in the mathematical model as it impacts greatly on total uranium recovery. These blocking aspects have been modeled in this PhD work. The scientific novelty of this research provides a mathematical model for simulating uranium in-situ leaching process by accounting secondary mineral precipitation and reaction surface blocking.**

Monitoring and predicting methods developed for the extraction of minerals through ISL process are currently inefficient and have extremely low accuracy despite the tremendous works and attempts made since the late 70's to develop accurate ISL mathematical model. One of the first works in this direction was done by Golubev et al. (1978) [27] and Golubev and Kravtsov and Krichevec (1983) [26] on 1D analytical solutions by taking into account the cyclicity and reversibility of reactions. They described the behavior through time of the uranium components in the solid phase, and calculated the amount of leached uranium applying mass balance equation to the mass transfer process in the porous media (Kravtsov and Krichevec, 1983 [26]).

A review of mathematical formulations of mass transfer problems depending on various types of chemical reactions, is given in the work by Rubin (1983) [60]. Further investigations on underground contamination due to migration of radioactive elements on groundwater system were made by Kalmazet et al. (1981) [32]. They have made a numerical simulation of probable migration process of heap leaching radioactive contaminants.

Bekri et al. (1995) [5] studied the microscopic changes of porous media due to acid injection but the precipitation mechanisms were neglected and porosity is considered as increasing function of dissolution process. As for other elements, the dissolution/precipitation mechanism is a heterogeneous process that occurs at the interface between solid and liquid during the leaching of uranium ores by sulfuric acid. The kinetic aspects of heterogeneous reactions have been reviewed by a number of authors. Usually, the rates of heterogeneous chemical reactions involving multi-steps are governed by the slower step process; they do not follow rate laws of homogeneous reaction.

Since the early 2000s, several software products developed in the Western countries can be used for modeling of ISL process, including ModFlow, MT3D, RT3D, and reactive transport models (Lagneau and Lee, 2010 [39]). In essence, these programs are of general use for simulating the migration of contaminants and are not specialized for modeling specifically ISL processes.

Zheng and Wang (1999) [67] have developed the MT3DMS software to calculate the migration of contaminants in soil. The authors built a 3D transport model in a porous medium for one-phase multi-component flow assuming no effects of the chemical reactions on the properties of the reservoir (no strong feedback from chemical processes to main flow). They studied the dispersion of pollutants in the soil accounting for the radioactive decay, the sorption and desorption of the pollutants onto the porous matrix.

Poezzhaev and Abdul'manova (2004) [55] have studied numerically the hydrodynamic process of ISL. They focused on improving the injection scheme of wells in order to reduce the contamination problems of upper and lateral aquifers by acid leaching injected solutions. The derived recommendations on how to improve hydrodynamic and geotechnical cycles, and to optimize the hydrodynamic fields of the injection schemes technologically accounting for the filtration velocity using the GMS3.1 fluid flow simulator. However, GMS3.1 takes into account only the hydrodynamic part of the problem without taking into account for the dissolution of the mineral in the formation. This is the major limitation of this work.

Pen'kovskij and Rybakova (1989) [52] and Danaev et al. (2005) [18] made similar work on porous media and applied it to the modeling of copper extraction by ISL. They differ from Zheng and Wang (1999) [67] by introducing the mass action law to describe equilibrium of various chemical species. An analytical solution for describing the *Cu* concentration in the liquid phase is obtained for homogeneous media (already plural), while the mineral dissolution kinetics and reagent transfer equations are solved numerically; the authors suggested an analytical solution for 1D problems. In addition, they obtained numerical leaching rate curves of copper oxide in case of sulfuric acid solution and for hexagonal wells location using a finite elements method.

Kancel (2008) [33] found self-similar approximated analytical solutions for predicting uranium recovery during ISL for the 1D problem. The solution describes the propagation of the front of the leached liquid solution, the extension of active dissolution zones, and the edge - boundary tail of the completely dissolved zones; effects of heterogeneities on the dynamics of the ISL process were studied numerically. In particular, it is shown that repeated re-precipitation of uranium may occur in front zones with low saturated uranium concentration.

The structure of the porous medium tend to be modified by dissolution and precipitation of solid phases which thus modify flow and transport properties, Lagneau and Lee (2010) [39] Buddhima et al. (2014) [11], investigated the coupled geochemistry and groundwater flow problem. Secondary minerals precipitation caused the appearance of geochemical barriers and reduction of hydraulic conductivity of the medium. Simulations made on commercial ModFlow and RT3D codes. These time dependent properties evolution cannot be explicitly simulated by representative elementary volume (REV) scale based models. However, such modifications can be included assuming specific geometries (simplified geometries for the porous medium (Kieffer et al., 1999; Lichtner, 1992; Lagneau, 2000 [35, 41, 38]), or validity of empirical laws (e.g. Kozeny–Carman for permeability (Carman, 1937; Chilingarian et al., 1992 [12, 14]), or Archie's law of

diffusion (Archie , 1942; Chilingarian et al., 1992 [2, 14]). No general relationship exists, and this subject is still an active research area.

Noskov et al. (2008) [47], Istomin et al.(2014) [31] and Regnault et al. (2014) [58] demonstrated benefits of applying numerical simulations for optimizing uranium extraction using ISL process. However, despite these pioneer works, current uranium mining sector in Kazakhstan does not yet use software packages for monitoring and managing uranium extraction by ISL process. Some experimental essays are recently conducted on pilot site at Katco. However, possibilities of mathematical modeling and modern Computational Fluid Dynamics (CFD) can help in conducting development and design of optimal technological ISL processes.

This review demonstrates that the major attempts for modeling uranium production by in-situ leaching methods remain at the level of mathematical model constructions, with some accounting for different parameters affecting the process; some approaches investigate simple well schemes (hexagonal centered mesh), the effects of changing composition of the injected solution on the recovery, including the liquid to solid ratio, and some of the kinetic coefficients.

1 EQUATIONS OF REACTIVE TRANSPORT IN POROUS MEDIA

1.1 DESCRIPTION OF A CHEMICAL REACTION

Elementary stoichiometric system

Among various types of reactions, it is important to distinguish:

- a homogeneous reaction, which occurs between the components of fluid;
- a heterogeneous reaction, which occurs between components of fluid and solid surface;
- a simple reaction, which takes place in one stage;
- a multi-step reaction, which represents a consecutive set of reactions taking place one after another;
- simultaneous system of reactions: several reactions happening at the same time;
- irreversible reaction, which happens only in one direction so that one can distinguish the reactives and the products;
- reversible reaction, which happens in both directions, so that all components are reactives and products at the same time;
- catalyzed reaction, which happens only in the presence of additional species which plays the role of catalyzer;
- auto-catalyzed reaction: several products of such reaction play the role of catalyzers of this reaction, so that the reaction changes its rate in time spontaneously.

Let the equation of a simple irreversible chemical reaction be:

$$\nu_1 R_1 + ... + \nu_r R_r = \nu_{r+1} R_{r+1} + ... + \nu_{r+p} R_{r+p} \qquad (1.1)$$

where R_1 and Pi are the chemical symbols of reactants and products; ν_i is the number of particles of component *i* in reaction ("the stoichiometric coefficient"); *r* is the number of reactants; *p* is the number of products.

Elementary stoichiometric system is the mixture of reactants where a number of minimal moles necessary to the reaction occurs: such system contains exactly ν_1 moles of component R_1 ,..., and ν_r moles of component R_r .For a reversible reaction, an elementary stoichiometric system contains all components of the reaction.

Reaction rate

For a reaction between the components of fluid, which happens within the overall fluid volume, the reaction rate ω is defined as the number of elementary stoichiometric systems in 1 m^3 of fluid, which have been entirely reacted during 1 sec.

For a reaction between fluid and solid, the reaction rate ω_s should be reported to 1 m^2 of the solid surface, but not to the fluid volume.

Several typical values of ω are:

$\omega \sim 10^{-10} \frac{1}{s \cdot m^3}$ is a slow reaction (1 m^3 of matter reacts during 300 years)

$\omega \sim 10^{-6} \frac{1}{s \cdot m^3}$ is a fast reaction (1 m^3 of matter reacts during 13 days)

1.2PARTICLE BALANCE IN REACTION

Let us consider the mixture in an ERV (elementary representative volume) of porous medium, in which a single reaction occurs between the fluid components. For component *i* of fluid or solid that participates in the reaction, the variation of the number of particles of this component (N_i) in time is:

Ω

$$\frac{dN_i}{dt} = \pm \left\{ \begin{array}{l} \text{The number of particles} \\ \text{of component } i \text{ in a} \\ \text{stoichiometric system,} \\ \text{of reaction } |\nu_i| \end{array} \right\} \left\{ \begin{array}{l} \text{The number of} \\ \text{stoichiometric systems} \\ \text{that have reacted during 1 s} \\ \text{in the volume of liquid, which} \\ \text{occupies the ERV, } \omega \end{array} \right\} \left\{ \begin{array}{l} \text{The volume of} \\ \text{liquid in ERV, } \Omega_{liq} \end{array} \right\}$$

Mathematically it is expressed as: $\frac{dN_i}{dt} = \gamma_i \nu_i \omega \Omega_{liq}$, $\gamma_i = \begin{cases} +1 & \text{for products,} \\ -1 & \text{for reactants.} \end{cases}$

In porous medium: $\frac{1}{\Omega} \frac{dN_i}{dt} = \gamma_i \nu_i \omega \phi$, where Ω is the ERV and ϕ is the medium porosity.

If component *i* of fluid participates in *M* reactions simultaneously, then the variation of the number of particles of this component in liquid is: $\frac{1}{\Omega}\frac{dN_i}{dt} = \phi\sum_{r=1}^{M}\gamma_{ir}\nu_{ir}\omega_r$, where ν_{ik} is the stoichiometric coefficient of component *I* in reaction *k*, ω_k is the rate of reaction *k*.

For a reaction between fluid and solid rocks, the variation of the number of particles of component *I* is:

$$\frac{dN_i}{dt} = \pm\left\{\begin{array}{l}\text{The number of particles}\\ \text{of this component in a}\\ \text{stoichiometric system,}\\ |\nu_i|\end{array}\right\}\left\{\begin{array}{l}\text{The number of}\\ \text{stoichiometric systems}\\ \text{that have reacted during 1 s}\\ \text{in contact with 1m}^2\text{ of the}\\ \text{solid surface, }\omega_s\end{array}\right\}\left\{\begin{array}{l}\text{The solid surface}\\ \text{in a ERV, S}\end{array}\right\}$$

or: $\frac{dN_i}{dt} = \gamma_i\nu_i\omega_{s,i}S$, where *S* is the solid surface in ERV.

1.3REACTION KINETICS: GULBERG-WAAGE'S LAW OF MASS ACTION

The definition of reaction rates ω , or ω_s is one of the main problems of chemical kinetics. The general relation for the reaction rate may be obtained from the following physical considerations. The reaction rate is determined by two circumstances:

- the probability of collision between all the particles of reactives determined by the stoichiometric equation at any point of space;
- the time of particle transformation after collision.

Let us consider a simple irreversible reaction. The probability for a particle *i*to be present at a space point is equal to its molar fraction C_i. The probability for ν_i particles of component *i* to collide between them at any space point is equal to the probability product: $C_i^{\nu_i}$, if all collisions are independent between them. Equation (1.1) requires that ν_i particles of each reactive (*i*= 1, ..., *r*) collide simultaneously. The probability of such event is: $C_1^{\nu_1}C_2^{\nu_1}\cdot\ldots\cdot C_r^{\nu_r}$. Then the reaction rate is determined as:

$$\omega = kC_1^{\nu_1}C_2^{\nu_1}\cdot\ldots\cdot C_r^{\nu_r} \qquad (1.2)$$

where *k* is the reaction constant value, which is the characteristic rate of particle transformation after all necessary collisions. Its dimension is [1/(m^3s)] for volumetric reactions (between fluid components), and [1/(m^2s)] for reactions between fluid and solid surface.

This fundamental equation is called the law of mass action.

The formulation (1.2) is given for a simple irreversible reaction, but it is easy to generalize it for any kind of more complicated reactions. The domain of validity of the mass action law is determined by the hypothesis of the independence between various collisions. So (1.2) is applicable in the following cases:

- if the fluid is ideal gas, in this case the collisions between particles are really independent events as the particles have no dimension;
- if the fluid is a diluted liquid solution.

For a multi-step reaction, the law (1.2) must be applied for each step, but not for the resulting reaction, which represents the formal sum of all steps. The sum of steps yields a wrong reaction kinetics.

For real gases it is necessary to use *the fugacity* instead of molar fractions. For real liquid solutions *the chemical activity* should replace the molar fraction. In these cases the exponents ν_i are not necessary the stoichiometric coefficients, but some empirical values obtained by fitting experimental data.

1.4REACTION CONSTANTS

To calculate k_i, it is possible to apply several methods.

Empirical rule of van't Hoff:

$$k(T_1) = k(T_2) \cdot \gamma^{(T_2 - T_1)/10}, \quad \gamma = 2 - 4$$

This rule shows that the reaction rate increases by four times when the temperature increases by 10 degrees.

This rule is applicable between $T = 0°C$ and $100°C$.

Arrhenius equation has demonstrated that the reaction is not caused by all collisions between reagents, but by the most active collisions which possess an excessive energy *(the active*

molecules). The fraction of active molecules is $e^{-E_\alpha / RT}$, where E_α is the activation energy. Then, for the reaction rate, one obtains:

$$k(T) = k_0 e^{-E_\alpha / RT}$$

Herein k_0 is the pre-exponential factor (also called factor of frequency) which takes into account the collision frequency and stearic effects.

For a large spectrum of reactions, $E_\alpha = 40 - 130 kJ / mol$.

1.5TRANSPORT WITH CHEMICAL REACTIONS

Examine the case when a part of fluid components react between each other (homogeneous reactions), and another part reacts with solid rocks (heterogeneous reactions). Let component *i*of the fluid make part of m_1 homogeneous reactions and m_2 heterogeneous reactions.

Taking into account that $\frac{1}{\Omega}\frac{dN_i}{dt} \equiv \frac{\partial(\phi\rho C_i)}{\partial t}$, we obtain for component *i* of the fluid, by the analogy with static case:

$$\frac{\partial(\phi\rho C_i)}{\partial t} + \underbrace{div(\rho C_i \vec{V})}_{advection} = \underbrace{div\left(\phi\rho \sum_{j=1}^{n} D_{ij} grad C_j\right)}_{diffusion} + \underbrace{\phi \sum_{k=1}^{m_1} \gamma_{ik} \nu_{ik} \omega_k}_{\substack{\text{homogeneous} \\ reactions}} + \underbrace{s_s \sum_{k=m_1}^{m_1+m_2} \gamma_{ik} \nu_{ik} \omega_{sk}}_{\substack{heterogeneou \\ reactions}} \qquad (1.3)$$

$i = 1,\ldots,n$

where ρ is the molar density of the phase [mol/m^3]; $\vec{V} = \sum_{k=1}^{n} C_k \vec{V}_k$ is the Darcy's velocity of advection (the mean molar Darcy's velocity of the fluid); D_{ij} are the binary diffusion coefficients; *n* is the total number of components in the fluid; $s_s = S/\Omega$ is the specific surface (the surface of pores in volume Ω divided by the volume).

The sum of all the equations (*) over the components present in liquid yields the balance equation for the overall liquid, in which the diffusion term should disappear. At the same time, the reaction term does not disappear, as the fluid composition varies due to reactions with solid rocks. For component *i* belonging to the solid rocks, the balance equation is:

$$\frac{\partial(1-\phi)\rho_s C_i}{\partial t} = \underbrace{s_s \sum_{k=m_1}^{m_1+m_2} \gamma_{ik} \nu_{ik} \omega_{sk}}_{\substack{heterogeneou \\ reactions}} \qquad (1.4)$$

where ρ_s is the molar density of the solid rocks [mol/m^3].

1.6EXAMPLE: THE SIMPLEST MODEL OF IN SITU LEACHING

The liquid phase consists of three components: H_2O, $H_2SO_4H_2SO_4$, and uranyl sulphate UO_2SO_4. The solid phase consists of UO_3 and all other solid components.

The balance equations for acid, uranyl sulphate and uranium trioxide are:

$$\frac{\partial\left(\phi\rho C_{H_2SO_4}\right)}{\partial t}+\underbrace{div\left(\rho C_{H_2SO_4}\vec{V}\right)}_{advection}=\underbrace{div\left(\phi\rho\sum_{j=1}^{n}D_{ij}\,grad C_j\right)}_{diffusion}-\underbrace{s_s\nu\omega}_{\substack{heterogeneou\\ reactions}}$$

$$\frac{\partial\left(\phi\rho C_{UO_2SO_4}\right)}{\partial t}+\underbrace{div\left(\rho C_{UO_2SO_4}\vec{V}\right)}_{advection}=\underbrace{div\left(\phi\rho\sum_{j=1}^{n}D_{ij}\,grad C_j\right)}_{diffusion}+\underbrace{s_s\nu\omega}_{\substack{heterogeneou\\ reactions}}$$

$$\frac{\partial(1-\phi)\rho_s C_{UO_3}}{\partial t}=-\underbrace{s_s\nu\omega}_{\substack{heterogeneou\\ reactions}}$$

In the present thesis we will use another chemical model, sufficiently more complicated, which takes into account for additional important reactions caused by acid injection.

2 OPTIMIZED CONCEPTUAL PHENOMENOLOGICAL MODEL OF ISL

2.1 PHYSICAL AND CHEMICAL MODEL

The uranium is present in rocks in the form of complex oxides (such as, uraninite, cofinite, branerite, ...). Its crystal lattice consists of molecules of UO_2 and UO_3 united in various ways by forming the complexes UO_2, $U_3O_8 \equiv UO_2 \times 2UO_3$ and $U_4O_9 \equiv 3UO_2 \times UO_3$ at various ratios. The link energy between UO_2 and UO_3 in uraninite is very high, the thermodynamic calculation yields:

$$3UO_2 + UO_3 = U_4O_9 + 36.4kJ,\ UO_2 + 2UO_3 = U_3O_8 + 46.1kJ.$$

In the zone of roll fronts, the uraninite is essentially present in the form of U_3O_8, while the presence of U_4O_9 is the lowest. Then we can accept that uraninite consists essentially of UO_2 and $U_3O_8 \equiv UO_2 \times 2UO_3$.

The direct oxidation of UO_2 by acid is a very energy consuming process (the consecutive reaction is endothermic) with respect to the reaction between the acid and uraninite U_3O_8. At the same time, the uranium dioxide UO_2 is rapidly oxidized by the ions of iron +3. The presence of these ions in liquid solution is due to the reaction between the solid iron +3 present in rocks and acid.

The sulfur acid reacts with several other elements present in rocks, but practically they are all reversible. The significant exception concerns the reaction of acid with carbonates, which causes the deposition of solid gypsum cake on pore walls insoluble in liquid within the large interval of pH between 1 and 12. The formation of the gypsum cake is non-instantaneous and occurs through several stages when initially small colloid particles of gypsum arise and form liquid suspension, after which the growing gypsum flakes are deposited on pore walls, thus, creating an insoluble sediment. This reduces the surface of contact between the acid and uranium oxides, which leads to the passivation of useful reactions and can significantly reduce the recovery efficiency.

Consequently we suggest the following system of four heterogeneous reactions happening during ISL:

Reaction I: $$\underbrace{UO_2 \times 2UO_3}_{s1} + \underbrace{2H_2SO_4}_{1} = \underbrace{UO_2}_{s2} + \underbrace{2UO_2SO_4}_{2} + \underbrace{2H_2O}_{3} \quad (2.1)$$

Reaction II: $$\underbrace{2Fe(OH)_3}_{s3} + \underbrace{3H_2SO_4}_{1} = \underbrace{Fe_2(SO_4)_3}_{4} + \underbrace{6H_2O}_{3} \quad (2.2)$$

Reaction III: $$\underbrace{UO_2}_{s2} + \underbrace{Fe_2(SO_4)_3}_{4} = \underbrace{UO_2SO_4}_{2} + \underbrace{2FeSO_4}_{5} \quad (2.3)$$

Reaction IV: $$\underbrace{CaCO_3}_{s4} + \underbrace{H_2SO_4}_{1} = \underbrace{CaSO_4}_{s5} + \underbrace{H_2CO_3}_{6} \quad (2.4)$$

Gypsum $CaSO_4$ is insoluble in water (if pH varies between 1 and 12).

Thus, the fluid is single-phase liquid. It consists of the following chemical components:

Component 1: sulfuric acid H_2SO_4,

Component 2: uranyl sulfate UO_2SO_4,

Component 3: water H_2O,

Component 4: iron(III) sulfate $Fe_2(SO_4)_3$,

Component 5: iron(II) sulfate $FeSO_4$,

Component 6: carbonic acid H_2CO_3.

The solid rock contains five main elements which are active with respect to fluid:

Component s1: uraninite $UO_2 \times 2UO_3$,

Component s2: uranium dioxide UO_2,

Component s3: iron hydroxide $Fe(OH)_3$,

Component s4: calcium carbonate $CaCO_3$,

Component s5: gypsum $CaSO_4$.

An elementary stoichiometric system contains 1 moles of uraninite, 6 moles of sulfuric acid, 2 moles of iron hydroxide, 1 moles of oxide of uranium, and 1 moles of carbonate.

2.2 BALANCE EQUATIONS

According to (3.2) and (3.3), the balance equations for the system described above are

$$\frac{\partial(1-\phi)\rho_s C^{(s1)}}{\partial t} = \nu_I^{(1)}\omega_I \tag{2.5a}$$

$$\frac{\partial(1-\phi)\rho_s C^{(s2)}}{\partial t} = \nu_I^{(3)}\omega_I + \nu_{III}^{(1)}\omega_{III} \tag{2.5b}$$

$$\frac{\partial(1-\phi)\rho_s C^{(s3)}}{\partial t} = \nu_{II}^{(1)}\omega_{II} \tag{2.5c}$$

$$\frac{\partial(1-\phi)\rho_s C^{(s4)}}{\partial t} = \nu_{IV}^{(1)}\omega_{IV} \tag{2.5d}$$

$$\frac{\partial(1-\phi)\rho_s C^{(s5)}}{\partial t} = \nu_{IV}^{(3)}\omega_{IV} \tag{2.5e}$$

$$\frac{\partial\rho_l\phi C^{(1)}}{\partial t} + div(\rho_l\phi C^{(1)}\vec{U}) = div\left(\rho_l\phi\sum_{k=1}^{n} D^{(1k)}\,gradC^{(k)}\right) + \left(\nu_I^{(2)}\omega_I + \nu_{II}^{(2)}\omega_{II} + \nu_{IV}^{(2)}\omega_{IV}\right) \tag{2.5f}$$

$$\frac{\partial\rho_l\phi C^{(2)}}{\partial t} + div(\rho_l\phi C^{(2)}\vec{U}) = div\left(\rho_l\phi\sum_{k=1}^{n} D^{(2k)}\,gradC^{(k)}\right) + \left(\nu_I^{(4)}\omega_I + \nu_{III}^{(3)}\omega_{III}\right) \tag{2.5g}$$

$$\frac{\partial\rho_l\phi C^{(3)}}{\partial t} + div(\rho_l\phi C^{(3)}\vec{U}) = div\left(\rho_l\phi\sum_{k=1}^{n} D^{(3k)}\,gradC^{(k)}\right) + \left(\nu_I^{(5)}\omega_I + \nu_{II}^{(4)}\omega_{II}\right) \tag{2.5h}$$

$$\frac{\partial\rho_l\phi C^{(4)}}{\partial t} + div(\rho_l\phi C^{(4)}\vec{U}) = div\left(\rho_l\phi\sum_{k=1}^{n} D^{(4k)}\,gradC^{(k)}\right) + \left(\nu_{II}^{(3)}\omega_{II} + \nu_{III}^{(2)}\omega_{III}\right) \tag{2.5i}$$

$$\frac{\partial\rho_l\phi C^{(5)}}{\partial t} + div(\rho_l\phi C^{(5)}\vec{U}) = div\left(\rho_l\phi\sum_{k=1}^{n} D^{(5k)}\,gradC^{(k)}\right) + \nu_{III}^{(4)}\omega_{III} \tag{2.5j}$$

$$\frac{\partial\rho_l\phi C^{(6)}}{\partial t} + div(\rho_l\phi C^{(6)}\vec{U}) = div\left(\rho_l\phi\sum_{k=1}^{n} D^{(6k)}\,gradC^{(k)}\right) + \nu_{IV}^{(4)}\omega_{IV} \tag{2.5k}$$

where

$$\omega_q = \omega_{s,q}\sigma \tag{2.6}$$

is the volumetric rate of reaction q (q= I, II, III, IV), $\omega_{s,q}$ is the superficial reaction rate, $\sigma = S/\Omega$ is the specific surface of the porous walls.

The overall balance equation for liquid is the sum of all individual equations, where we take into account that:

$$\sum_{i=1}^{n} C^{(i)} = 1, \quad n=6$$

Then

$$\frac{\partial \rho_l \phi}{\partial t} + div(\rho_l \vec{V}) = \omega_I \left(\nu_I^{(2)} + \nu_I^{(4)} + \nu_I^{(5)}\right) + \omega_{II}\left(\nu_{II}^{(2)} + \nu_{II}^{(3)} + \nu_{II}^{(4)}\right) + \\ + \omega_{III}\left(\nu_{III}^{(2)} + \nu_{III}^{(3)} + \nu_{III}^{(4)}\right) + \omega_{IV}\left(\nu_{IV}^{(2)} + \nu_{IV}^{(4)}\right) \tag{2.7}$$

The right-hand side of the equation (2.7) can be neglected by saying that chemical reactions don't affect overall mass balance of the liquid.

$$\frac{\partial \rho_l \phi}{\partial t} + div(\rho_l \vec{V}) = 0 \tag{2.8}$$

The diffusion must disappear in the total balance equation. Due to it, the diffusion coefficients must satisfy additional conditions:

$$\sum_{i,k=1}^{n} D^{(ki)} grad C^{(k)} = 0 \tag{2.9}$$

2.3REDUCTION TO THE CONCENTRATION TRANSPORT EQUATIONS

Let us differentiate (2.5f) by parts, then we obtain for *i* = 1:

$$\rho_l \phi \left[\frac{\partial C^{(1)}}{\partial t} + \vec{U} grad C^{(1)}\right] + C^{(1)}\left[\frac{\partial \rho_l \phi}{\partial t} + div(\rho_l \phi \vec{U})\right] = div\left(\rho_l \phi \sum_{k=1}^{n} D^{(1k)} grad C^{(k)}\right) + \\ + \nu_I^{(2)}\omega_I + \nu_{II}^{(2)}\omega_{II} + \nu_{IV}^{(2)}\omega_{IV}$$

and subtract (2.8)

$$\rho_l \phi \left[\frac{\partial C^{(1)}}{\partial t} + \vec{U} grad C^{(1)}\right] = div\left(\rho_l \phi \sum_{k=1}^{n} D^{(1k)} grad C^{(k)}\right) + \\ + \nu_I^{(2)}\omega_I + \nu_{II}^{(2)}\omega_{II} + \nu_{IV}^{(2)}\omega_{IV}$$

or

$$\frac{\partial C^{(1)}}{\partial t} + \vec{U} grad C^{(1)} = \frac{1}{\rho_l \phi} div\left(\rho_l \phi \sum_{k=1}^{n} D^{(1k)} grad C^{(k)}\right) + \\ + \frac{\nu_I^{(2)}\omega_I + \nu_{II}^{(2)}\omega_{II} + \nu_{IV}^{(2)}\omega_{IV}}{\rho_l \phi} \tag{2.10}$$

2.4MODEL FOR ALMOST BINARY INCOMPRESSIBLE SOLUTION

Let the concentration of water in liquid be largely dominating, then the molar density of liquid is independent of liquid composition. We also assume that it does not depend on pressure. The variation of porosity and solid density due to chemical reactions is neglecting. The Eigen diffusion coefficient $D^{(ii)} \equiv D^{(i)}$ is dominant for each component *i*. Then the balance equations (2.5) become:

$$div\vec{V} = 0 \; \vec{V} = -Kgrad(h) \tag{2.11a}$$

$$\frac{\partial C^{(s1)}}{\partial t} = \frac{\nu_I^{(1)}\omega_I}{(1-\phi)\rho_s} \tag{2.11b}$$

$$\frac{\partial C^{(s2)}}{\partial t} = \frac{\nu_I^{(3)}\omega_I + \nu_{III}^{(1)}\omega_{III}}{(1-\phi)\rho_s} \tag{2.11c}$$

$$\frac{\partial C^{(s3)}}{\partial t} = \frac{\nu_{II}^{(1)}\omega_{II}}{(1-\phi)\rho_s} \tag{2.11d}$$

$$\frac{\partial C^{(s4)}}{\partial t} = \frac{\nu_{IV}^{(1)}\omega_{IV}}{(1-\phi)\rho_s} \tag{2.11e}$$

$$\frac{\partial C^{(s5)}}{\partial t} = \frac{\nu_{IV}^{(3)}\omega_{IV}}{(1-\phi)\rho_s} \tag{2.11f}$$

$$\frac{\partial C^{(1)}}{\partial t} + \vec{U}gradC^{(1)} = div\left(D^{(1)}gradC^{(1)}\right) + \frac{\left(\nu_I^{(2)}\omega_I + \nu_{II}^{(2)}\omega_{II} + \nu_{IV}^{(2)}\omega_{IV}\right)}{\rho_l\phi} \tag{2.11g}$$

$$\frac{\partial C^{(2)}}{\partial t} + \vec{U}gradC^{(2)} = div\left(D^{(2)}gradC^{(2)}\right) + \frac{\left(\nu_I^{(4)}\omega_I + \nu_{III}^{(3)}\omega_{III}\right)}{\rho_l\phi} \tag{2.11h}$$

$$\frac{\partial C^{(3)}}{\partial t} + \vec{U}gradC^{(3)} = div\left(D^{(3)}gradC^{(3)}\right) + \frac{\left(\nu_I^{(5)}\omega_I + \nu_{II}^{(4)}\omega_{II}\right)}{\rho_l\phi} \tag{2.11i}$$

$$\frac{\partial \rho_l\phi C^{(4)}}{\partial t} + div(\rho_l\phi C^{(4)}\vec{U}) = div\left(\rho_l\phi\sum_{k=1}^{n} D^{(4k)}gradC^{(k)}\right) + \frac{\left(\nu_{II}^{(3)}\omega_{II} + \nu_{III}^{(2)}\omega_{III}\right)}{\rho_l\phi} \tag{2.11j}$$

$$\frac{\partial C^{(5)}}{\partial t} + \vec{U}gradC^{(5)} = div\left(D^{(5)}gradC^{(5)}\right) + \frac{\nu_{III}^{(4)}\omega_{III}}{\rho_l\phi} \tag{2.11k}$$

$$\frac{\partial C^{(6)}}{\partial t} + \vec{U}gradC^{(6)} = div\left(D^{(6)}gradC^{(6)}\right) + \frac{\nu_{IV}^{(4)}\omega_{IV}}{\rho_l\phi} \tag{2.11m}$$

Where *h* is the hydraulic head, $\vec{U} = \vec{V} / \phi$

This system of thirteen equations is closed with respect to thirteen variables: V , h , $C^{(s1)}$, $C^{(s2)}$, $C^{(s2)}$,..., $C^{(s5)}$ and $C^{(1)}$, $C^{(2)}$,..., $C^{(6)}$.

Instead of (2.9) the diffusion coefficients must satisfy the following conditions:

$$\sum_{i=1}^{n} D^{(i)} grad C^{(i)} = 0 \tag{2.12}$$

or

$$\sum_{i=1}^{n-1} D^{(i)} grad C^{(i)} + D^{(5)} grad\left(1 - \sum_{k=1}^{n-1} C^{(k)}\right) = 0$$

or

$$\sum_{i=1}^{n-1} \left(D^{(i)} - D^{(n)}\right) grad C^{(i)} = 0$$

Therefore, the diffusion coefficient must be identical in order to be independent of concentrations:

$$D^{(1)} = D^{(2)} = ... = D^{(n)} \equiv D \tag{2.13}$$

2.5REACTION KINETICS

Taking into account that the considered liquid mixture is a diluted solution, we can apply the law of mass action for reaction kinetics. Then according to …, the reaction rates for four reactions (2.1) – (2.4) are:

$$\omega_I = k_I C^{(s1)}\left(C^{(1)}\right)^2, \quad \omega_{II} = k_{II}\left(C^{(s3)}\right)^2\left(C^{(1)}\right)^3$$
$$\omega_{III} = k_{III} C^{(s2)} C^{(4)}, \quad \omega_{IV} = k_{IV} C^{(s4)} C^{(1)} \tag{2.14}$$

Parameters k_I, k_{II}, k_{III}, k_{IV}, are called the reaction constants. In reality, the reaction constants k_i are not exactly "constant values", as they depend significantly on the temperature. Indeed, the high temperature increases the intensity of particle fluctuations, which increases the probability of collisions. As a result, the reaction rate grows. However, the analyzed process is isothermal, consequently k_i are constant.

2.6 MODEL IN THE FORM OF TRANSPORT EQUATION

According to the accepted assumptions, the system (2.11) becomes:

$$div\vec{U}\phi = 0 \qquad \vec{U}\phi = -Kgrad(h) \tag{2.15a}$$

$$\frac{\partial C^{(s1)}}{\partial t} = -\frac{k_I C^{(s1)}\left(C^{(1)}\right)^2}{(1-\phi)\rho_s} \tag{2.15b}$$

$$\frac{\partial C^{(s2)}}{\partial t} = \frac{k_I C^{(s1)}\left(C^{(1)}\right)^2 - k_{III} C^{(s2)} C^{(4)}}{(1-\phi)\rho_s} \tag{2.15c}$$

$$\frac{\partial C^{(s3)}}{\partial t} = -\frac{2k_{II}\left(C^{(s3)}\right)^2\left(C^{(1)}\right)^3}{(1-\phi)\rho_s} \tag{2.15d}$$

$$\frac{\partial C^{(s4)}}{\partial t} = -\frac{k_{IV} C^{(s4)} C^{(1)}}{(1-\phi)\rho_s} \tag{2.15e}$$

$$\frac{\partial C^{(s5)}}{\partial t} = \frac{k_{IV} C^{(s4)} C^{(1)}}{(1-\phi)\rho_s} \tag{2.15f}$$

$$\frac{\partial C^{(1)}}{\partial t} + \vec{U} grad C^{(1)} = divD^{(1)} grad C^{(1)} + \\ + \frac{1}{\phi\rho_l}\left(-2k_I C^{(s1)}\left(C^{(1)}\right)^2 - 3k_{II}\left(C^{(s3)}\right)^2\left(C^{(1)}\right)^3 - k_{IV} C^{(s4)} C^{(1)}\right) \tag{2.15g}$$

$$\frac{\partial C^{(2)}}{\partial t} + \vec{U} grad C^{(2)} = divD^{(2)} grad C^{(2)} + \frac{1}{\theta\rho_l}\left(2k_I C^{s1}\left(C^{(1)}\right)^2 + k_{III} C^{(s2)} C^{(4)}\right) \tag{2.15h}$$

$$\frac{\partial C^{(3)}}{\partial t}+\vec{U}gradC^{(3)}=divD^{(3)}gradC^{(3)}+\frac{1}{\phi\rho_l}\left(2k_I C^{s1}\left(C^{(1)}\right)^2+6k_{II}\left(C^{(s3)}\right)^2\left(C^{(1)}\right)^3\right) \quad (2.15i)$$

$$\frac{\partial C^{(4)}}{\partial t}+\vec{U}gradC^{(4)}=divD^{(4)}gradC^{(4)}+\frac{1}{\phi\rho_l}\left(k_{II}\left(C^{(s3)}\right)^2\left(C^{(1)}\right)^3-k_{III}C^{(s2)}C^{(4)}\right) \quad (2.15j)$$

$$\frac{\partial C^{(5)}}{\partial t}+\vec{U}gradC^{(5)}=divD^{(5)}gradC^{(5)}+\frac{2k_{III}C^{(s2)}C^{(4)}}{\phi\rho_l} \quad (2.15k)$$

$$\frac{\partial C^{(6)}}{\partial t}+\vec{U}gradC^{(6)}=divD^{(6)}gradC^{(6)}+\frac{k_{IV}C^{(s4)}C^{(1)}}{\phi\rho_l} \quad (2.15m)$$

2.7 MODEL OF GYPSUM PRECIPITATION. CRUST POROSITY AND DIMENSIONS

The appearance of gyps means formation of a solid film (a crust) on the surface of the rocks which can retard both chemical reactions. A crust is characterized by three main parameters: its porosity, its specific surface, and its thickness.

The porosity of a crust may be estimated on the basis of the so-called Pilling-Bedworth ratio (1923) [54], α which is the volume of the formed crust $CaSO_4$ divided by the volume of the issuing material ($CaCO_3$). It is calculated as:

$$\alpha=\frac{M_{CaSO_4}\rho_{CaCO_3}}{M_{CaCO_3}\rho_{CaSO_4}}$$

where $M_{CaSO_4}=116$ and $M_{CaCO_3}=80$ are the molar masses, while $\rho_{CaSO_4}=2.3g/cm^3$, and $\rho_{CaCO_3}=2.71g/cm^3$ are the densities.

According to Pilling and Bedworth (1923) [54], if α< 1, then the crust is porous and penetrable;

If α> 2, then the crust is fragile and easily broken; if α = 1 – 2, then the crust is continuous and impenetrable for reactive substances.

For the considered case, α = 1.7, which means that the crust passivates both chemical reactions once formed.

Within the framework of the assumption that the precipitation does not influence the medium porosity and permeability, the thickness of the crust has no significance. In contrast, the surface occupied by the crust is very important. The crust is formed exactly over calcite inclusions, but may also be partially displaced by the moving fluid to the neighboring sites while covering uranium minerals. So the crust represents a system of isolated spots, or a continuous film but with holes. In any case, the crust reduces to the active surface *S* (or the specific active surface *σ*) of contact between fluid and solid which enters in the relation for the reaction rate (2.14).

The crust spots are higher in the areas when the calcite concentration is higher, so we can assume that the contact surface reduces linearly as the function of $C^{(s5)}$:

$$\sigma = \sigma_0 (1 - \beta C^{(s5)}) \tag{2.16}$$

where σ_0 is the specific surface of porous walls before calcite precipitation, β is an empirical parameter.

Then, we obtain for all volumetric reaction rates:

$$\begin{aligned} &\omega_I = k_I C^{(s1)} \left(C^{(1)}\right)^2 \left(1 - \beta C^{(s5)}\right), \qquad && \omega_{II} = k_{II} \left(C^{(s3)}\right)^2 \left(C^{(1)}\right)^3 \left(1 - \beta C^{(s5)}\right), \\ &\omega_{III} = k_{III} C^{(s2)} C^{(4)} \left(1 - \beta C^{(s5)}\right), \qquad && \omega_{IV} = k_{IV} C^{(s4)} C^{(1)} \left(1 - \beta C^{(s5)}\right). \end{aligned} \tag{2.17}$$

2.8 CLOSED MODEL WITH PRECIPITATION

Model (2.15) may be reduced to equation for the hydraulic head *h* and seven equations for concentrations:

$$div\vec{U}\phi = 0 \qquad \vec{U}\phi = -Kgrad(h) \tag{2.18a}$$

$$\frac{\partial C^{(s1)}}{\partial t} = -\frac{k_I}{(1-\phi)\rho_s} C^{(s1)} \left(C^{(1)}\right)^2 \left(1 - \beta C^{(s5)}\right) \tag{2.18b}$$

$$\frac{\partial C^{(s2)}}{\partial t} = \frac{1}{(1-\phi)\rho_s} \left(k_I C^{(s1)} \left(C^{(1)}\right)^2 - k_{III} C^{(s2)} C^{(4)} \right) \left(1 - \beta C^{(s5)}\right) \tag{2.18c}$$

$$\frac{\partial C^{(s3)}}{\partial t} = -\frac{2k_{II}}{(1-\phi)\rho_s} \left(C^{(s3)}\right)^2 \left(C^{(1)}\right)^3 \left(1 - \beta C^{(s5)}\right) \tag{2.18d}$$

$$\frac{\partial C^{(s4)}}{\partial t} = -\frac{k_{IV}}{(1-\phi)\rho_s} C^{(s4)} C^{(1)} \left(1 - \beta C^{(s5)}\right) \tag{2.18e}$$

$$\frac{\partial C^{(s5)}}{\partial t} = \frac{k_{IV}}{(1-\phi)\rho_s} C^{(s4)} C^{(1)} \left(1 - \beta C^{(s5)}\right) \tag{2.18f}$$

$$\begin{aligned} \frac{\partial C^{(1)}}{\partial t} + \vec{U} grad C^{(1)} &= div D^{(1)} grad C^{(1)} + \\ &+ \frac{1}{\phi\rho_l}\left(-2k_I C^{s1}\left(C^{(1)}\right)^2 - 3k_{II}\left(C^{(s3)}\right)^2\left(C^{(1)}\right)^3 - k_{IV} C^{(s4)} C^{(1)}\right)\left(1 - \beta C^{(s5)}\right) \end{aligned} \tag{2.18g}$$

$$\begin{aligned} \frac{\partial C^{(4)}}{\partial t} + \vec{U} grad C^{(4)} &= div D^{(4)} grad C^{(4)} + \\ &+ \frac{1}{\phi\rho_l}\left(k_{II}\left(C^{(s3)}\right)^2\left(C^{(1)}\right)^3 - k_{III} C^{(s2)} C^{(4)}\right)\left(1 - \beta C^{(s5)}\right) \end{aligned} \tag{2.18h}$$

Other concentrations can be calculated after the system is solved:

$$\begin{aligned} \frac{\partial C^{(2)}}{\partial t} + \vec{U} grad C^{(2)} &= div D^{(2)} grad C^{(2)} + \\ &+ \frac{1}{\phi\rho_l}\left(2k_I C^{s1}\left(C^{(1)}\right)^2 + k_{III} C^{(s2)} C^{(4)}\right)\left(1 - \beta C^{(s5)}\right) \end{aligned} \tag{2.19a}$$

$$\begin{aligned} \frac{\partial C^{(3)}}{\partial t} + \vec{U} grad C^{(3)} &= div D^{(3)} grad C^{(3)} + \\ &+ \frac{1}{\phi\rho_l}\left(2k_I C^{s1}\left(C^{(1)}\right)^2 + 6k_{II}\left(C^{(s3)}\right)^2\left(C^{(1)}\right)^3\right)(1 - \beta C^{(s5)}) \end{aligned} \tag{2.19b}$$

$$\frac{\partial C^{(5)}}{\partial t} + \vec{U} grad C^{(5)} = div D^{(5)} grad C^{(5)} + \frac{2k_{III}}{\phi\rho_l} C^{(s2)} C^{(4)} \left(1 - \beta C^{(s5)}\right) \tag{2.19c}$$

$$\frac{\partial C^{(6)}}{\partial t} + \vec{U} grad C^{(6)} = div D^{(6)} grad C^{(6)} + \frac{k_{IV}}{\phi\rho_l} C^{(s4)} C^{(1)} \left(1 - \beta C^{(s5)}\right) \tag{2.19d}$$

To conclude, this last set of five coupled equations describes the evolution of species concentration over time for a closed system. Analytical solutions for different cases reviewed above will be discussed in the following chapter.

3 1D ANALYTICAL SOLUTIONS: ASYMPTOTIC METHOD OF SPLITTING NONLINEAR AND COMPOSITIONAL EFFECTS

3.1SETTING OF THE PROBLEM OF UNDERGROUND LEACHING

We consider the problem of injection of the aqueous solution of acid at a fixed concentration $C^{(1*)}$, $C^{(4*)}$ from the left-hand boundary in the reservoir initially containing minerals s1, s3 and s4.The initial fluid in the reservoir is water (component 3).

Let us assume that:

- the diffusion is neglected;
- the reservoir is homogeneous
- the initial distribution of minerals is homogeneous in space;
- the concentration of injected acid $C^{(1*)}$, $C^{(4*)}$ is much higher than other concentrations (except for water).

The model (2.18) becomes:

$$U = const \tag{3.1a}$$

$$\frac{\partial C^{(s1)}}{\partial t} = -\lambda_1 C^{(s1)} \left(C^{(1)}\right)^2 \left(1 - \beta C^{(s5)}\right) \tag{3.1b}$$

$$\frac{\partial C^{(s2)}}{\partial t} = \left(\lambda_1 C^{(s1)} \left(C^{(1)}\right)^2 - \lambda_3 C^{(s2)} C^{(4)}\right)\left(1 - \beta C^{(s5)}\right) \tag{3.1c}$$

$$\frac{\partial C^{(s3)}}{\partial t} = -2\lambda_2 \left(C^{(s3)}\right)^2 \left(C^{(1)}\right)^3 \left(1 - \beta C^{(s5)}\right) \tag{3.1d}$$

$$\frac{\partial C^{(s4)}}{\partial t} = -\lambda_4 C^{(s4)} C^{(1)} \left(1 - \beta C^{(s5)}\right) \tag{3.1e}$$

$$\frac{\partial C^{(s5)}}{\partial t} = \lambda_4 C^{(s4)} C^{(1)} \left(1 - \beta C^{(s5)}\right) \tag{3.1f}$$

$$\frac{\partial C^{(1)}}{\partial t} + U \frac{\partial C^{(1)}}{\partial x} = \lambda_5 \left(-2\lambda_1 C^{s1} \left(C^{(1)}\right)^2 - 3\lambda_2 \left(C^{(s3)}\right)^2 \left(C^{(1)}\right)^3 - \lambda_4 C^{(s4)} C^{(1)}\right)\left(1 - \beta C^{(s5)}\right) \tag{3.1g}$$

$$\frac{\partial C^{(4)}}{\partial t} + U \frac{\partial C^{(4)}}{\partial x} = \lambda_5 \left(\lambda_2 \left(C^{(s3)}\right)^2 \left(C^{(1)}\right)^3 - \lambda_3 C^{(s2)} C^{(4)}\right)\left(1 - \beta C^{(s5)}\right) \tag{3.1h}$$

$$\frac{\partial C^{(2)}}{\partial t}+U\frac{\partial C^{(2)}}{\partial x}=\lambda_5\left(\lambda_1 C^{(s1)}\left(C^{(1)}\right)^2+\lambda_3 C^{(s2)}C^{(4)}\right)\left(1-\beta C^{(s5)}\right) \tag{3.1i}$$

where

$$\lambda_1\equiv\frac{k_I}{\rho_s(1-\phi)},\ \lambda_2\equiv\frac{k_{II}}{\rho_s(1-\phi)},\ \lambda_3\equiv\frac{k_{III}}{\rho_s(1-\phi)},\ \lambda_4\equiv\frac{k_{IV}}{\rho_s(1-\phi)},\ \lambda_5\equiv\frac{\rho_s(1-\phi)}{\rho_l\phi}$$

Initial and boundary conditions are:

$$\begin{aligned}
&C^{(s1)}\big|_{t=0}=C^{(s1,0)},\quad C^{(s2)}\big|_{t=0}=0,\\
&C^{(s3)}\big|_{t=0}=0,\qquad C^{(s4)}\big|_{t=0}=C^{(s4,0)},\qquad C^{(s5)}\big|_{t=0}=0\\
&C^{(1)}\big|_{t=0}=0,\qquad C^{(4)}\big|_{t=0}=0,\\
&C^{(1)}\big|_{x=0}=C^{1*}\qquad C^{(4)}\big|_{x=0}=C^{4*}
\end{aligned} \tag{3.2}$$

3.2ASYMTOTIC METHOD OF SPLITTING NONLINEAR AND COMPOSITIONAL EFFECTS (SNCE)

The main problems of multi-component transport with chemical reactions are:

- the nonlinearity introduced by chemical kinetics and multi-component diffusion (the Stephane-Maxwell diffusion is sufficiently nonlinear);
- The high number of differential equations equal to the number of chemical components.

To overcome these problems we suggest the asymptotic approach that enables us to split the nonlinear and compositional effects. It is based on approximating the phase composition as a diluted mixture, i.e. we assume that the phase consists essentially of one chemical component, while all other components are present in small quantities. The maximum value of the concentrations of non-dominating components represents a small parameter of the problem, ε. Respectively the solution of our nonlinear multi-component problem, u, can be presented in the form of an asymptotic series: $u=u_0+\varepsilon u_1+\ldots$. The zero-order term contains nonlinearity, but corresponds, obviously, to a mono-component fluid. Therefore it does not contain diffusion (as the diffusion has no meaning in a mono-component system), and chemical reactions (as a reaction

requires to have at least two reactants and one product). All the compositional effects are kept in the first approximation u_1, which is however linear.

This gives us the possibility to obtain analytical solution of a complicated nonlinear problem of high dimension.

Method SNCE was developed in the theory of reservoir engineering for two-phase gas-oil and gas-condensate systems, when gas is considered to consist essentially of methane, while liquid consists essentially of a heavy component, and all other intermediate components are present in small quantities (Panfilov, 1986, [49]), (Panfilov and Shilovich, 2000, [50]), (Abadpour and Panfilov, 2010, [1]). For single-phase natural flow of multi-component aqueous solution, this method was applied in (Felder, Oltean, Panfilov M., and Buès, 2004, [23]) where the liquid was considered as a diluted mixture dominated by H_2O.

Evidently method SNCE represents a particular interest for problems with chemical reactions giving the opportunity to treat high-order system of nonlinear equations efficiently.

In the present thesis we develop modification of the method SNCE, by assuming that the reservoir liquid is binary, i.e. consists essentially of H_2O and the injected acid H_2SO_4, while the concentrations of all other components are small. Respectively, we obtain the single-phase flow of water and H_2SO_4 in the zero-order approximation, in which chemical reactions do not occur. All compositional effects related to chemical reactions appear in the first approximation, which is described by linear system of equations. Despite the large number of equations this system has an exact analytical solution.

3.3 ASYMPTOTIC EXPANSION

The technology of leaching is characterized by small concentrations of acid in the injected aqueous solution. On the other hand, the uranium ores represent microscopic inclusions in rocks, molar fractions of which are much lower than 1. Respectively the fraction of uranium dissolved in liquid will also be small. This means that the reservoir liquid can be considered as a diluted solution.

Let us assume that the concentration of the injected acid ($C^{(1)}, C^{(4)}$) is much higher than all other concentrations. Let the small concentrations $C^{(s1)}, C^{(s2)}, ..., C^{(s5)}$ be of order ε where,

$$0 < \varepsilon << 1$$

is a characteristic value of all non-dominant concentrations (for instance, ε may be selected as $C^{(s1,0)}$).

In order to keep the effect of calcite precipitation at least in the first approximation, we assume that

$$\beta \sim \varepsilon^{-1}$$

The solution of the problem (3.1), (3.2) may be searched in the form of the following asymptotic series:

$$\begin{aligned} &C^{(1)} = C_0^{(1)} + \varepsilon C_1^{(1)} + \varepsilon^2 ...; \qquad C^{(4)} = C_0^{(4)} + \varepsilon C_1^{(4)} ...; \\ &C^{(si)} = \varepsilon C_1^{(si)} + \varepsilon^2 ..., \qquad (i = 1,2,3,4,5) \end{aligned} \tag{3.3}$$

3.4 ZERO ORDER APPROXIMATION

Substituting the series (3.3) into (3.1) and (3.2), we obtain equations for zero approximation:

$$\begin{aligned} &\frac{\partial C_0^{(1)}}{\partial t} + U\frac{\partial C_0^{(1)}}{\partial x} = 0, \qquad C_0^{(1)}\Big|_{t=0,x>0} = 0, \quad C_0^{(1)}\Big|_{x=0,t>0} = C^{1*}; \\ &\frac{\partial C_0^{(4)}}{\partial t} + U\frac{\partial C_0^{(4)}}{\partial x} = 0, \qquad C_0^{(4)}\Big|_{t=0,x>0} = 0, \quad C_0^{(4)}\Big|_{x=0,t>0} = C^{4*} \end{aligned} \tag{3.4}$$

This linear problem of convective transport with the initial shock has the following exact solution:

$$\boxed{\begin{aligned} C_0^{(1)}(x,t) &= \begin{cases} C^{1*}, \ x \le x_f(t) = Ut, \ \ U = const \\ 0, \quad x > x_f(t) \end{cases} \\ C_0^{(4)}(x,t) &= \begin{cases} C^{4*}, \ x \le x_f(t) = Ut, \ \ U = const \\ 0, \quad x > x_f(t) \end{cases} \end{aligned}} \tag{3.5}$$

So, the zero-order solutions are piecewise constant.

3.4 SPLITTING OF THE FIRST ORDER PROBLEM

The problem for the first approximation is split into several problems. The fundamental role plays the problem for $C^{(s4)}$ and $C^{(s5)}$ which is independent:

$$\begin{cases} \dfrac{\partial C_1^{(s4)}}{\partial t} = -\lambda_4 C_1^{(s4)} C_0^{(1)} \left(1 - \beta\varepsilon C_1^{(s5)}\right) \\ \dfrac{\partial C_1^{(s5)}}{\partial t} = \lambda_4 C_1^{(s4)} C_0^{(1)} \left(1 - \beta\varepsilon C_1^{(s5)}\right) \\ C_1^{s4}\Big|_{t=0} = \dfrac{C^{s4,0}}{\varepsilon} \\ C_1^{s5}\Big|_{t=0} = 0 \end{cases} \tag{3.6}$$

Once this problem is solved, it is possible to solve other problems for the remaining concentrations:

$$\begin{cases} \dfrac{\partial C_1^{(s1)}}{\partial t} = -\lambda_1 C_1^{(s1)} \left(C_0^{(1)}\right)^2 \left(1 - \beta\varepsilon C_1^{(s5)}\right) \\ C_1^{(s1)}\Big|_{t=0} = \dfrac{C^{s1,0}}{\varepsilon} \end{cases} \tag{3.7}$$

$$\begin{cases} \dfrac{\partial C_1^{(s2)}}{\partial t} = \left(\lambda_1 C_1^{(s1)} \left(C_0^{(1)}\right)^2 - \lambda_3 C_1^{(s2)} C_0^{(4)}\right)\left(1 - \beta\varepsilon C_1^{(s5)}\right) \\ C_1^{(s2)}\Big|_{t=0} = 0 \end{cases} \tag{3.8}$$

$$\begin{cases} \dfrac{\partial C_1^{(1)}}{\partial t} + U\dfrac{\partial C_1^{(1)}}{\partial x} = \lambda_5 \left(-2\lambda_1 C_1^{(s1)} \left(C_0^{(1)}\right)^2 - \lambda_4 C_1^{(s4)} C_0^{(1)}\right)\left(1 - \beta\varepsilon C_1^{(s5)}\right) \\ C_1^{(1)}\Big|_{t=0,x>0} = 0 \\ C_1^{(1)}\Big|_{x=0,t>0} = 0 \end{cases} \tag{3.9}$$

$$\begin{cases} \dfrac{\partial C_1^{(2)}}{\partial t} + U\dfrac{\partial C_1^{(2)}}{\partial x} = \lambda_5 \left(2\lambda_2 C_1^{(s1)} \left(C_0^{(1)}\right)^2 + \lambda_3 C_1^{(s2)} C_0^{(4)}\right)\left(1 - \beta\varepsilon C_1^{(s5)}\right) \\ C_1^{(2)}\Big|_{t=0,x>0} = 0 \\ C_1^{(2)}\Big|_{x=0,t>0} = 0 \end{cases} \tag{3.10}$$

After that we can solve equations for the rest of the concentrations in liquid phase $C^{(2)}, C^{(3)}, C^{(5)}, C^{(6)}$.

3.5 SOLUTION OF THE MAIN FIRST-ORDER PROBLEM

Let us examine problem (3.6) which becomes, while taking into account for (3.3), (3.5):

For $0 < t < x/U$

$$\boxed{C_1^{(s4)} \equiv \frac{C^{s4,0}}{\varepsilon}}, \quad \boxed{C_1^{(s5)} \equiv 0.} \tag{3.11}$$

For $t \geq x/U$:

$$\boxed{\begin{cases} \dfrac{\partial C_1^{(s4)}}{\partial t} = -\lambda_4 C_1^{(s4)} C_0^{(1)} \left(1 - \beta\varepsilon C_1^{(s5)}\right) & C_1^{(s4)}\Big|_{t=x/U} = \dfrac{C^{s4,0}}{\varepsilon} \\ \dfrac{\partial C_1^{(s5)}}{\partial t} = \lambda_4 C_1^{(s4)} C_0^{(1)} \left(1 - \beta\varepsilon C_1^{(s5)}\right) & C_1^{(s5)}\Big|_{t=x/U} = 0. \end{cases}} \tag{3.12}$$

Summarizing two equations in (3.12) gives

$$C_1^{(s4)} = Const_1 - C_1^{(s5)} \tag{3.13}$$

Using the initial conditions we obtain

$$Const_1 = \frac{C^{s4,0}}{\varepsilon} \tag{3.14}$$

Then (3.13) becomes

$$\boxed{C_1^{(s4)} = \frac{C^{s4,0}}{\varepsilon} - C_1^{(s5)}} \tag{3.15}$$

By substituting (3.15) into (3.12) we obtain a differential equation for $C_1^{(s5)}$

$$\begin{cases} \dfrac{\partial C_1^{(s5)}}{\partial t} = \lambda_4 C^{1*}\left(\dfrac{C^{s4,0}}{\varepsilon} - C_1^{(s5)}\right)\left(1-\beta\varepsilon C_1^{(s5)}\right) \\ C_1^{(s5)}\Big|_{t=x/U} = 0 \end{cases} \tag{3.16}$$

Equation (3.16) can be modified as

$$\begin{cases} \dfrac{\partial C_1^{(s5)}}{\partial t}\left[\dfrac{1}{\left(\dfrac{C^{s4,0}}{\varepsilon} - C_1^{(s5)}\right)\left(1-\beta\varepsilon C_1^{(s5)}\right)}\right] = \lambda_4 C^{1*} \\ C_1^{(s5)}\Big|_{t=x/U} = 0 \end{cases} \tag{3.17}$$

Further modification of equation (3.17)

$$\begin{cases} \dfrac{\partial C_1^{(s5)}}{\partial t}\left[\dfrac{1}{\left(1-\beta C^{s4,0}\right)\left(\dfrac{C^{s4,0}}{\varepsilon} - C_1^{(s5)}\right)} - \dfrac{\beta\varepsilon}{\left(1-\beta C^{s4,0}\right)\left(1-\beta\varepsilon C_1^{(s5)}\right)}\right] = \lambda_4 C^{1*} \\ C_1^{(s5)}\Big|_{t=x/U} = 0 \end{cases} \tag{3.18}$$

Integration yields:

$$\left(\frac{1}{1-\omega}\right)\ln\left(\frac{1-\beta\varepsilon C_1^{(s5)}}{\dfrac{C^{s4,0}}{\varepsilon} - C_1^{(s5)}}\right) = \lambda_4 C^{1*} t + Const_2 \tag{3.19}$$

where

$$\boxed{\omega = \beta C^{s4,0}} \tag{3.20}$$

Let us consider the case when $\omega = \beta C^{s4,0} \neq 1$. After using initial condition for $C_1^{(s5)}$ the integration constant will be:

$$Const_2 = -\left(\frac{1}{1-\omega}\right)\ln\left(\frac{C^{s4,0}}{\varepsilon}\right) - \lambda_4 C^{l*}\frac{x}{U} \tag{3.21}$$

Using expression (3.21) in equation (3.19), we obtain:

$$\left(\frac{1}{1-\omega}\right)\ln\left(\frac{1-\beta\varepsilon C_1^{(s5)}}{\frac{C^{s4,0}}{\varepsilon}-C_1^{(s5)}}\right) = \lambda_4 C^{l*}\left(t-\frac{x}{U}\right) - \left(\frac{1}{1-\omega}\right)\ln\left(\frac{C^{s4,0}}{\varepsilon}\right) \tag{3.22}$$

Thus, find $C_1^{(s5)}$

$$C_1^{(s5)} = \frac{C^{s4,0}}{\varepsilon}\left(\frac{e^{A\left(t-\frac{x}{U}\right)}-1}{e^{A\left(t-\frac{x}{U}\right)}-\omega}\right) = \frac{C^{s4,0}}{\varepsilon}\left(1-\frac{1-\omega}{e^{-\frac{A}{U}(x-Ut)}-\omega}\right) \tag{3.23}$$

where

$$\boxed{A = \lambda_4 C^{l*}(1-\omega)} \tag{3.24}$$

By introducing a new function $f(\eta)$ for simplicity,

$$\boxed{f(\eta) \equiv \frac{1-\omega}{e^{-\frac{A}{U}\eta}-\omega}} \tag{3.25}$$

We can write the solution for $C_1^{(s5)}$ in a simple form:

$$\boxed{\begin{cases} C_1^{(s5)} = 0, & t < x/U \\ C_1^{(s5)} = \dfrac{C^{s4,0}}{\varepsilon}\left(1-f(x-Ut)\right), & t \geq x/U \end{cases}} \tag{3.26}$$

From (3.15) and (3.26) for $C_1^{(s4)}$

$$\boxed{\begin{cases} C_1^{(s4)} = \dfrac{C^{s4,0}}{\varepsilon}, & t < x/U \\ C_1^{(s4)} = \dfrac{C^{s4,0}}{\varepsilon} f(x-Ut), & t \geq x/U \end{cases}} \tag{3.27}$$

Note that when $\boxed{\omega = 1}$,the solution of the system (3.6) becomes:

$$\begin{cases} C_1^{(s5)} = 0, & t < x/U \\ C_1^{(s5)} = \dfrac{C^{s4,0}}{\varepsilon}\left[1 - \dfrac{1}{-\lambda_4 \dfrac{C^{1*}}{U}(x - Ut) + 1}\right], & t \geq x/U \end{cases} \tag{3.28}$$

By defining a new function $f_{\omega=1}$ as $\boxed{f_{\omega=1}(\eta) \equiv \dfrac{1}{-\lambda_4 \dfrac{C^{1*}}{U}\eta + 1}}$,we can write (3.28)

$$\boxed{\begin{cases} C_1^{(s5)} = 0, & t < x/U \\ C_1^{(s5)} = \dfrac{C^{s4,0}}{\varepsilon}\left[1 - f_{\omega=1}(x - Ut)\right], & t \geq x/U \end{cases}} \tag{3.29}$$

Also, using the defined function $f_{\omega=1}$ in the following expression

$$\begin{cases} C_1^{(s4)} = \dfrac{C^{s4,0}}{\varepsilon}, & t < x/U \\ C_1^{(s4)} = \dfrac{C^{s4,0}}{\varepsilon}\left[\dfrac{1}{-\lambda_4 \dfrac{C^{1*}}{U}(x - Ut) + 1}\right], & t \geq x/U \end{cases} \tag{3.30}$$

we obtain

$$\boxed{\begin{cases} C_1^{(s4)} = \dfrac{C^{s4,0}}{\varepsilon}, & t < x/U \\ C_1^{(s4)} = \dfrac{C^{s4,0}}{\varepsilon}\left[f_{\omega=1}(x - Ut)\right], & t \geq x/U \end{cases}} \tag{3.30a}$$

3.6SOLUTION FOR OTHER VARIABLES OF THE FIRST-ORDER PROBLEM

Now, let us consider concentrations $C_1^{(s1)}$ and $C_1^{(s2)}$

From (3.7) and (3.28) for $t \geq x/U$:

$$\begin{cases} \dfrac{\partial C_1^{(s1)}}{\partial t} = -\lambda_1 C_1^{(s1)} \left(C^{1*}\right)^2 \left[\dfrac{(1-\omega) e^{-\frac{A}{U}(x-Ut)}}{e^{-\frac{A}{U}(x-Ut)} - \omega} \right], \\ C_1^{(s1)}\Big|_{t=\mathbf{x}/U} = \dfrac{C^{s1,0}}{\varepsilon} \end{cases} \tag{3.31}$$

or knowing that $1-\beta\varepsilon C_1^{(s5)} = 1-\omega+\omega f\left(x-Ut\right)$

$$\frac{\partial \ln\left(C_1^{(s1)}\right)}{\partial t} = -\lambda_1 \left(C^{1*}\right)^2 \left[\frac{(1-\omega) e^{-\frac{A}{U}(x-Ut)}}{e^{-\frac{A}{U}(x-Ut)} - \omega} \right]$$

The integration through the replacement of variables $z = e^{-\frac{A}{U}(x-Ut)} - \omega$ and using the initial condition yields:

$$\ln C_1^{(s1)} = \ln\left(\frac{C^{s1,0}}{\varepsilon} \frac{1}{(1-\omega)^{-\sigma_1}} \left(e^{-\frac{A}{U}(x-Ut)} - \omega \right)^{-\sigma_1} \right)$$

Then we obtain a formula for $C_1^{(s1)}$ which is

$$C_1^{(s1)} = \begin{cases} \dfrac{C^{(s1,0)}}{\varepsilon}, & t < x/U \\ \dfrac{C^{s1,0}}{\varepsilon} \left(\dfrac{1-\omega}{e^{-\frac{A}{U}(x-Ut)} - \omega} \right)^{\sigma_1}, & t \geq x/U \end{cases} \tag{3.32}$$

or, using defined function $f(\eta)$

$$C_1^{(s1)} = \begin{cases} \dfrac{C^{(s1,0)}}{\varepsilon}, & t < x/U \\ \dfrac{C^{s1,0}}{\varepsilon} \left[f\left(x-Ut\right) \right]^{\sigma_1}, & t \geq x/U \end{cases} \tag{3.33}$$

where

$$\boxed{\sigma_1 \equiv \frac{\lambda_1}{\lambda_4} C^{1*}} \tag{3.34}$$

For the case when $\omega = 1$:

$$\boxed{C_1^{(s1)} = \begin{cases} \dfrac{C^{(s1,0)}}{\varepsilon}, & t < x/U \\ \dfrac{C^{s1,0}}{\varepsilon} \left(\dfrac{1}{-\dfrac{\lambda_1 C^{1*}}{U}(x - Ut) + 1} \right)^{\sigma_1}, & t \geq x/U \end{cases}} \tag{3.35}$$

or, using $f_{\omega=1}$, obtain

$$\boxed{C_1^{(s1)} = \begin{cases} \dfrac{C^{(s1,0)}}{\varepsilon}, & t < x/U \\ \dfrac{C^{s1,0}}{\varepsilon} \left[f_{\omega=1}(x - Ut) \right]^{\sigma_1}, & t \geq x/U \end{cases}} \tag{3.36a}$$

Let us consider the equation for $C_1^{(s2)}$

$$\boxed{\begin{cases} \dfrac{\partial C_1^{(s2)}}{\partial t} = \left(\lambda_1 C_1^{(s1)} \left(C_0^{(1)} \right)^2 - \lambda_3 C_1^{(s2)} C_0^{(4)} \right) \left(1 - \beta \varepsilon C_1^{(s5)} \right) \\ C_1^{(s2)} \Big|_{t=0} = 0 \end{cases}} \tag{3.37}$$

This is a first order, non-homogeneous, linear equation which can be solved by the method of variation of constant.

The first step is to solve the homogeneous part of the equation (3.23) and the second is to solve an equation for variation constant.

Let us consider the homogeneous case of (3.37)

$$\frac{\partial C_1^{(s2)}}{\partial t} = -\lambda_3 C_1^{(s2)} C_0^{(4)} \left(1 - \beta \varepsilon C_1^{(s5)} \right) \tag{3.38}$$

or

$$\frac{\partial \ln\left(C_1^{(s2)}\right)}{\partial t} = -\lambda_3 C^{4*}\left[\frac{(1-\omega)e^{-\frac{A}{U}(x-Ut)}}{e^{-\frac{A}{U}(x-Ut)}-\omega}\right] \tag{3.39}$$

Solution procedure is similar to problem (3.31), after integrating (3.39) the integration constant is taken as a variable.

$$\boxed{C_1^{(s2)} = \left(e^{-\frac{A}{U}(x-Ut)}-\omega\right)^{-\sigma_2}\tilde{C}(t)} \tag{3.40}$$

$$\boxed{\sigma_2 = \frac{\lambda_3 C^{4*}}{\lambda_4 C^{1*}}} \tag{3.41}$$

After substituting (3.40) into (3.37) we obtain a first order differential equation for integration constant of homogeneous part of the problem (3.37).

$$\frac{\partial \tilde{C}(t)}{\partial t}\left(e^{-\frac{A}{U}(x-Ut)}-\omega\right)^{-\sigma_2} = \frac{\lambda_1\left(C^{1*}\right)^2 C^{s1,0}}{\varepsilon}\left(\frac{(\omega-1)}{e^{-\frac{A}{U}(x-Ut)}-\omega}\right)^{\sigma_1}\left(\frac{(\omega-1)e^{-\frac{A}{U}(x-Ut)}}{e^{-\frac{A}{U}(x-Ut)}-\omega}\right) \tag{3.42}$$

$$\frac{\partial \tilde{C}(t)}{\partial t} = \frac{\lambda_1\left(C^{1*}\right)^2 C^{s1,0}}{\varepsilon(\omega-1)^{-\sigma_2}} e^{-\frac{A}{U}(x-Ut)}\left(\frac{1-\omega}{e^{-\frac{A}{U}(x-Ut)}-\omega}\right)^{\sigma_1-\sigma_2+1} \tag{3.43}$$

and by continuing the simplification of the last expression, obtain

$$\frac{\partial \tilde{C}(t)}{\partial t} = \frac{\lambda_1\left(C^{1*}\right)^2 C^{s1,0}(\omega-1)^{\sigma_1+1}}{\varepsilon} e^{-\frac{A}{U}(x-Ut)}\left(e^{-\frac{A}{U}(x-Ut)}-\omega\right)^{\sigma_2-\sigma_1-1} \tag{3.44}$$

Integration of (3.44) yields

$$\tilde{C}(t) = \frac{\lambda_1 C^{1*} C^{s1,0}(\omega-1)^{\sigma_1}}{\lambda_4 \varepsilon(\sigma_2-\sigma_1)}\left(e^{-\frac{A}{U}(x-Ut)}-\omega\right)^{\sigma_2-\sigma_1} + Const \tag{3.45}$$

By substituting (3.45) into (3.40) and using the initial conditions we obtain

$$Const = -\frac{\lambda_1 C^{1*} C^{s1,0} (\omega - 1)^{\sigma_2}}{\lambda_4 \varepsilon (\sigma_2 - \sigma_1)}$$

Final result first order approximation will be

$$\boxed{C_1^{(s2)} = \frac{C^{s1,0}}{\varepsilon} \frac{\sigma_1}{(\sigma_2 - \sigma_1)} \left[\left(\frac{1-\omega}{e^{-\frac{A}{U}(x-Ut)} - \omega} \right)^{\sigma_1} - \left(\frac{1-\omega}{e^{-\frac{A}{U}(x-Ut)} - \omega} \right)^{\sigma_2} \right]} \quad (3.46)$$

further using the defined function

$$\boxed{C_1^{(s2)} = \frac{C^{s1,0}}{\varepsilon} \frac{\sigma_1}{(\sigma_2 - \sigma_1)} \left[(f(x-Ut))^{\sigma_1} - (f(x-Ut))^{\sigma_2} \right]} \quad (3.47)$$

With the same technique for the particular case when $\omega = 1$, we will obtain the following expression for $C_1^{(s2)}$

$$\boxed{\begin{cases} C_1^{(s2)} = 0, & t < x/U \\ C_1^{(s2)} = \frac{C^{s1,0}}{\varepsilon} \frac{\sigma_1}{(\sigma_2 - \sigma_1)} \left[\left(\frac{1}{-\frac{\lambda_1 C^{1*}}{U}(x-Ut)+1} \right)^{\sigma_1} - \left(\frac{1}{-\frac{\lambda_1 C^{1*}}{U}(x-Ut)+1} \right)^{\sigma_2} \right], & t \geq x/U \end{cases}} \quad (3.48)$$

or using $f_{\omega=1}$ in formula (3.48), we obtain

$$\boxed{\begin{cases} C_1^{(s2)} = 0, & t < x/U \\ C_1^{(s2)} = \frac{C^{s1,0}}{\varepsilon} \frac{\sigma_1}{(\sigma_2 - \sigma_1)} \left[(f_{\omega=1}(x-Ut))^{\sigma_1} - (f_{\omega=1}(x-Ut))^{\sigma_2} \right], & t \geq x/U \end{cases}} \quad (3.49)$$

There is the case for solution of $C_1^{(s2)}$ when $\sigma_2 = \sigma_1$. We can resolve the differential equation (3.37) for such particular case and will obtain:

$$\frac{\partial \ln\left(C_1^{(s2)}\right)}{\partial t} = -\lambda_3 C^{4*}\left[\frac{(1-\omega)e^{-\frac{A}{U}(x-Ut)}}{e^{-\frac{A}{U}(x-Ut)}-\omega}\right] \tag{3.50}$$

Solution procedure is similar to problem (3.39), after integration, the integration constant is taken as a variable.

$$\boxed{C_1^{(s2)} = \left(e^{-\frac{A}{U}(x-Ut)}-\omega\right)^{-\sigma_2}\tilde{C}(t)} \tag{3.51}$$

$$\boxed{\sigma_2 = \sigma_1} \tag{3.52}$$

After substituting (3.51) into (3.37) we obtain a first order differential equation for integration constant of homogeneous part of the problem (3.37).

$$\frac{\partial \tilde{C}(t)}{\partial t}\left(e^{-\frac{A}{U}(x-Ut)}-\omega\right)^{-\sigma_1} = \frac{\lambda_1\left(C^{1*}\right)^2 C^{s1,0}}{\varepsilon}\left(\frac{(\omega-1)}{e^{-\frac{A}{U}(x-Ut)}-\omega}\right)^{\sigma_1}\left(\frac{(\omega-1)e^{-\frac{A}{U}(x-Ut)}}{e^{-\frac{A}{U}(x-Ut)}-\omega}\right) \tag{3.53}$$

$$\frac{\partial \tilde{C}(t)}{\partial t} = \frac{\lambda_1\left(C^{1*}\right)^2 C^{s1,0}}{\varepsilon(\omega-1)^{-\sigma_1}} e^{-\frac{A}{U}(x-Ut)}\left(\frac{1-\omega}{e^{-\frac{A}{U}(x-Ut)}-\omega}\right) \tag{3.54}$$

further simplifying

$$\frac{\partial \tilde{C}(t)}{\partial t} = \frac{\lambda_1\left(C^{1*}\right)^2 C^{s1,0}(\omega-1)^{\sigma_1+1}}{\varepsilon}\left(\frac{e^{-\frac{A}{U}(x-Ut)}}{e^{-\frac{A}{U}(x-Ut)}-\omega}\right) \tag{3.55}$$

Integration of (3.55)gives

$$\tilde{C}(t) = \frac{\lambda_1 C^{1*} C^{s1,0}(\omega-1)^{\sigma_1}}{\lambda_4 \varepsilon}\ln\left(e^{-\frac{A}{U}(x-Ut)}-\omega\right) + Const \tag{3.56}$$

By substituting (3.56) into (3.51) and using the initial conditions we obtain

$$Const = -\frac{\lambda_1 C^{1*} C^{s1,0} (\omega - 1)^{\sigma_2}}{\lambda_4 \varepsilon} \ln(1-\omega)$$

The result is

$$C_1^{(s2)} = -\frac{C^{s1,0}}{\varepsilon} \sigma_1 (1-\omega)^{\sigma_1+1} \left[\frac{e^{-\frac{A}{U}(x-Ut)} - \omega}{1-\omega} \right] \ln\left(\frac{1-\omega}{e^{-\frac{A}{U}(x-Ut)} - \omega} \right) \tag{3.57}$$

or in terms of the defined function

$$C_1^{(s2)} = -\frac{C^{s1,0}}{\varepsilon} \frac{\sigma_1 (1-\omega)^{\sigma_1+1}}{f(x-Ut)} \ln\left(f(x-Ut)\right) \tag{3.58}$$

Solution (3.58) has a sub-particular case when $\omega = 1$

Solution for main species of liquid phase

$$\begin{cases} \dfrac{\partial C_1^{(2)}}{\partial t} + U \dfrac{\partial C_1^{(2)}}{\partial x} = \lambda_5 \left(2\lambda_1 C_1^{(s1)} \left(C^{1*} \right)^2 + \lambda_3 C_1^{(s2)} C^{4*} \right) \left(1 - \beta\varepsilon C_1^{(s5)} \right) \\ C_1^{(2)}\Big|_{t=0, x>0} = 0 \\ C_1^{(2)}\Big|_{x=0, t>0} = 0 \end{cases} \tag{3.59}$$

Solution of equation (3.59) will be:

$$C_1^{(2)} = \lambda_5 \left(2\lambda_1 C_1^{(s1)} \left(C_0^{(1)} \right)^2 + \lambda_3 C_1^{(s2)} C_0^{(4)} \right) \left(1 - \beta\varepsilon C_1^{(s5)} \right) \frac{x}{U} \tag{3.60}$$

or using defined function $f(\eta)$

$$C_1^{(2)} = \lambda_5 \frac{C_1^{s1,0}}{\varepsilon}\left[2\lambda_1\left(C^{1*}\right)^2\left(f\left(x-Ut\right)\right)^{\sigma_1} + \lambda_3 C^{4*}\frac{\sigma_1}{\sigma_2-\sigma_1}\left(\left(f\left(x-Ut\right)\right)^{\sigma_1} - \left(f\left(x-Ut\right)\right)^{\sigma_2}\right)\right]\times$$
$$\times\left[1-\omega+\omega f\left(x-Ut\right)\right]\frac{x}{U} \qquad (3.61)$$

I: $$\underbrace{UO_2}_{s1}\times\underbrace{2UO_3}+\underbrace{2H_2SO_4}_{1}=\underbrace{UO_2}_{s2}+\underbrace{2UO_2SO_4}_{2}+\underbrace{2H_2O}_{3}$$

II: $$\underbrace{2Fe(OH)_3}_{s3}+\underbrace{3H_2SO_4}_{1}=\underbrace{Fe_2(SO_4)_3}_{4}+\underbrace{6H_2O}_{3}$$

III: $$\underbrace{UO_2}_{s2}+\underbrace{Fe_2(SO_4)_3}_{4}=\underbrace{UO_2SO_4}_{2}+\underbrace{2FeSO_4}_{5}$$

IV: $$\underbrace{CaCO_3}_{s4}+\underbrace{H_2SO_4}_{1}=\underbrace{CaSO_4}_{s5}+\underbrace{H_2CO_3}_{6}$$

Solutions for the main components of the solid and liquid phases $(\omega\neq 1)$

Results of the problems (3.6) through (3.10) are shown in the following tables:

Table 3 – Analytical solution of system of equations (3.6-3.10)

$$C^{(s5)}=\begin{cases}0, & t<x/U\\ C^{s4,0}\left(1-f\left(x-Ut\right)\right), & t\geq x/U\end{cases}$$

$$C^{(s4)}=\begin{cases}C^{s4,0}, & t<x/U\\ C^{s4,0}f\left(x-Ut\right), & t\geq x/U\end{cases}$$

$$C^{(s1)}=\begin{cases}C^{(s1,0)}, & t<x/U\\ C^{(s1,0)}\left[f\left(x-Ut\right)\right]^{\sigma_1}, & t\geq x/U\end{cases}$$

$$C^{(s2)}=\begin{cases}0, & t<x/U\\ C^{s1,0}\dfrac{\sigma_1}{\left(\sigma_2-\sigma_1\right)}\left[\left(f\left(x-Ut\right)\right)^{\sigma_1}-\left(f\left(x-Ut\right)\right)^{\sigma_2}\right], & t\geq x/U\end{cases}$$

$$C^{(2)}=\begin{cases}0, & t<x/U\\ \lambda_5C^{s1,0}\left[2\lambda_1\left(C^{1*}\right)^2\left(f\left(x-Ut\right)\right)^{\sigma_1}+\lambda_3C^{4*}\dfrac{\sigma_1}{\sigma_2-\sigma_1}\left(\left(f\left(x-Ut\right)\right)^{\sigma_1}-\left(f\left(x-Ut\right)\right)^{\sigma_2}\right)\right]\times & \\ \times\left[1-\omega+\omega f\left(x-Ut\right)\right]\dfrac{x}{U}, & t\geq x/U\end{cases}$$

Where	$\omega=\beta C^{s4,0}$ $A=\lambda_4C^{1*}\left(1-\omega\right)$	$f\left(\eta\right)=\dfrac{1-\omega}{e^{-\frac{A}{U}\eta}-\omega}$	$\sigma_1=\dfrac{\lambda_1}{\lambda_4}C^{1*}$	$\sigma_2=\dfrac{\lambda_3C^{4*}}{\lambda_4C^{1*}}$

I: $\underbrace{UO_2}_{s1} \times 2\underbrace{UO_3} + \underbrace{2H_2SO_4} = \underbrace{UO_2}_{s2} + \underbrace{2UO_2SO_4}_{2} + \underbrace{2H_2O}_{3}$

II: $\underbrace{2Fe(OH)_3}_{s3} + \underbrace{3H_2SO_4}_{1} = \underbrace{Fe_2(SO_4)_3}_{4} + \underbrace{6H_2O}_{3}$

III: $\underbrace{UO_2}_{s2} + \underbrace{Fe_2(SO_4)_3}_{4} = \underbrace{UO_2SO_4}_{2} + \underbrace{2FeSO_4}_{5}$

IV: $\underbrace{CaCO_3}_{s4} + \underbrace{H_2SO_4}_{1} = \underbrace{CaSO_4}_{s5} + \underbrace{H_2CO_3}_{6}$

Solutions for the main components of the solid and liquid phases $(\omega = 1)$

Table 4 – Analytical solution of system of equations (3.6 - 3.10) for $\omega = 1$.

$$C^{(s5)} = \begin{cases} 0, & t < x/U \\ C^{s4,0}\left[1 - f_{\omega=1}(x - Ut)\right], & t \geq x/U \end{cases}$$

$$C^{(s4)} = \begin{cases} C^{s4,0}, & t < x/U \\ C^{s4,0}\left[f_{\omega=1}(x - Ut)\right], & t \geq x/U \end{cases}$$

$$C^{(s1)} = \begin{cases} C^{(s1,0)}, & t < x/U \\ C^{(s1,0)}\left[f_{\omega=1}(x - Ut)\right]^{\sigma_1}, & t \geq x/U \end{cases}$$

$$C^{(s2)} = \begin{cases} 0, & t < x/U \\ C^{s1,0}\dfrac{\sigma_1}{(\sigma_2 - \sigma_1)}\left[\left(f_{\omega=1}(x - Ut)\right)^{\sigma_1} - \left(f_{\omega=1}(x - Ut)\right)^{\sigma_2}\right], & t \geq x/U \end{cases}$$

$$C^{(2)} = \begin{cases} 0, & t < x/U \\ \lambda_5 C^{s1,0}\left[2\lambda_1\left(C^{1*}\right)^2\left(f_{\omega=1}(x - Ut)\right)^{\sigma_1} + \lambda_3 C^{4*}\dfrac{\sigma_1}{\sigma_2 - \sigma_1}\left(\left(f_{\omega=1}(x - Ut)\right)^{\sigma_1} - \left(f_{\omega=1}(x - Ut)\right)^{\sigma_2}\right)\right] \times \\ \quad \times\left[f_{\omega=1}(x - Ut)\right]\dfrac{x}{U}, & t \geq x/U \end{cases}$$

Where	$f_{\omega=1}(\eta) \equiv \dfrac{1}{-\lambda_4 \dfrac{C^{1*}}{U}\eta + 1}$	$\sigma_1 = \dfrac{\lambda_1}{\lambda_4} C^{1*}$	$\sigma_2 = \dfrac{\lambda_3 C^{4*}}{\lambda_4 C^{1*}}$

The results of analytical solution for evolution of calcium carbonate $CaCO_3$ (Figure6), calcium sulfate $CaSO_4$ (Figure 7), uranium dioxide UO_2 (Figure 8), uraninite-$UO_2X_2UO_3$ (Figure 9) and dissolved useful component UO_2SO_4 (Figure 10) are obtained for different time steps. Curves on right hand side correspond to concentrations at different time.

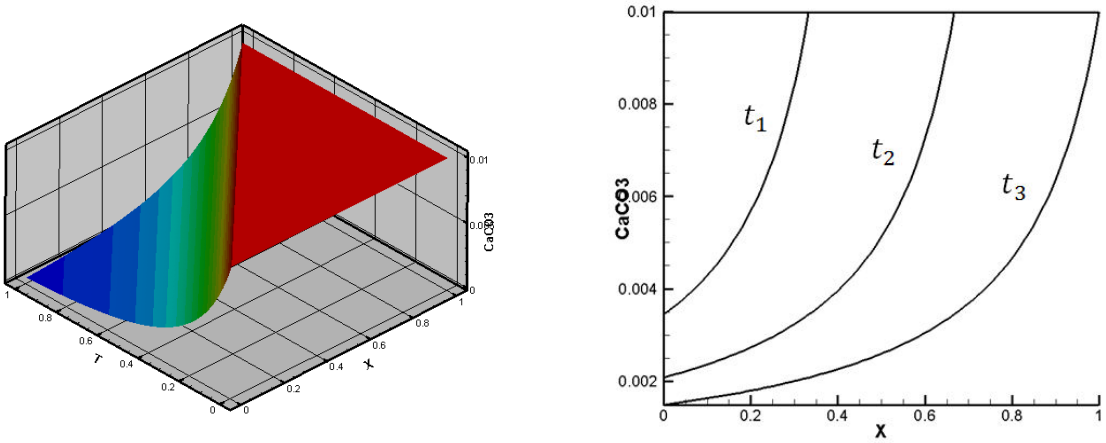

Figure6 - Evolution over time (T) of$CaCO_3$against distance (x) to the injector (dimensionless formulation)

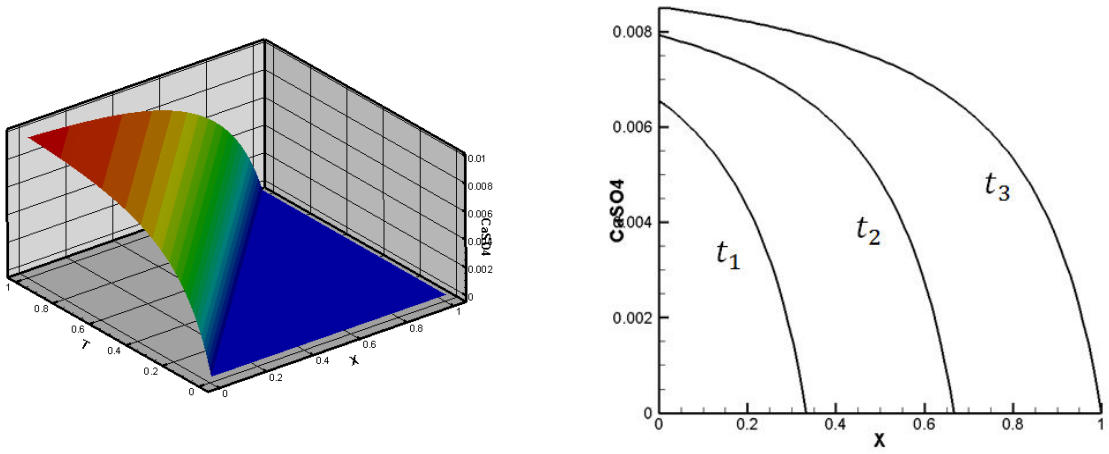

Figure 7 - Evolution over time (T) of$CaSO_4$against distance (x) to the injector (dimensionless formulation)

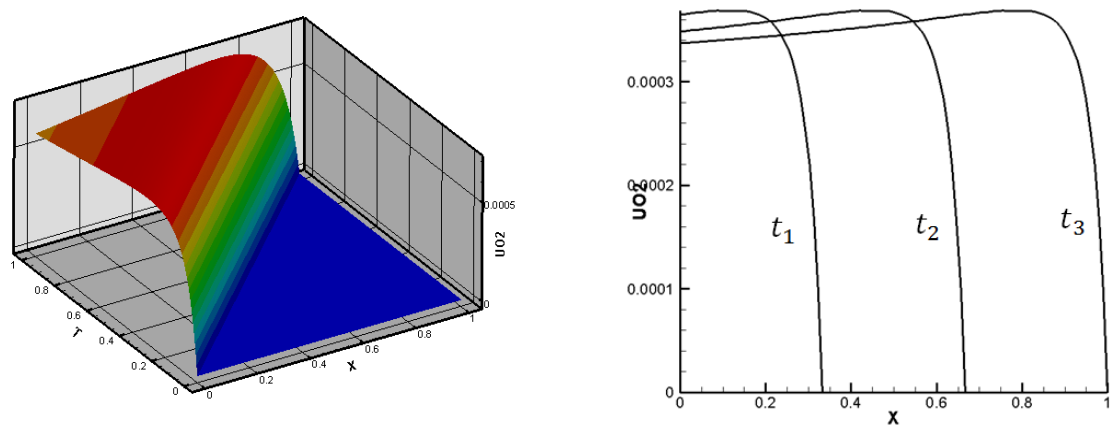

Figure 8Evolution over time (T) ofUO_2against distance (x) to the injector (dimensionless formulation)

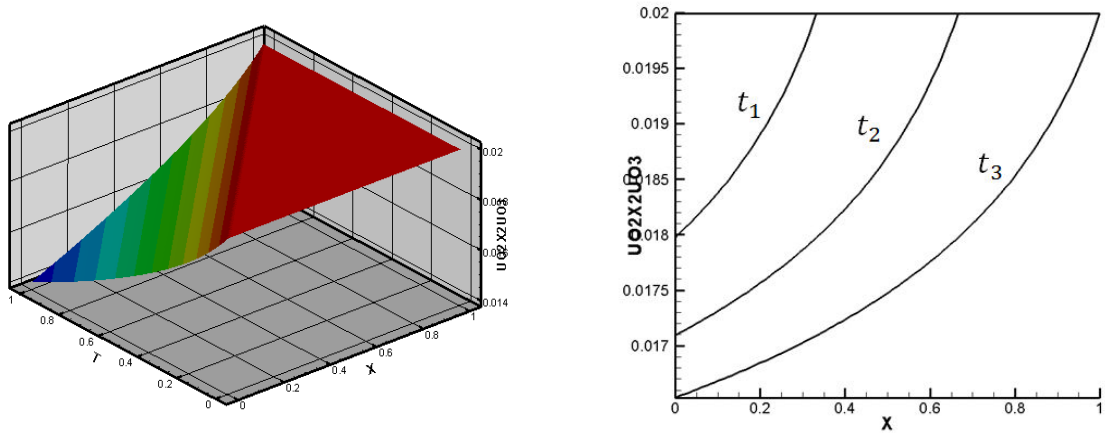

Figure 9 - Evolution over time (T) of uraninite (UO_2x2UO_3) against distance (x) to the injector (dimensionless formulation)

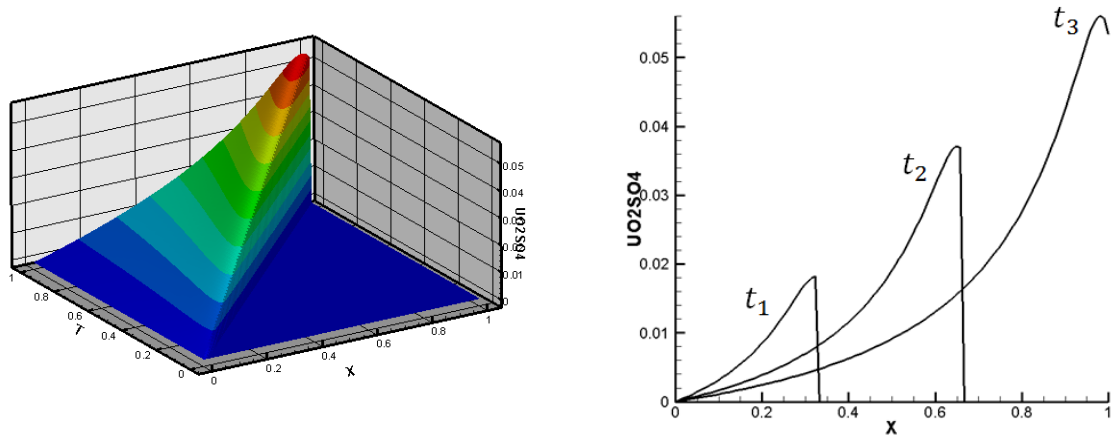

Figure 10 - Evolution over time (T) ofUO_2SO_4against distance (x) to the injector (dimensionless formulation)

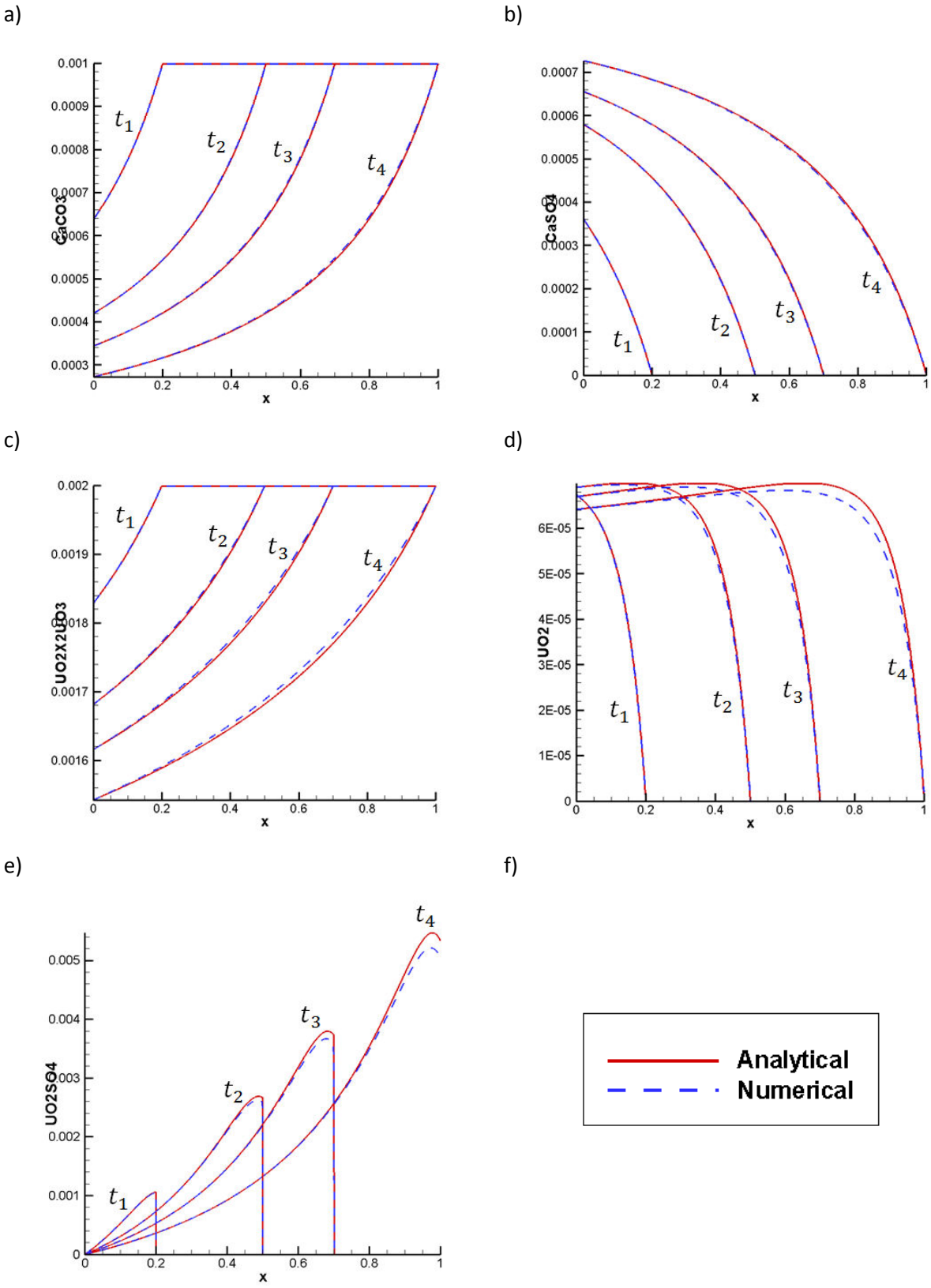

Figure 11 - Comparison with numerical solutions for:

a)$CaCO_3$; b)$CaSO_4$; c)UO_2X2UO_3; d)UO_2; e) UO_2SO_4.

Curves are correspond to concentrations at different times $t = t_1, t_2, t_3, t_4$

Comparison of analytical solution with numerical solutions for calcium carbonate*CaCO₃* (a), calcium sulfate *CaSO₄* (b), uraninite*UO₂ x 2UO₃* (c), uranium dioxide *UO₂* (d), dissolved useful component *UO₂SO₄* (e) are shown at Figure 11 where a solid line represents analytical results and a dotted line - numerical results. Curves correspond to concentrations at different times.

Extraction degree strongly depends on passivation rate $\omega = \beta C^{s4,0}$ (Figure 12). Figure 13 demonstrates dependence of extraction degree on passivation rates. It can be seen that extraction reduces with decreased passivation rate.

Dependence of the reactive surface $\sigma / \sigma_0 = (1 - \beta C^{(s5)})$ on passivation rate $\omega = \beta C^{s4,0}$ (at the fixed point by time and space) is presented on Figure 14.

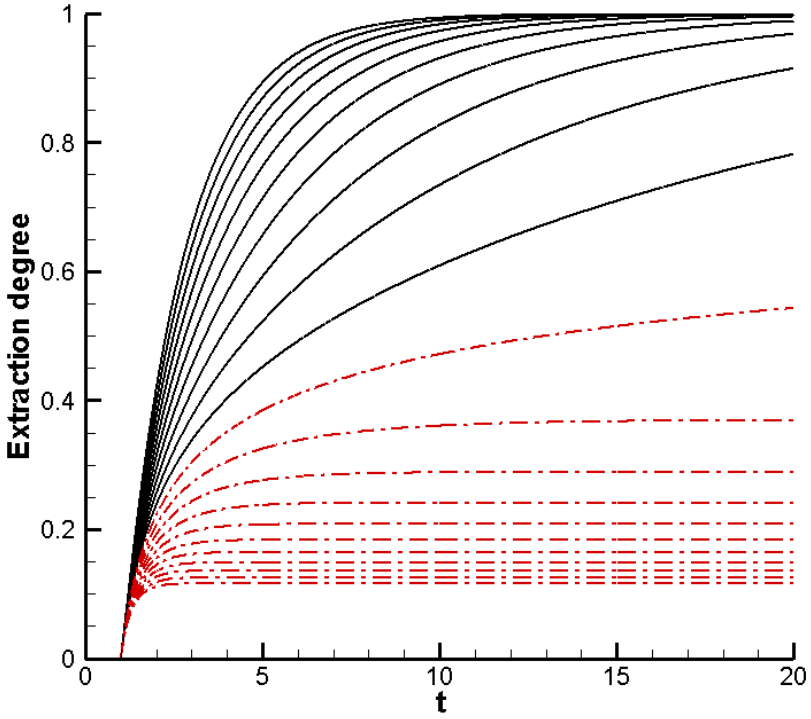

Figure 12 - Extraction degree for various values of $\omega = \beta C^{s4,0}$

$\omega \in [0;1) \quad step = 0.1,$

$\omega \in [1;2] \quad step = 0.1$

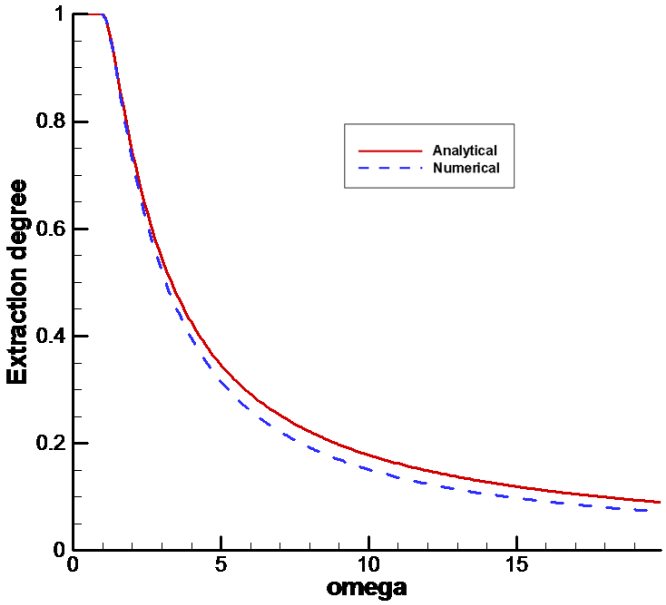

Figure 13 - Dependence of extraction degree on passivation rate $\omega = \beta C^{s4,0}$

(at the infinite integration time)

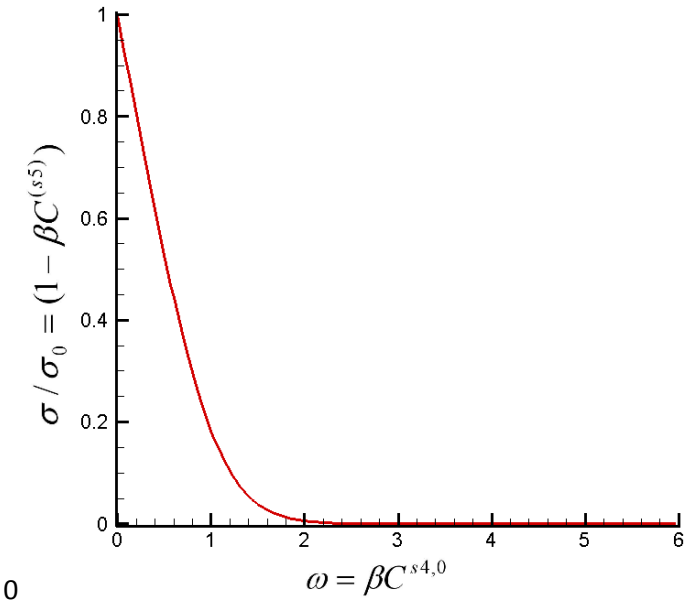

0

Figure 14 - Dependence of the reactive surface $\sigma / \sigma_0 = (1 - \beta C^{(s5)})$ on passivation rate $\omega = \beta C^{s4,0}$

(at the fixed point by time and space)

4 3D REACTIVE TRANSPORT STREAMLINE SIMULATOR

4.1 INTRODUCTION

A mathematical model for simulating the in-situ leaching method which accounts for reaction slow-down (passivation) was developed according to chemical kinetics theory developed in the previous chapters. The model consists of 13 equations including the Darcy's law, the mass balance equation, and 11 transport equations for chemical components in solid and liquid phase. These coupled equations have to be solved simultaneously in the 3D domain, accounting from boundary conditions. Numerical solution of this system of partial differential equations by finite difference or finite element methods requires powerful computing resources. An approximated solution of the systems can be found using a streamline technology that by essence divides3D problems into multiple one-dimensional ones (Blunt et al. 1996 [8], Oladyshkin, Royer and Panfilov 2008 [48]).

Streamline flow simulation has been used in oil industry since the 1950's. The interest in this method has reappeared in the last two decades (Blunt et al. 1996[8], Bratvedt et al. 1996[9]). Significant contribution to the development of streamline-based flow simulation method was made by scientists, such as, Pollock 1988 [56], Datta-Gupta and King 2007 [19], Bratvedt et al. 1996 [9], Batycky 1997 [3], Blunt et al. 1996 [8] and others.

Streamline simulation is based on the concept of time of flight, i.e. the time necessary to go from one point to the other along a trajectory. In case of steady state flow, the stream lines correspond to the trajectories of a particle flown by a given velocity field, strictly speaking it is tangent curve to the velocity field (or the normal to the iso-potential surfaces). It is usually built using a meshed grid (regular or irregular) on which the velocity is stored. Knowing the entry point in a given cell, the Pollock's algorithm gives the particle travel time through the cell together with the out point on the leaving face of the cell. The sum of times of flight on the cells crossed by the particle gives the overall traveling time of the particle.

In the problems investigated in this work, only the steady-state case is considered [i.e. main flow characteristics (hydraulic head, velocity field etc.] are constant over time); this is the most convenient case because the simulation is easier. In principle, there is no restriction to extend streamline simulations to transient flows, but it is necessary to remap the streamline solutions on the 3D grid at each step, re-estimate the velocity field, re-build the streamlines, and solve the transport equation for species again; and back and forth. This introduces inaccuracy in the solution compared to the classical 3D full resolution. It can be considered as one of its weaknesses of the streamline approach compared to conventional finite-difference methods. All advantages and disadvantages of the streamline approach will not be discussed here, but it should be mentioned and always kept in mind that significant errors can be introduced when mapping the

solutions form the x, y and z coordinates system to the time of flight coordinates, and vice versa (flows with strong feedback require this kind of procedure).

According to the assumptions made, the use of the streamline simulation for solving the mathematical model describing the leaching process, involves the following basic steps:

1. Solve the hydraulic head equation on an Eulerian grid and define the velocity field;
2. Trace the streamlines on the basis of the resulting velocity field;
3. Compute particle travel time or time of flight along the streamlines;
4. Solve the transport equations (concentrations) along the streamlines. The transport calculations are performed in the time-of-flight coordinate, effectively decoupling heterogeneity effects and significantly simplifying calculations;
5. If the conditions of main flow changed (flow rates of wells are changed, new wells integrated to the existing system etc.), then map the 1D solutions calculated along the streamlines onto the initial finite-difference grid and repeat all of the above steps from the beginning till the integration time is reached.

4.2 MATHEMATICAL MODEL

In chapter 2 the transport model of leaching solute species and dissolution of solid components in layer was developed taking into account the slow downs (passivation) of reactions due to precipitation of gypsum. Let us rewrite the system of partial differential equations describing the transport of species in the three-dimensional groundwater system which accounts for reaction passivation (2.18), (2.19):

$$div\vec{U}\phi = 0 \qquad \vec{U}\phi = -Kgrad(h) \tag{4.1a}$$

$$\frac{\partial C^{(s1)}}{\partial t} = -\frac{k_I}{(1-\phi)\rho_s} C^{(s1)} \left(C^{(1)}\right)^2 \left(1-\beta C^{(s5)}\right) \tag{4.1b}$$

$$\frac{\partial C^{(s2)}}{\partial t} = \frac{1}{(1-\phi)\rho_s} \left(k_I C^{(s1)} \left(C^{(1)}\right)^2 - k_{III} C^{(s2)} C^{(4)} \right) \left(1-\beta C^{(s5)}\right) \tag{4.1c}$$

$$\frac{\partial C^{(s3)}}{\partial t} = -\frac{2k_{II}}{(1-\phi)\rho_s} \left(C^{(s3)}\right)^2 \left(C^{(1)}\right)^3 \left(1-\beta C^{(s5)}\right) \tag{4.1d}$$

$$\frac{\partial C^{(s4)}}{\partial t} = -\frac{k_{IV}}{(1-\phi)\rho_s} C^{(s4)} C^{(1)} \left(1-\beta C^{(s5)}\right) \tag{4.1e}$$

$$\frac{\partial C^{(s5)}}{\partial t} = \frac{k_{IV}}{(1-\phi)\rho_s} C^{(s4)} C^{(1)} \left(1 - \beta C^{(s5)}\right) \tag{4.1f}$$

$$\frac{\partial C^{(1)}}{\partial t} + \vec{U} grad C^{(1)} = div\left(D^{(1)} grad C^{(1)}\right) + \\ + \frac{1}{\phi\rho_l}\left(-2k_I C^{s1}\left(C^{(1)}\right)^2 - 3k_{II}\left(C^{(s3)}\right)^2\left(C^{(1)}\right)^3 - k_{IV} C^{(s4)} C^{(1)}\right)\left(1 - \beta C^{(s5)}\right) \tag{4.1g}$$

$$\frac{\partial C^{(4)}}{\partial t} + \vec{U} grad C^{(4)} = div D^{(4)} grad C^{(4)} + \\ + \frac{1}{\phi\rho_l}\left(k_{II}\left(C^{(s3)}\right)^2\left(C^{(1)}\right)^3 - k_{III} C^{(s2)} C^{(4)}\right)\left(1 - \beta C^{(s5)}\right) \tag{4.1h}$$

$$\frac{\partial C^{(2)}}{\partial t} + \vec{U} grad C^{(2)} = div D^{(2)} grad C^{(2)} + \\ + \frac{1}{\phi\rho_l}\left(2k_I C^{s1}\left(C^{(1)}\right)^2 + k_{III} C^{(s2)} C^{(4)}\right)\left(1 - \beta C^{(s5)}\right) \tag{4.1i}$$

$$\frac{\partial C^{(3)}}{\partial t} + \vec{U} grad C^{(3)} = div D^{(3)} grad C^{(3)} + \\ + \frac{1}{\phi\rho_l}\left(2k_I C^{s1}\left(C^{(1)}\right)^2 + 6k_{II}\left(C^{(s3)}\right)^2\left(C^{(1)}\right)^3\right)(1 - \beta C^{(s5)}) \tag{4.1j}$$

$$\frac{\partial C^{(5)}}{\partial t} + \vec{U} grad C^{(5)} = div D^{(5)} grad C^{(5)} + \frac{2k_{III}}{\phi\rho_l} C^{(s2)} C^{(4)} \left(1 - \beta C^{(s5)}\right) \tag{4.1k}$$

$$\frac{\partial C^{(6)}}{\partial t} + \vec{U} grad C^{(6)} = div D^{(6)} grad C^{(6)} + \frac{k_{IV}}{\phi\rho_l} C^{(s4)} C^{(1)} \left(1 - \beta C^{(s5)}\right) \tag{4.1m}$$

In practice, the mining industry used only two types of wells arrangements (linear and hexagonal patterns) for implementing the ISL technology (www.kazatomprom.kz2013 [64], Brovin and Grabovnikov 1997[10]).For uranium exploitation, the distances between wells are usually about 40 to 50 m in a mining block; they are displayed according to hexagonal patterns, about 10-15 hexagonal cells cover the mining block. Let us consider only a part of an exploited block with injection and production wells assumed symmetry boundary conditions. In addition, the diffusion of species is neglected due to short distance between the wells (Figure 15).

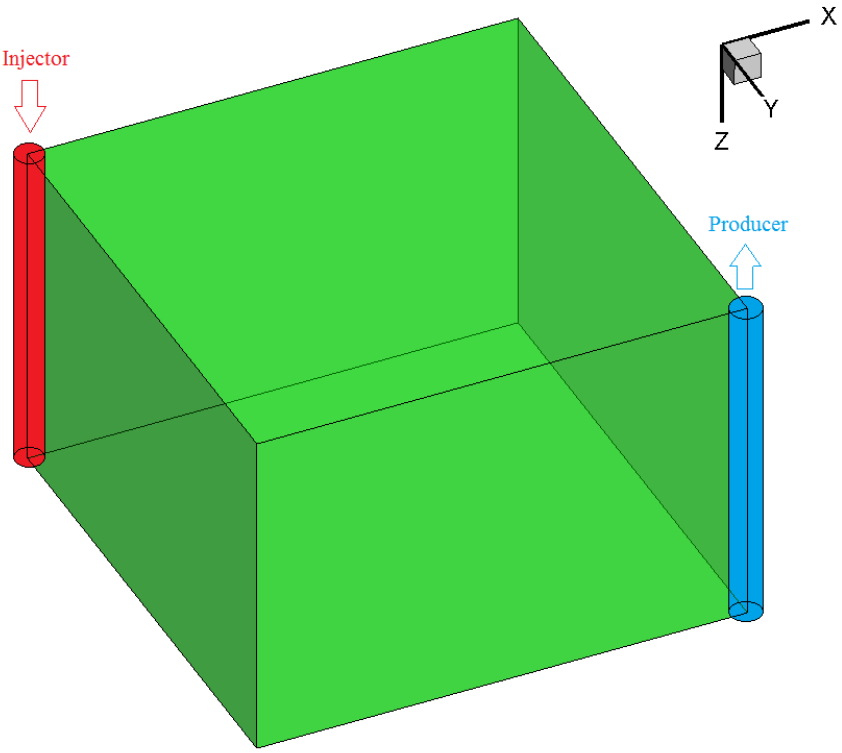

Figure 15 - Calculation domain

4.3 SOLUTION OF PRESSURE EQUATION AND DETERMINING OF THE VELOCITY FIELD

As discussed previously, uranium deposits are exploited using injection and production wells. Leaching solution containing sulfuric acid is injected into the ore laying zone and pumped back to the surface by production wells. During this process, the sulfuric acid reacts with uranium oxides and dissolves them. Dissolved uranium oxides become mobile and start getting transported to the surface by main flow through the system of wells.

The equations (4.1a) are the mass balance equation and the Darcy's Law. By substituting the Darcy's Law in to the balance equation we will obtain the following hydraulic head equation.

$$div(K\ grad(h)) = 0\,, \tag{4.2}$$

where *K* is the diagonal hydraulic conductivity tensor (written in its main components). The values of the hydraulic conductivity tensor depend on the choice of the coordinates system *x, y, z*. In case of natural stratified porous media (transverse isotropic media), the permeability tensor is isotropic along the planes of the strata along which the permeability is maximum, an anisotropic along the direction perpendicular to the strata corresponding to lower permeability. In this case, the diagonalization of the permeability tensor can be performed by choosing one direction of the main tensor axes, *z* for example, perpendicularly to the stratification planes, and the two others, *x* and *y,* in any directions along the stratification plane, it comes:

$$K_{xx} = K_{yy} = K_h \quad ; \quad K_{zz} = K_v \text{, and } \quad K_{yx} = K_{xz} = K_{yx} = K_{yz} = K_{zx} = K_{zy} = 0 .$$

For the isotropic case, it simplifies into:

$$K_{xx} = K_{yy} = K_{zz} = K \text{, and } \quad K_{yx} = K_{xz} = K_{yx} = K_{yz} = K_{zx} = K_{zy} = 0 .$$

It is assumed that the medium is isotropic. This last assumption is incorporated in most commonly used finite-difference groundwater flow models (Zheng and Wang 1999 [67]).

Equation (4.2) describes the main three-dimensional groundwater flow. Injected or produced flow rates at well location can be represented as point sink/source terms in the conservation equation. The fluid sink/source terms describe the solute mass entering the domain through sources, or solute mass leaving the domain through sinks. In case of 3D classical finite difference approach the concentrations of source/sink species have to be specified at the source/sink points (i.e at the wells). When using the streamline approach, as shown in the next section, the composition of the injected fluid is only needed to be imposed as a boundary condition to 1D transport equations along each streamline, the main flow equation for the hydraulic head is then related to the transport equations through the velocity field.

Let us rewrite (4.2) using point source/sink terms to represent the injection and production wells:

$$div(K\ grad\ (h)) = \sum_{m=1}^{M} Q_{inj}^{k} \delta(\vec{r} - \vec{r}_{inj}^{k}) + \sum_{l=1}^{L} Q_{pr}^{l} \delta(\vec{r} - \vec{r}_{pr}^{l}) \qquad (4.3)$$

where

$Q_{inj}^{k},\ Q_{pr}^{l}$ - is the volumetric flow rate per unit volume of aquifer representing fluid sources (positive) and sinks (negative).

δ - Dirac delta function,

M, L - number of injection and production wells, respectively.

For two wells (one injector and one producer), the equation (4.3) could be rewritten as

$$\frac{\partial}{\partial x}\left(K\frac{\partial h}{\partial x}\right)+\frac{\partial}{\partial y}\left(K\frac{\partial h}{\partial y}\right)+\frac{\partial}{\partial z}\left(K\frac{\partial h}{\partial z}\right)=Q_{inj}\delta(\vec{r}-\vec{r}_{inj})+Q_{pr}\delta(\vec{r}-\vec{r}_{pr})\,. \qquad (4.4)$$

Generally equation (4.4) is nonlinear because of aquifer heterogeneity or anisotropy, and it is solved by an iterative alternately-triangular method. Calculations are implemented on ex-centered grid: hydraulic head is calculated at the cell center, while the velocity at the face center (Figure 16)(Chung 2006[15]).The numerical scheme for the 3D case is illustrated in Figure 17.

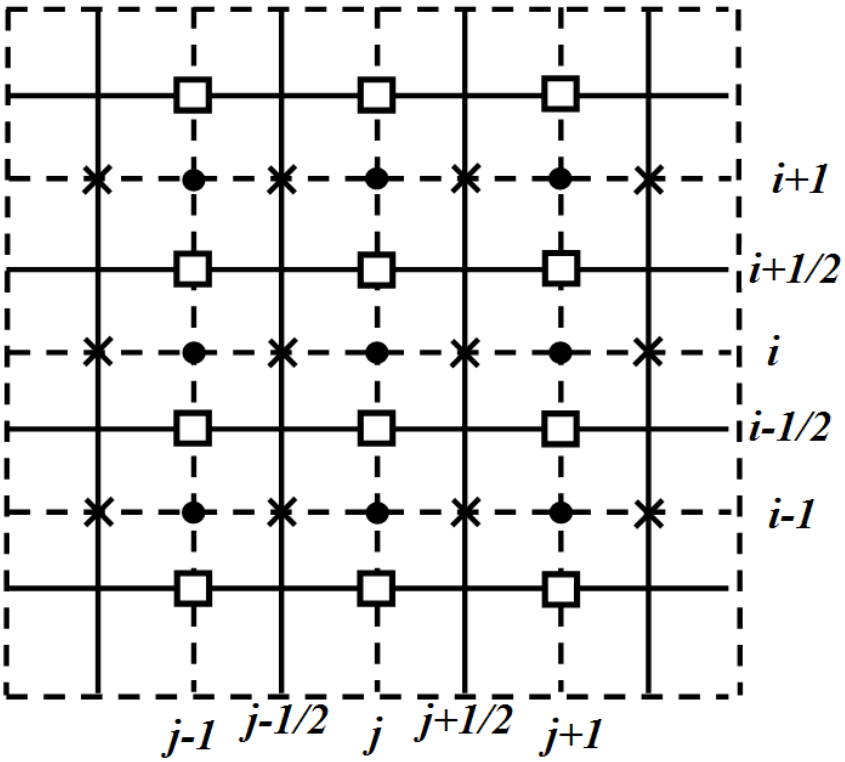

● - node for the calculation of hydraulic head and other scalar variables

× - node for the calculation of longitudinal velocity components

□ - node for the calculation transversal velocity components

Figure 16 - The scheme of numerical excentered grid in 2D

Calculation on excentered grid allows obtaining velocity components with the second order accuracy from Darsy's law using values of head pressure in two neighbor nodes and naturally approximate the equations in the divergent form.

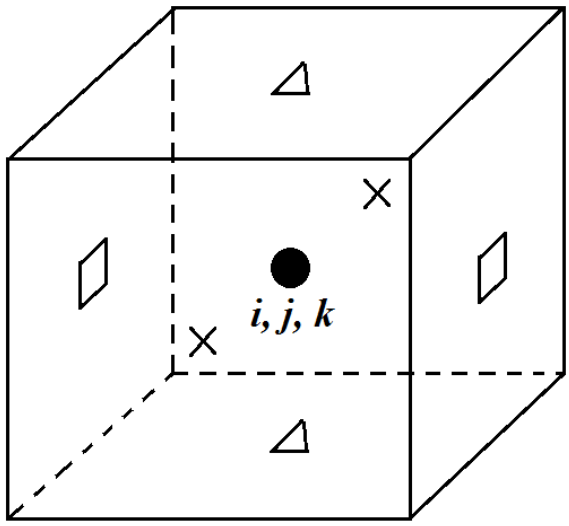

● - node for the calculation of the head pressure and other scalar variables

× - node for the calculation of the component of the velocity along the x axe

□ - node for the calculation of the component of velocity vector along the y axe

△ - node for the calculation of the component of velocity vector along the z axe

Figure 17 - The scheme of numerical excentered grid in 3D

Equation (4.4) is solved by the iterative method. The errors at each step of the iterative method are corrected in the subsequent step, thus round-off errors are usually not a concern (Chung 2006[15]). The iterations are stopped when the difference between solutions on all grid nodes for two consecutive steps is less than a given tolerance ε.

$$\left|h_{ijk}^{l+1} - h_{ijk}^{l}\right| \prec \varepsilon ,$$

Where ε is the permissible error on hydraulic head values.

The velocity field is determined from the Darcy's law using defined values for the hydraulic head. Velocity components are calculated on the cells faces (Figure 17) and determined with second order accuracy

$$u_{i+1/2\,jk} = -K_{i+1/2\,jk}\frac{h_{i+1\,jk} - h_{ijk}}{\Delta x},$$

$$v_{ij+1/2k} = -K_{ij+1/2k}\frac{h_{ij+1k} - h_{ijk}}{\Delta y}, \qquad (4.5)$$

$$w_{ijk+1/2} = -K_{ijk+1/2}\frac{h_{ijk+1} - h_{ijk}}{\Delta z}.$$

Defined velocity field will be used for determining the streamline paths and the times of flight.

4.4 TRACING STREAMLINES IN A 3D DOMAIN

For tracing the streamline from injector to producers we use the Pollock's 3D tracing method through a Cartesian cell grid (Figure 18). Pollock's method is simple, analytical, and is formulated in terms of time-of-flight (TOF). To apply Pollock's method to any cell, the total flux in and out of each boundary is calculated using the Darcy's Law. With the flux known the algorithm centers on determining the exit point of a streamline and the time to exit a given entry point assuming a piece-wise linear approximation of the velocity field in each coordinate direction.

$$v_x = v_{x0} + g_x(x - x_0), \qquad g_x = \frac{v_{x+\Delta x} - v_{x0}}{\Delta x}$$

where v_{x0} is x-velocity at x=x_0 and g_x is velocity gradient in x-direction. Since $v_x = dx/dt$ we can integrate the expression of x-velocity (and in analogous fashion in y- and z- direction) to get exit times out of each face given an arbitrary entry point (x_i, y_i, z_i)

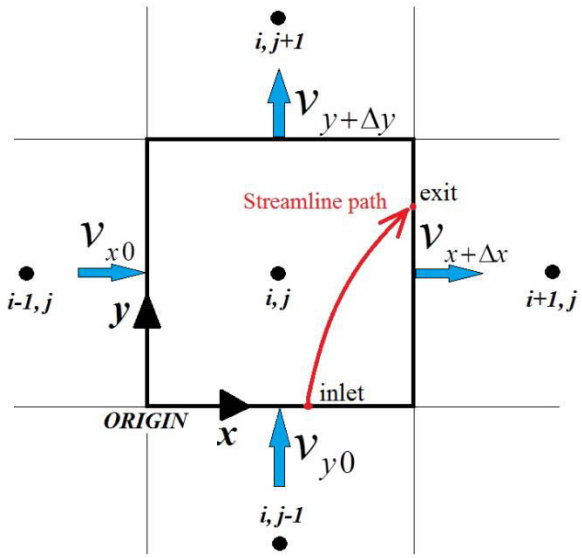

Figure 18- Pollock's 3D tracing method through a Cartesian cell. Given an arbitrary entry point, the time to exit and the exit point can be determined analytically (from Batycky et al. 1997[92])

$$\Delta t_x = \frac{1}{g_x}\ln\left(\frac{v_{x0}+g_x(x_e-x_0)}{v_{x0}+g_x(x_i-x_0)}\right)$$

$$\Delta t_y = \frac{1}{g_y}\ln\left(\frac{v_{y0}+g_y(y_e-y_0)}{v_{y0}+g_y(y_i-y_0)}\right) \tag{4.6}$$

$$\Delta t_z = \frac{1}{g_z}\ln\left(\frac{v_{z0}+g_z(z_e-z_0)}{v_{z0}+g_z(z_i-z_0)}\right)$$

where $(x_e,\ y_e,\ z_e)$ are the exit coordinates. Since the streamline must exit from the face having the smallest travel time $\Delta t_{\min} = \min(\Delta t_x, \Delta t_y, \Delta t_z)$, the exit locations are easily calculated by re-solving for $(x_e,\ y_e,\ z_e)$ using the minimum time:

$$x_e = \frac{1}{g_x}\ln\left[v_{xi}\exp(g_x\Delta t_{\min})-v_{x0}\right]+x_0$$

$$y_e = \frac{1}{g_y}\ln\left[v_{yi}\exp(g_y\Delta t_{\min})-v_{y0}\right]+y_0 \tag{4.7}$$

$$z_e = \frac{1}{g_z}\ln\left[v_{zi}\exp(g_z\Delta t_{\min})-v_{z0}\right]+z_0$$

4.5 THE TIME-OF-FLIGHT

The time-of-flight (TOF) is the time required to reach a given distance *s* along the streamline based on the velocity field along the streamline. The TOF concept has been used in the ground water literature for some time as a method for calculating the capture radii of well [63]. More recently Datta-Gupta and King 2007 [19] used the TOF concept for modeling flow in oil reservoirs. Mathematically, the time-of-flight τ is defined as

$$\tau(s) = \int_0^s \frac{\phi(\zeta)}{\left|\vec{U}(\zeta)\right|}d\zeta. \tag{4.8}$$

where $\phi(\zeta)$ is the porosity at location ζ, $\left|\vec{U}(\zeta)\right|$ is the velocity magnitude at location ζ.

The above integral is evaluated analytically using (4.6) such that

$$\tau = \sum_{i=1}^{N_{blocks}} \Delta t_{e,i} \tag{4.9}$$

where $\Delta t_{e,i}$ is the calculated incremental time-of-flight through grid block *i*.

4.6 SOLUTION OF THE TRANSPORT EQUATION ALONG STREAMLINE AND MAPPING 1D SOLUTION TO A STREAMLINE

Blunt et al. 1996 [8] outlined the following coordinate transform by first rewriting equation (4.8) as

$$\frac{\partial \tau}{\partial s} = \frac{\phi}{\left|\vec{U}\right|} \quad \Leftrightarrow \quad \left|\vec{U}\right| \frac{\partial}{\partial s} = \phi \frac{\partial}{\partial \tau} \tag{4.10}$$

which can be further rewritten as

$$\left|\vec{U}\right| \frac{\partial}{\partial s} \equiv \vec{U} \cdot \nabla = \phi \frac{\partial}{\partial \tau} \tag{4.10*}$$

Substitution (4.10*) into (4.1) gives

$$\frac{\partial C^{(s1)}}{\partial t} = -\frac{k_I}{(1-\phi)\rho_s} C^{(s1)} \left(C^{(1)}\right)^2 \left(1 - \beta C^{(s5)}\right) \tag{4.11a}$$

$$\frac{\partial C^{(s2)}}{\partial t} = \frac{1}{(1-\phi)\rho_s} \left(k_I C^{(s1)} \left(C^{(1)}\right)^2 - k_{III} C^{(s2)} C^{(4)} \right) \left(1 - \beta C^{(s5)}\right) \tag{4.11b}$$

$$\frac{\partial C^{(s3)}}{\partial t} = -\frac{2k_{II}}{(1-\phi)\rho_s} \left(C^{(s3)}\right)^2 \left(C^{(1)}\right)^3 \left(1 - \beta C^{(s5)}\right) \tag{4.11c}$$

$$\frac{\partial C^{(s4)}}{\partial t} = -\frac{k_{IV}}{(1-\phi)\rho_s} C^{(s4)} C^{(1)} \left(1 - \beta C^{(s5)}\right) \tag{4.11d}$$

$$\frac{\partial C^{(s5)}}{\partial t} = \frac{k_{IV}}{(1-\phi)\rho_s} C^{(s4)} C^{(1)} \left(1 - \beta C^{(s5)}\right) \tag{4.11e}$$

$$\frac{\partial C^{(1)}}{\partial t} + \phi \frac{\partial C^{(1)}}{\partial \tau} = \frac{1}{\phi \rho_l} \left(-2k_I \left(C^{(s1)}\right)^2 C^{(1)} - 3k_{II} \left(C^{(s3)}\right)^2 \left(C^{(1)}\right)^3 - k_{IV} C^{(s4)} C^{(1)} \right) \left(1 - \beta C^{(s5)}\right) \tag{4.11f}$$

$$\frac{\partial C^{(4)}}{\partial t} + \phi \frac{\partial C^{(4)}}{\partial \tau} = \frac{1}{\phi \rho_l} \left(k_{II} \left(C^{(s3)}\right)^2 \left(C^{(1)}\right)^3 - k_{III} C^{(s2)} C^{(4)} \right) \left(1 - \beta C^{(s5)}\right) \tag{4.11g}$$

$$\frac{\partial C^{(2)}}{\partial t} + \phi \frac{\partial C^{(2)}}{\partial \tau} = \frac{1}{\phi \rho_l} \left(2k_I \left(C^{(s1)}\right)^2 C^{(1)} + k_{III} C^{(s2)} C^{(4)} \right) \left(1 - \beta C^{(s5)}\right) \tag{4.11h}$$

$$\frac{\partial C^{(3)}}{\partial t} + \phi \frac{\partial C^{(3)}}{\partial \tau} = \frac{1}{\phi \rho_l} \left(2k_I \left(C^{(s1)}\right)^2 C^{(1)} + 6k_{II} \left(C^{(s3)}\right)^2 \left(C^{(1)}\right)^3 \right) (1 - \beta C^{(s5)}) \tag{4.11i}$$

$$\frac{\partial C^{(5)}}{\partial t} + \phi \frac{\partial C^{(5)}}{\partial \tau} = \frac{2k_{III}}{\phi \rho_l} C^{(s2)} C^{(4)} \left(1 - \beta C^{(s5)}\right) \tag{4.11j}$$

$$\frac{\partial C^{(6)}}{\partial t} + \phi \frac{\partial C^{(6)}}{\partial \tau} = \frac{k_{IV}}{\phi \rho_l} C^{(s4)} C^{(1)} \left(1 - \beta C^{(s5)}\right) \tag{4.11k}$$

The transport equations are solved along the stream lines using the time of flight instead

of the spatial coordinates. For discretization along the streamline a natural choice would be to select the $\Delta\tau$ intervals generated during the integration of the numerical velocity field as shown in Figure 19.

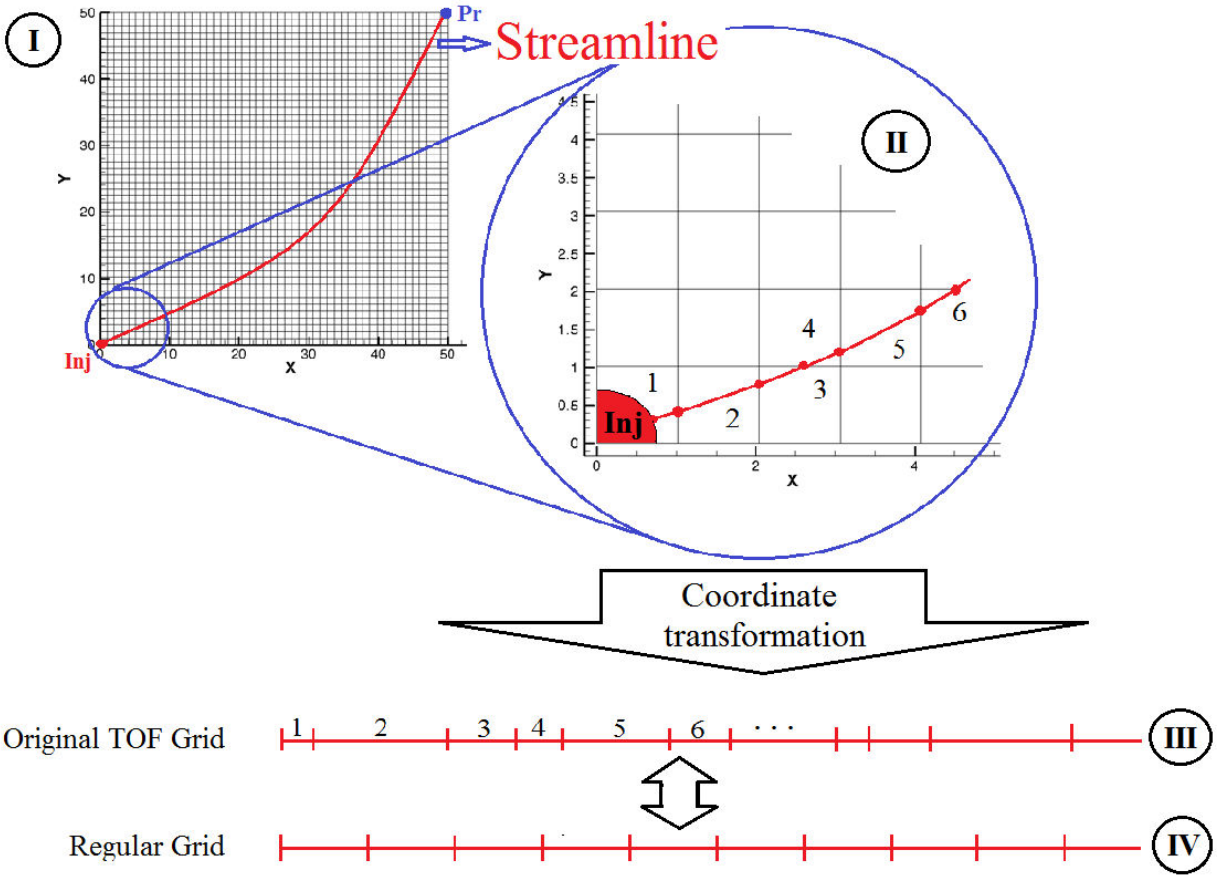

Figure 19- Transformation from Cartesian grid to time-of-flight coordinate system

Overall time of flight from injector to producer depends on the length of each streamline. If the length of the streamline is long, then the time that takes the particle to travel such way will be longer (Figure 21). We will consider multiple 1D problems after determination of the overall time of flights for each streamline. The differential equations for each streamline will be the same, difference for each streamline is only in initial and boundary conditions. As it was noticed before, each 1D domain has its own length, initial and boundary conditions. The time step size in the numerical solution will be limited by the smallest residence time $\Delta\tau$ (Figure 19, step III). To eliminate this problem we will map the concentration distribution on each 1D meshed streamline at a uniform $\Delta\tau$ step (Figure 19, step IV).

In Figure 20, the time of flight for a single streamline is shown. It passes 70 gridblocks travelling from the injector to the producer. Residence time for the particle in each cell depends on the cell average velocity and on the streamline length inside the gridblock (Figure 19, step II). In general, the residence time reduces with increasing velocity especially near the wells or in zones with high hydraulic conductivity.

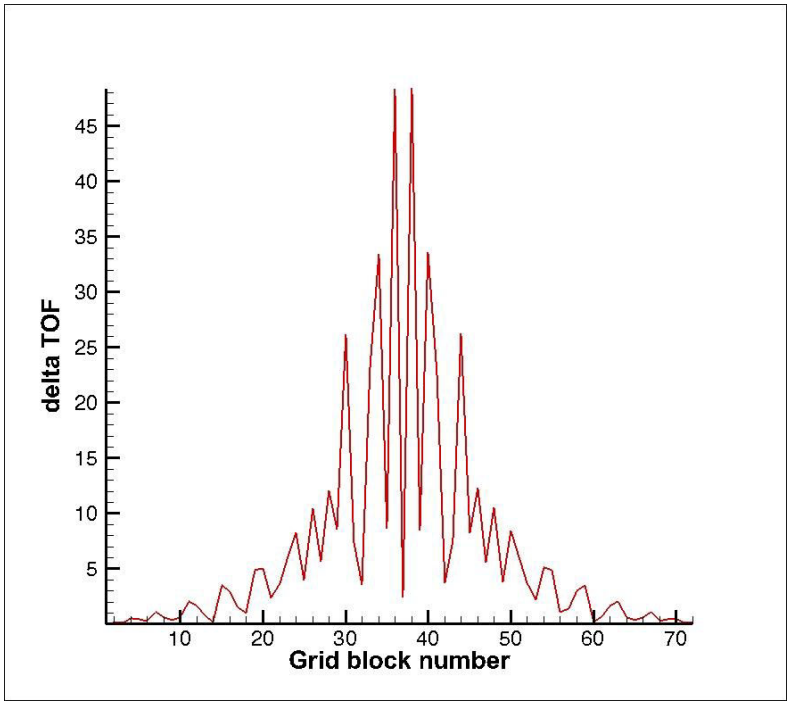

Figure 20- Dependence of $\Delta\tau$ on grid block number for isotropic porous media

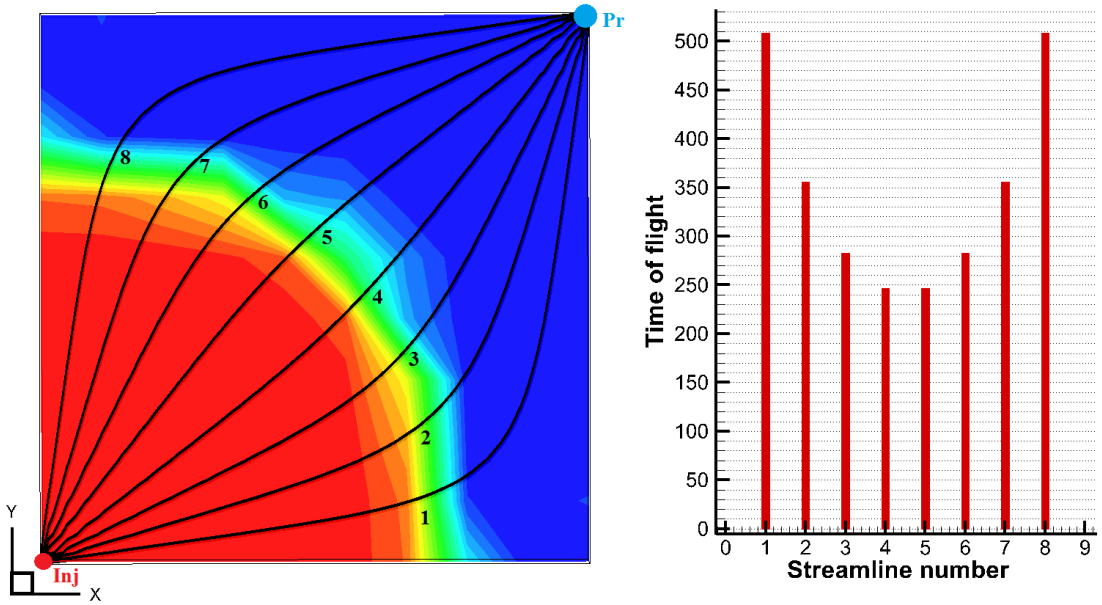

Figure 21- Time of flight values dependency on streamline number for isotropic porous media

4.7 TEST CASE CALCULATIONS

In order to verify developed streamline code let us consider the acid injection problem without taking into account chemical reactions. So, we consider this problem in both streamline and finite-difference approaches at the impermeable cubic domain with 1 injector and 1 producer (Figure 15).

$$\frac{\partial C}{\partial t}+\vec{U}gracC=\delta(\vec{r}-\vec{r}_{inj})Q_{inj}C^{inj}+\delta(\vec{r}-\vec{r}_{pr})Q_{pr}C;\quad \left.\frac{\partial C}{\partial \vec{n}}\right|_{\Omega}=0; \tag{4.12}$$

Where the right hand side term $\delta(\vec{r}-\vec{r}_{inj})Q_{inj}C^{inj}+\delta(\vec{r}-\vec{r}_{pr})Q_{pr}C$ represents the wells.

If we apply the time of flight coordinate transformation on this equation then we obtain the next 1D equations which has exact analytical solutions:

$$\frac{\partial C_i}{\partial t}+\phi\frac{\partial C_i}{\partial \tau}=0;\quad C_i\big|_{\tau=0}=C^{inj},\quad \left.\frac{\partial C_i}{\partial \tau}\right|_{\tau=T_i}=0;\ i=\overline{1,N} \tag{4.13}$$

where *N* is number of streamlines and T_i is time of flight of each streamline *i.*

Solution of equation (4.13) will be:

$$C=\begin{cases}C^{inj} & if\ \ \tau\le\phi t\\ 0 & if\ \ \tau>\phi t\end{cases} \tag{4.14}$$

Equation (4.12), in general, represents wave propagation. For this kind of hyperbolic equations various numerical finite difference schemes can be applied. In order to solve the equation (4.12) we use the simple Euler's upstream scheme 1st order accurate in time and space.

It is obvious that due to lack of diffusive effects information travels forward in time and the solution of (4.12) has to be discontinuous in space and in strong dependence on velocity field. Analytical solution of such partial differential equations is difficult to find but is easier to predict its qualitative behavior. Finite-difference schemes introduces numerical diffusion which is nonphysical (Chung 2006 [15]).

Analytical solutions along streamlines can be directly mapped to the time of flight variable and then to the x, y, z coordinate system. These solutions are free from numerical diffusion and allow greater time step in case of quasi-stationary flow, otherwise, solution is known at any simulation time as in (4.14).

Qualitative comparison of injected acid front propagation is shown in Figure 22. Numerical diffusion is specific to finite-difference simulation rather than streamline method. Figure 22- Symmetric representation of injected solution front propagation:
left) SL simulation; right) FD simulation.

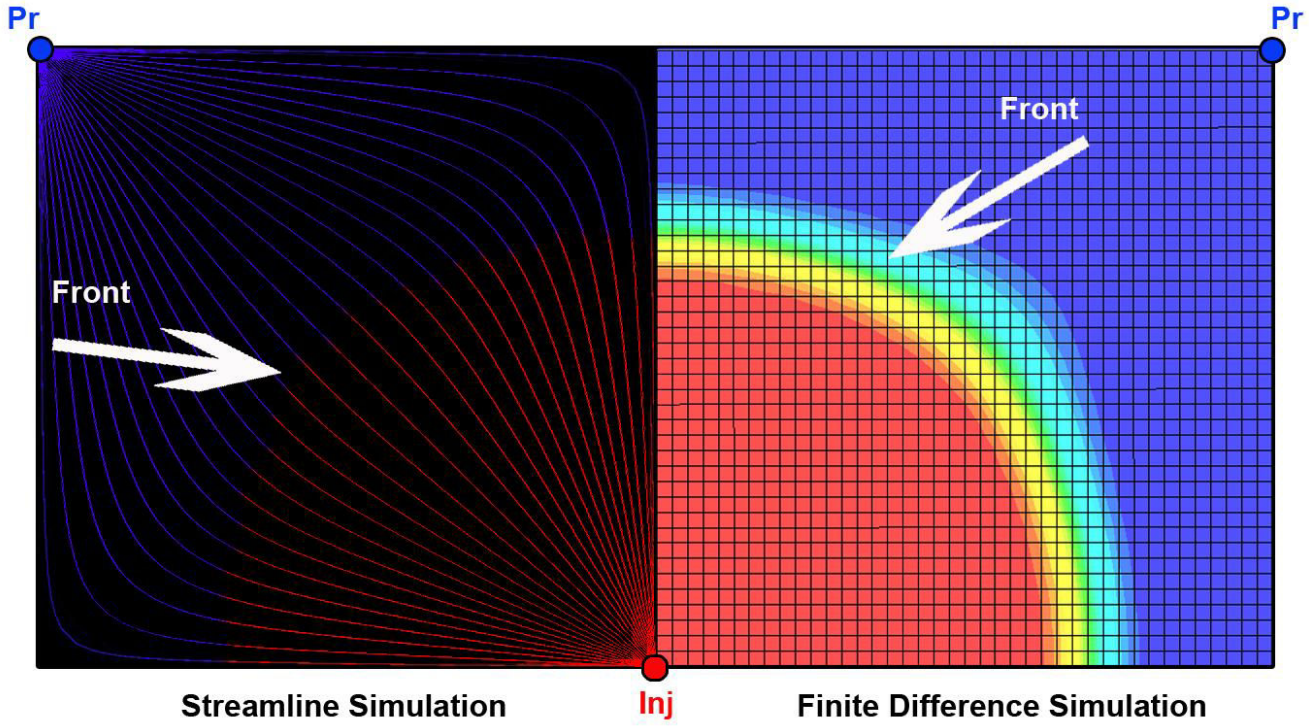

Figure 22- Symmetric representation of injected solution front propagation:
left) SL simulation; right) FD simulation.

To be better represented, difference between FD and streamline approaches was considered along injector to producer straight path line cut from both solutions. The smoothed front by FD simulation is shown in Figure 23 (in red), while streamline method shows the propagation of shock (in blue), which is more physical for (4.12).

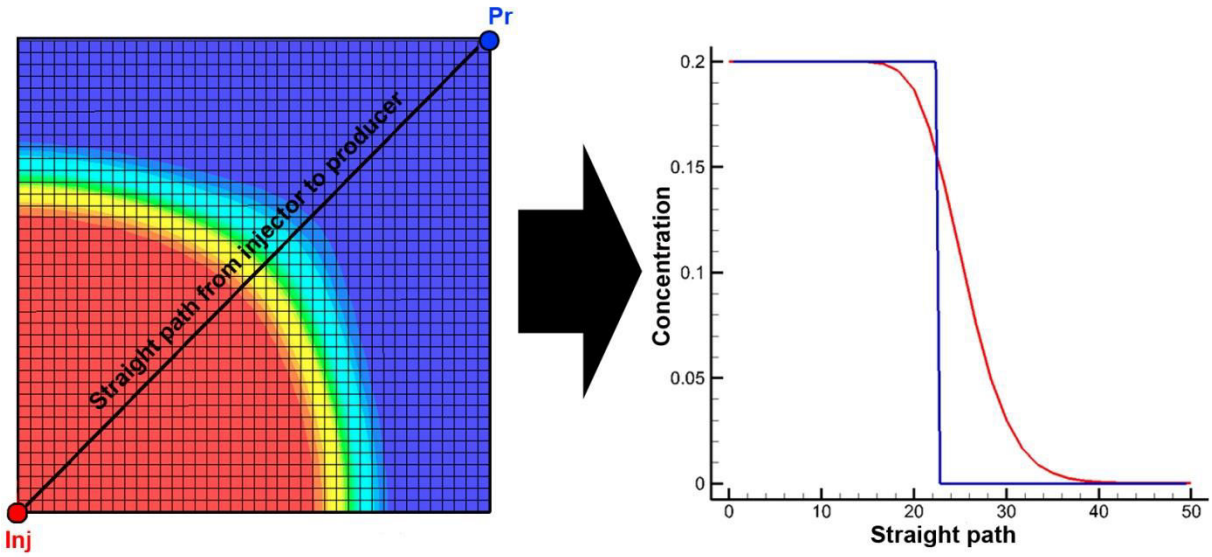

Figure 23- Injected solution front propagation along the straight line from injector to producer: blue) streamline simulation; red) FD simulation.

According to spatial distribution of the ore into the layer, the wells are cross-cutting mineralized formation and are open along the whole thickness of the ore body (perfect well), or localized in highest mineralized zones. In the latter case, the well may be open only on levels where the grade content is higher (imperfect well). Roll-front uranium deposits have an impermeable layer of clay at the bottom and at the top of the mineralized zone most of the time. It can be reasonably assumed that in this case most of the wells are perfect. In some cases, the mineralized uranium zones are hanging without the presence of an impermeable confining layer; in this case, the wells can be considered as imperfect. Figure 24 and Figure 25 show streamlines in case of perfect and imperfect wells, respectively.

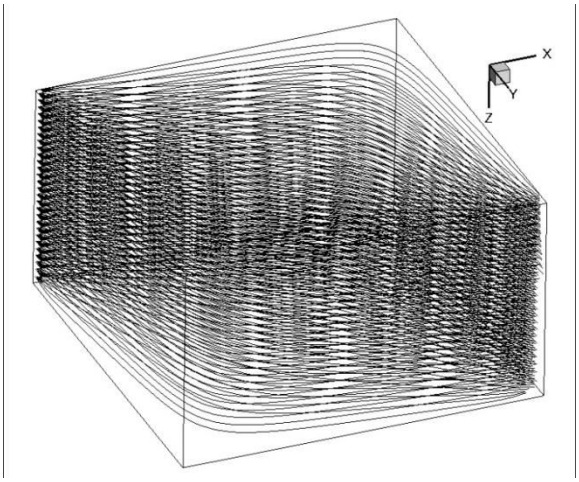

Figure 24- Streamline tracing in 3D geometry for isotropic permeability

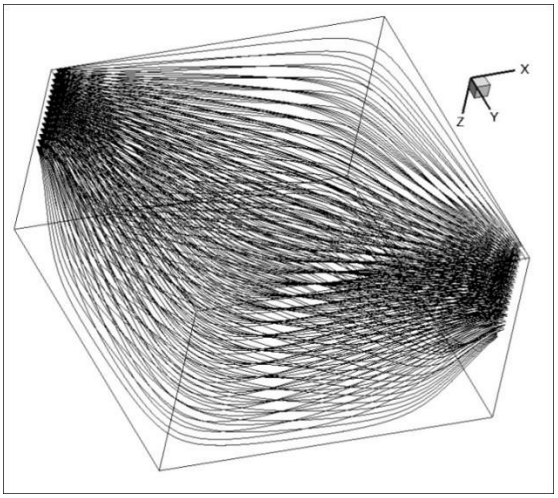

Figure 25- Streamline tracing in 3D geometry for imperfect wells

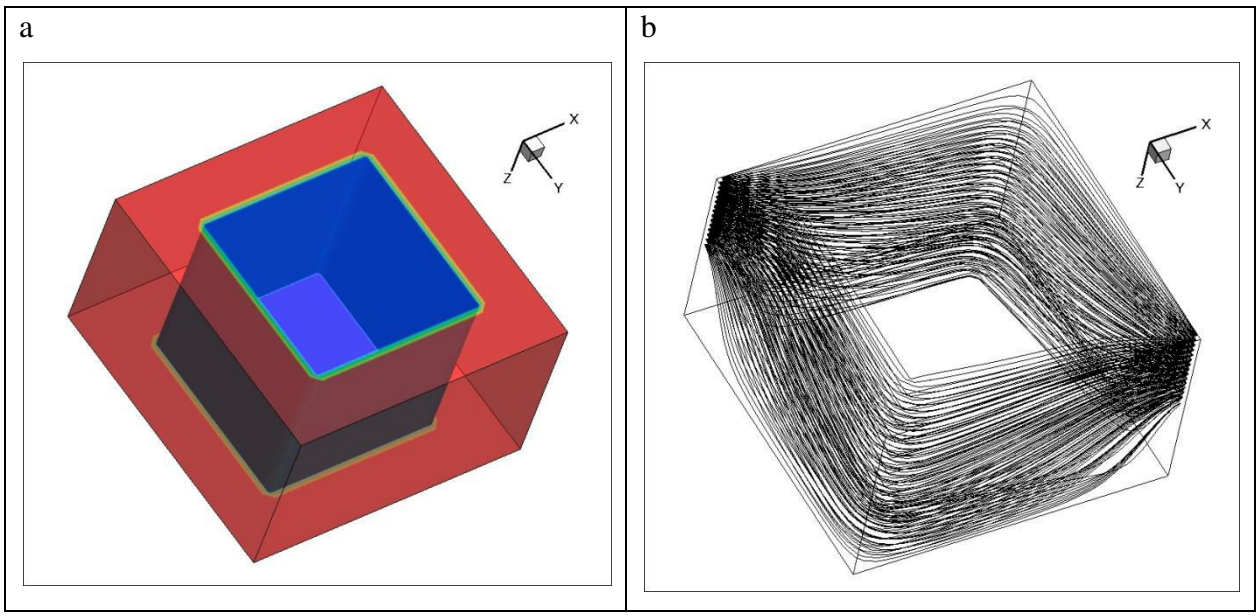

Figure 26- Permeability distribution (a) and corresponding streamline (b)

In order to validate the solver developed on streamlines, a test case constituted by a gigogne permeable and sub-impermeable cubes has been considered. The permeability distribution is shown on Figure 26(a) and the corresponding streamlines on Figure 26 (b). The results show that the streamlines avoid the impermeable cubic sub-domain and confirm the reliability of the results.

The solution to the transport equations along the streamline can be found numerically or using the analytical solution given in Chapter 2. However, this analytical solution is only valid in the

case of a homogeneously mineralized ore body i.e. the initial concentration of the solid species are constant everywhere. This is a serious limitation to use in practice for the analytical solution. This is why, a numerical approach has been developed to solve the transport equation along the streamlines.

Once the step time is defined, the transport equations are numerically solved along streamlines using a finite-difference method. Mapping time of flight along streamlines provides a way to visualize the flow in the reservoir. 1D transport equations are solved along streamlines in the time-of-flight coordinate system accounting for the heterogeneity of the reservoir (permeability, initial spatial distribution of the solid species, non-constant spatial velocity, ...). Calculations are carried out for domain presented at Figure 15. The corresponding solutions for the pressure distribution and the velocity field are presented in Figure 27 and Figure 28 assuming a stationary velocity field. Streamline traced in 3D for an isotropic permeability case, is shown in Figure 24.

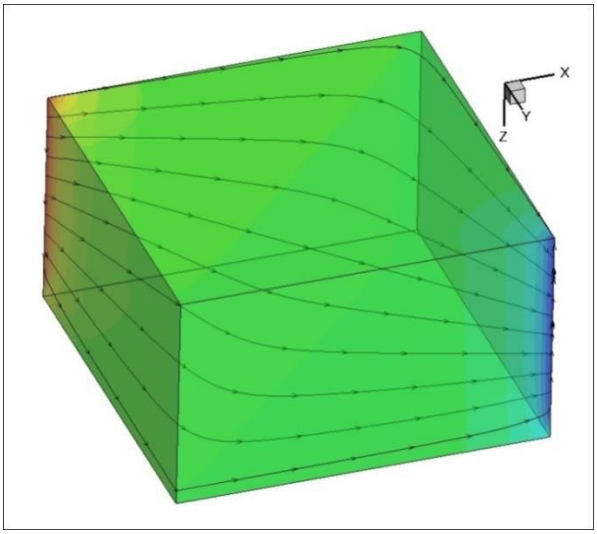

Figure 27- Pressure distribution

The transport equation for species were solved using the stream lines approach in the case of imperfect wells and assuming an isotropic distribution of the mineralization (Figure 25). The corresponding iso-surfaces for the sulfuric acid (a), solid mineral (b), dissolved mineral (c) and gypsum (d) are represented on Figure 29. Figure 30 represents the hydraulic head (a), the distributions of solid mineral (b), the sulfuric acid/reactant ratio (c) and the dissolved mineral (d) along the streamlines.

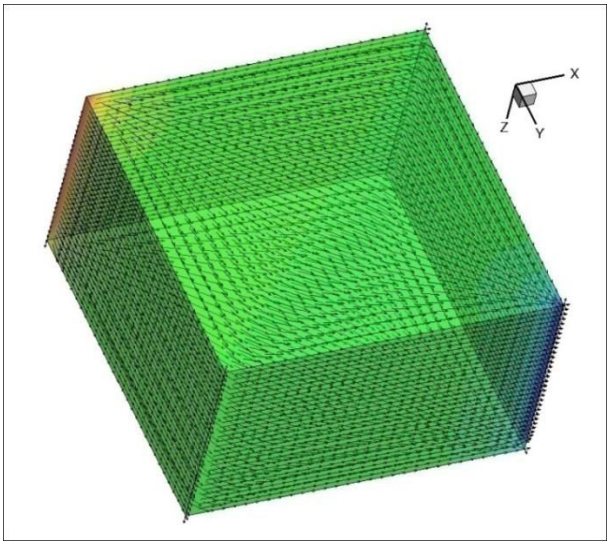

Figure 28- Velocity distribution

a

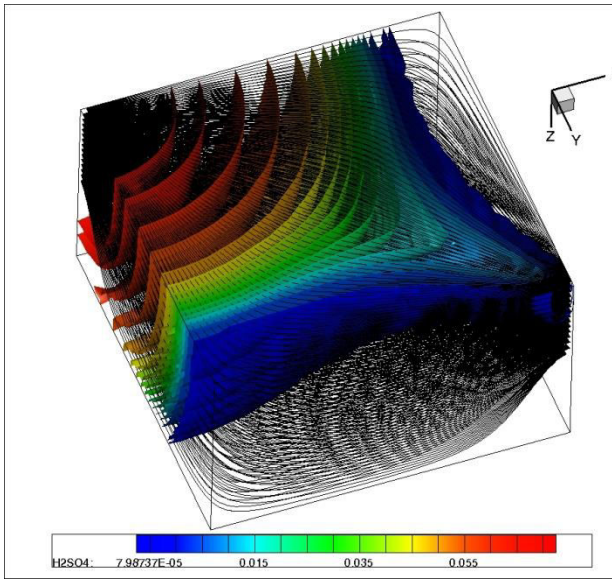

b

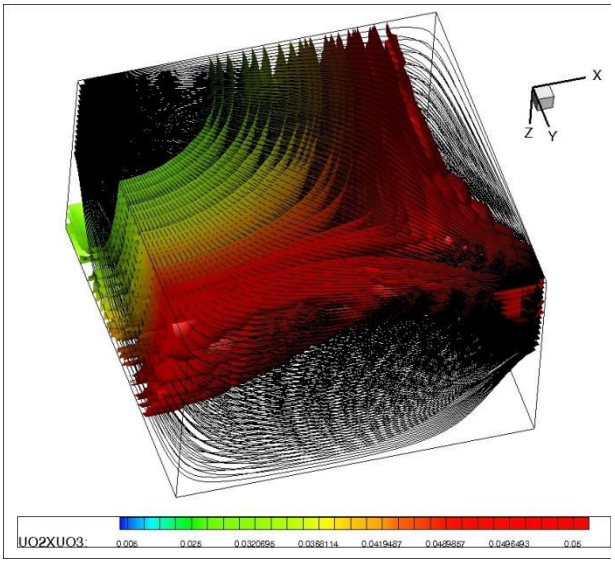

c

d

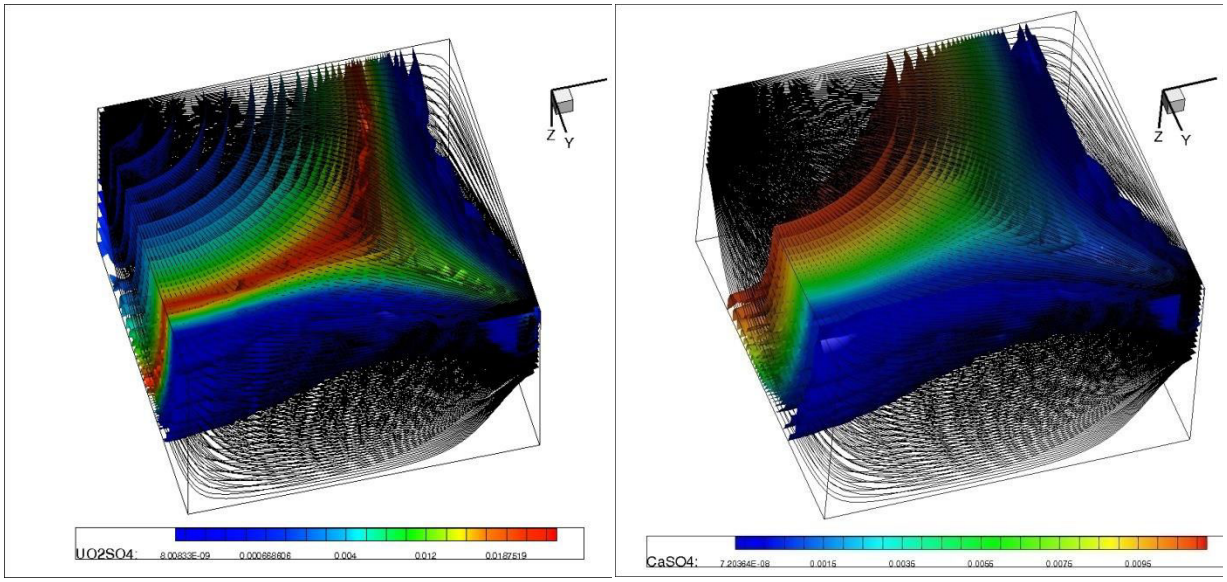

Figure 29 - Distribution of sulfuric acid (a), solid mineral (b), dissolved mineral (c) and gypsum (d)

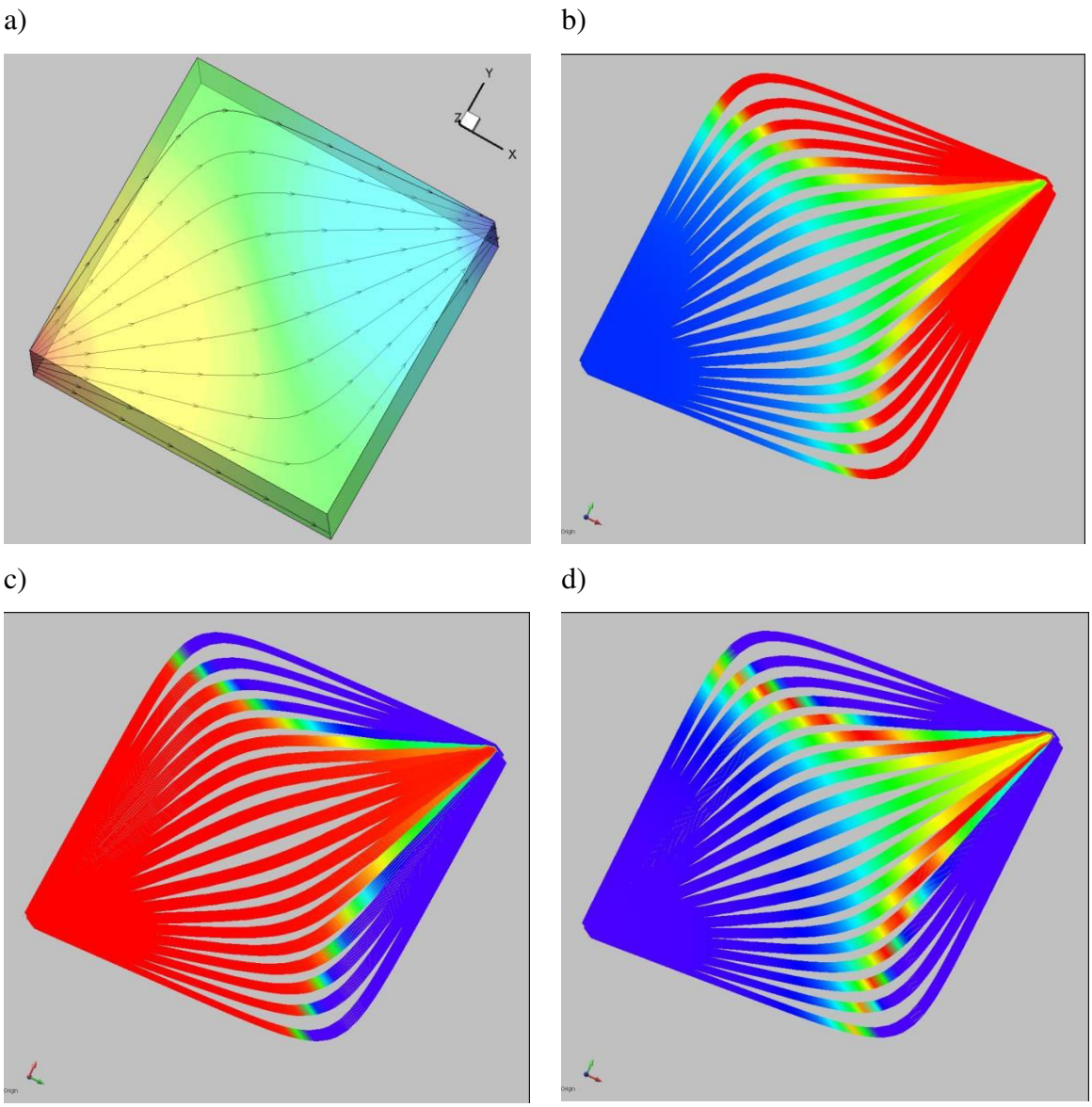

Figure 30 - Hydraulic head (a), distribution of solid mineral(b), sulfuric acid/reactant (c) and dissolved mineral (d) along streamlines

To validate accuracy of streamline simulation (SL), the same problem was solved by finite-difference method (FDM) in 3D. The distribution of the reactant in the layer obtained by FDM with a grid size of 30x30x30 is represented on Figure 31(a), while the streamline solution (SLM) is shown on Figure 31(b) for the same boundary condition. Qualitatively, the FDM and SLM solutions (with 1000 stream lines approximated by 500 nodes) for the reactant spatial distribution show consistent results. In details, numerical diffusion appears when solving using the 3D FDM methods, especially in the dominant convection case.

a b

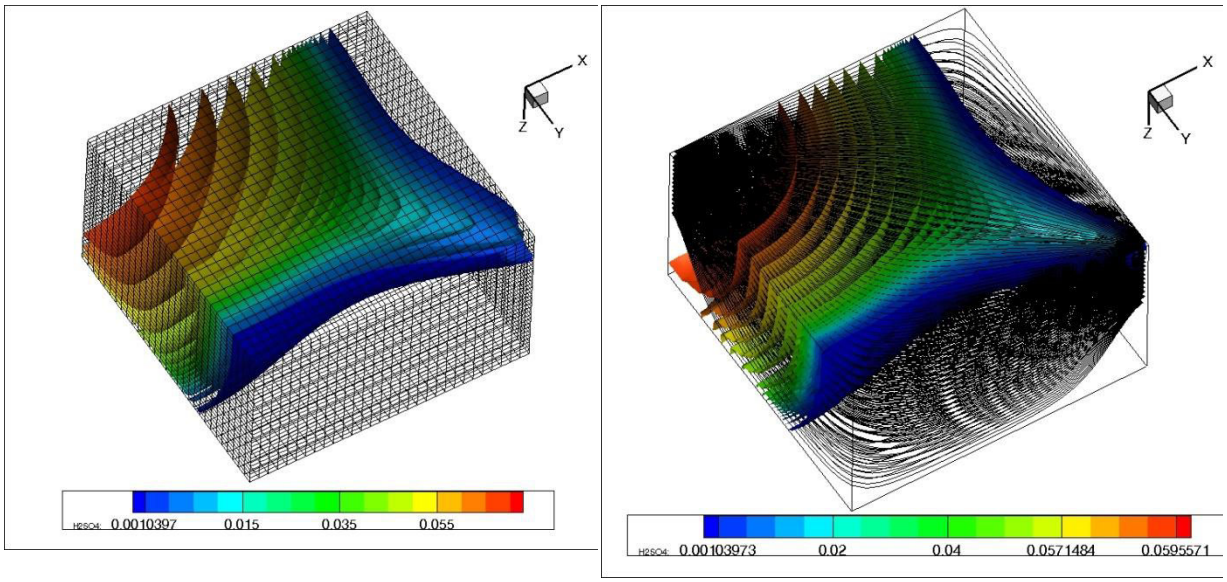

Figure 31 - Qualitative comparison of solutions in finite-differences method and streamline simulation for reactant distribution

The Courant–Friedrichs–Lewy(CFL) condition is better respected in the case of streamlines and provides more accurate results than in the 3D case as the velocity is included in the time of flight, and the meshing is adapted to the TOF. Another advantage of the SL based simulation is the computational time which is considerably reduced (by a factor 14) compared to the 3D approach. Figure 32 compares calculation time for finite differences and streamline methods.

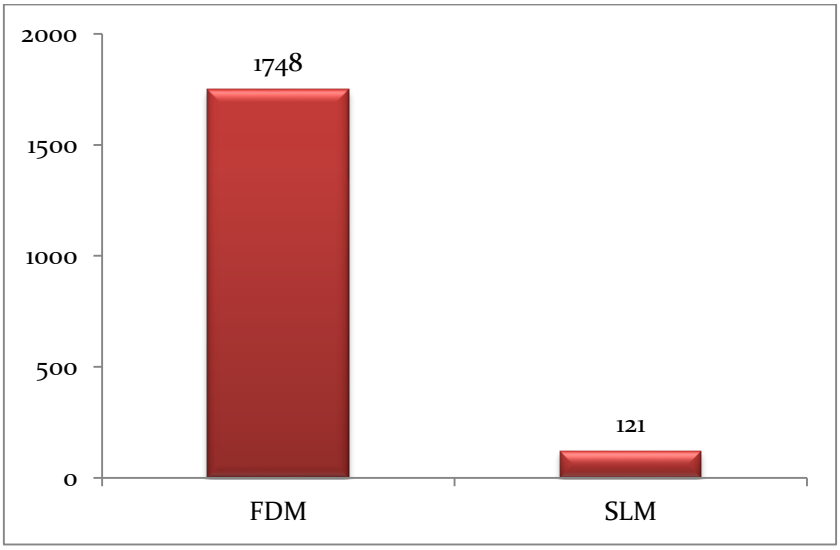

Figure 32 - Calculation time for finite differences (grid size 30x30x30) and streamline methods (1000 stream lines by 500 nodes on each streamline)

Results show that calculation time for streamlines is much lower compared to finite difference methods as equations are solved independently from one streamline to another. The streamline approach can be easy parallelized, a burden task to do in the case of 3D FDM. Moreover, advanced parallelized methods based on the exploitation of the GPU can be easily implemented in the case of streamline solution, open the possibility to use very refined mesh and thousands of streamlines. The drawbacks of this approach are to solve the pressure equation, the chemistry being not a problem.

Sulfuric acid solution reacts with the ore-forming rocks leading to the dissolution of mineral species (carbonate, clays, silicates ...) contained in the ore-bearing rocks, which can precipitate further along the fluid path as secondary minerals (in particular gyps). Thus, the contact surface of reacting minerals (uranium species) can be plugged and covered by thin layers which limit or even prevent access of acid to the uranium compounds, reducing consequently the uranium extraction yield. As a result of such sedimentation of chemical reaction products, the pore space is clogged up, and permeability is reduced in the formation creating apparent geochemical barriers, this last case is not considered in this work.

To investigate the influence of pore space clogging, we simulate the mineral extraction by ISL method with different chemical kinetics. We consider three different problems based from equation (2.1) – (2.4):

i. simple chemical model of uraninite dissolution by sulfuric acid (I);
ii. chemical model of interaction of sulfuric acid with uraninite and carbonate with pore space clogging by gyps (I), (IV);
iii. detailed chemical model of interaction of sulfuric acid with uraninite, iron hydroxide and carbonate with oxidation of oxide of uranium and clogging of pore space (I)-(IV).

Distribution of sulfuric acid (a), solid mineral (b), calcium carbonate (c), dissolved mineral (d) and gypsum (e) against time of flight are shown in Figure 33 for different values of passivation rate(chemical reactions (II) and (III) are neglected).Results show that the kinetics of the chemical reactions become slower when the passivation rate increases. Even for gypsum, the apparent precipitation rate seems to diminish because it starts to passivate itself, a phenomenon observed also in corrosion problems as reported by Pilling and Bedworth [54]. The composition of solute and the concentrations of the solid components change against the time of flight, they are shown for cases (i), (ii) and (iii) in Figure 34, Figure 35 and Figure 36, respectively.

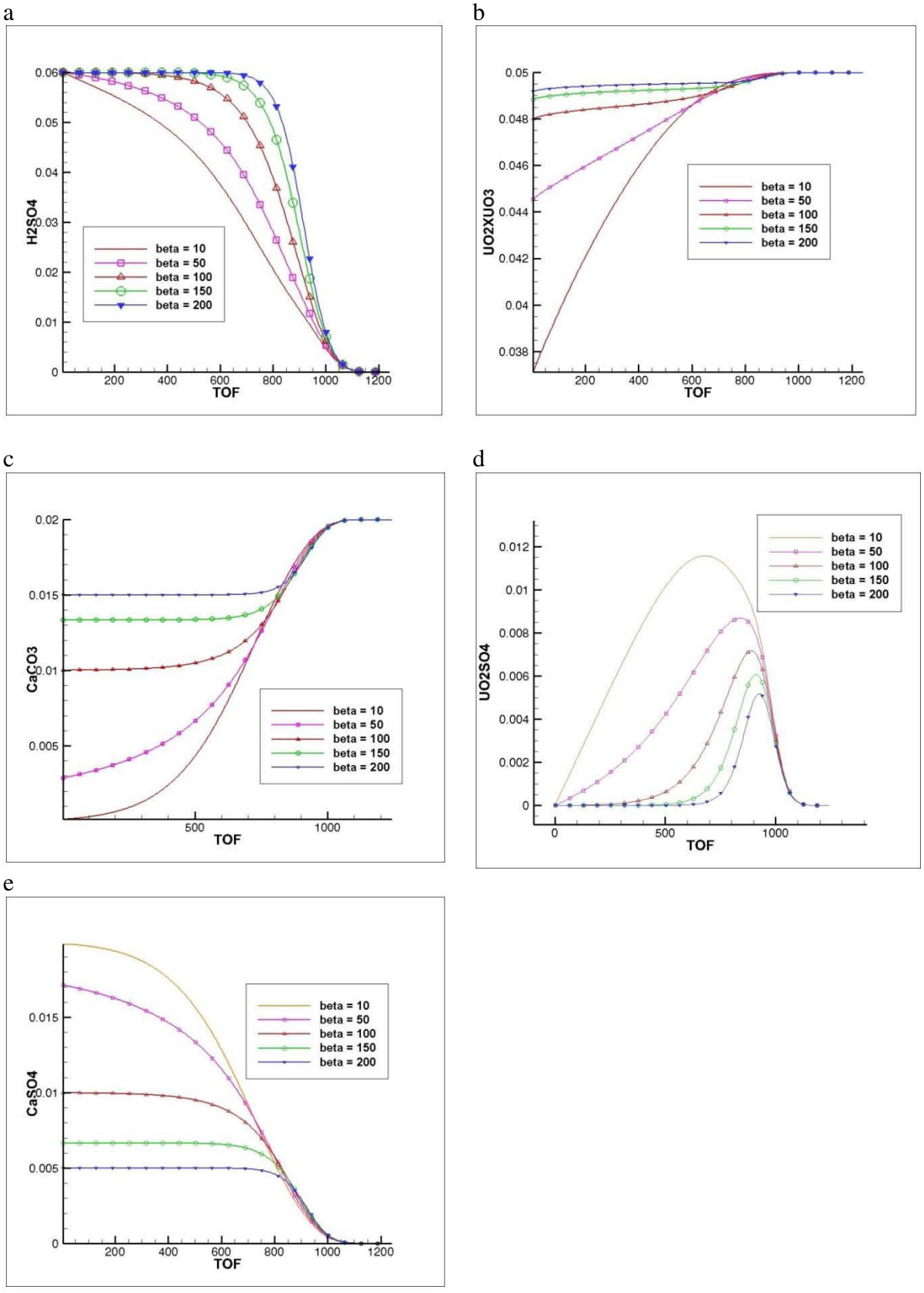

Figure 33 - Distribution of sulfuric acid (a), solid mineral (b), calcium carbonate (c), dissolved mineral (d) and gypsum (e) in time of flight variable for different passivation rate (chemical reactions (II) and (III) are neglected

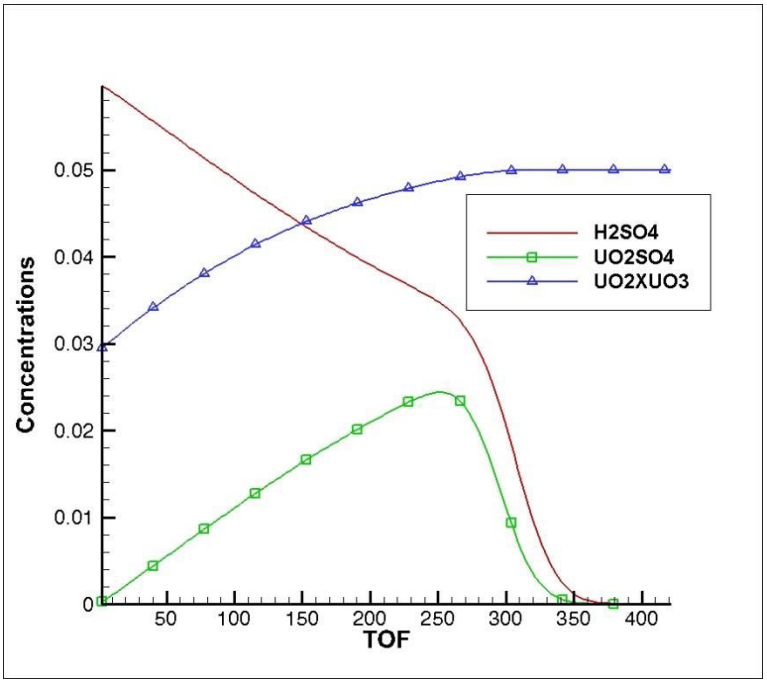

Figure 34- Changing of solute mixture and solid components in time of flight variable with taking to account chemical reactions (I)

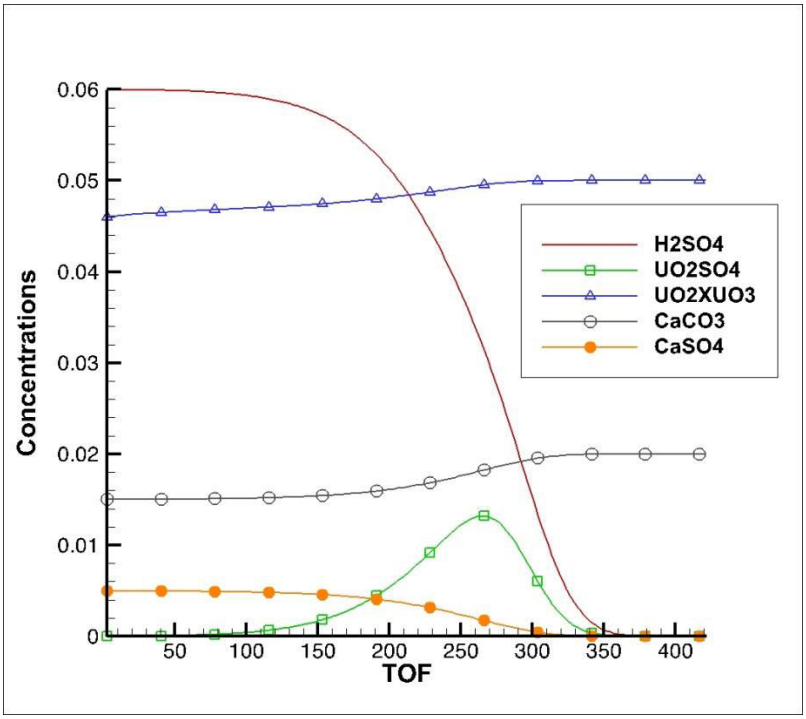

Figure 35 -Changing of solute mixture and solid components in time of flight variable with taking to account chemical reactions (I) and (IV)

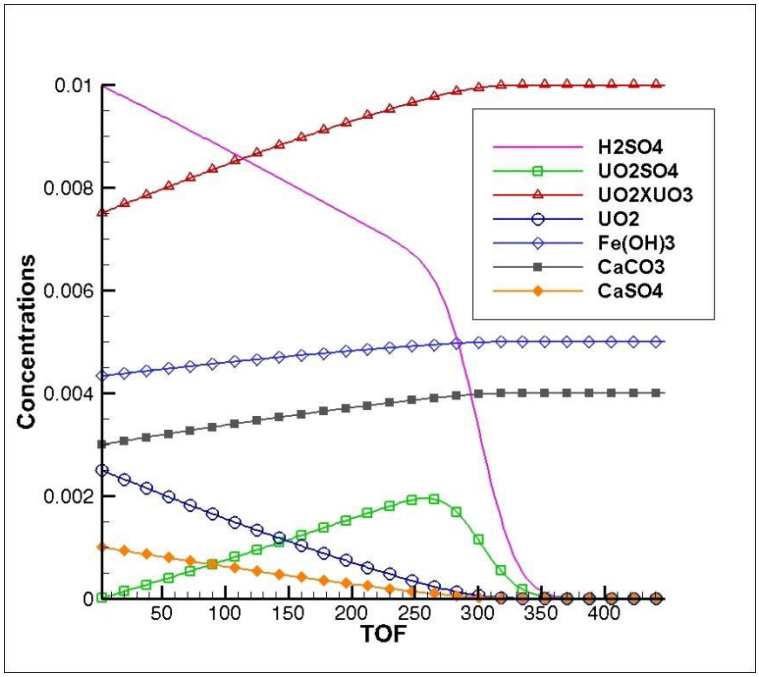

Figure 36 -Changing of solute mixture and solid components in time of flight variable for full chemical reactions (I)-(IV)

Obviously, in the case of detailed chemical kinetics (I)-(IV), it becomes possible to accurately calculate the sulfuric acid consumption.

SLM are carried out on several virtual case studies: (i) for a non-uniform initial spatial distribution of the solid mineral; (ii) for a mineralized ore distributed into a cube placed at the center of the studied area (Figure 37); the amount of uranium in the liquid phase is shown on Figure 38, in case of a non-uniform initial distribution of the solid mineral.

a b

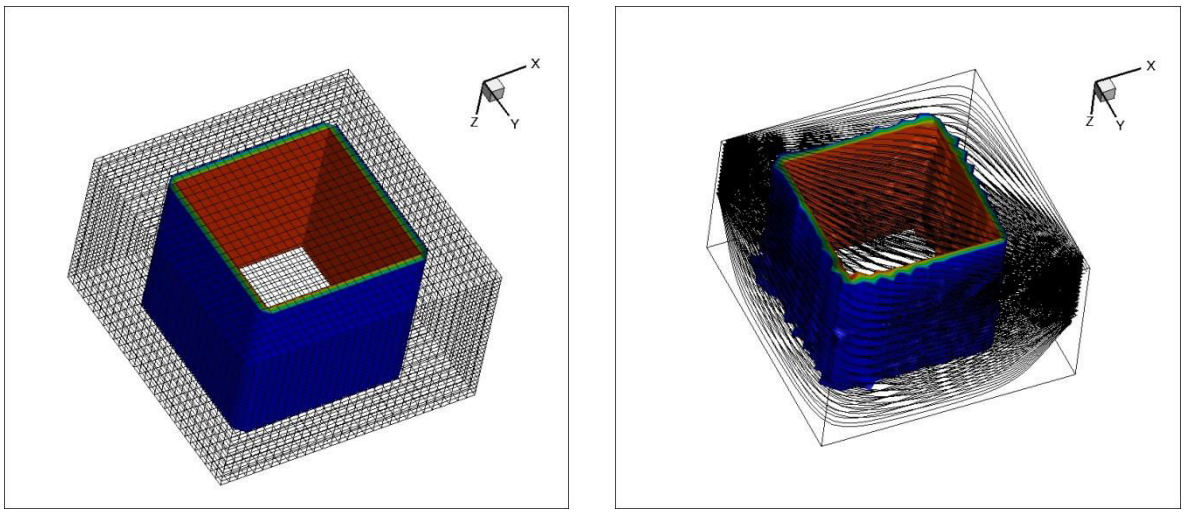

Figure 37 -Using the stream line method for non-uniform initial distribution of solid mineral

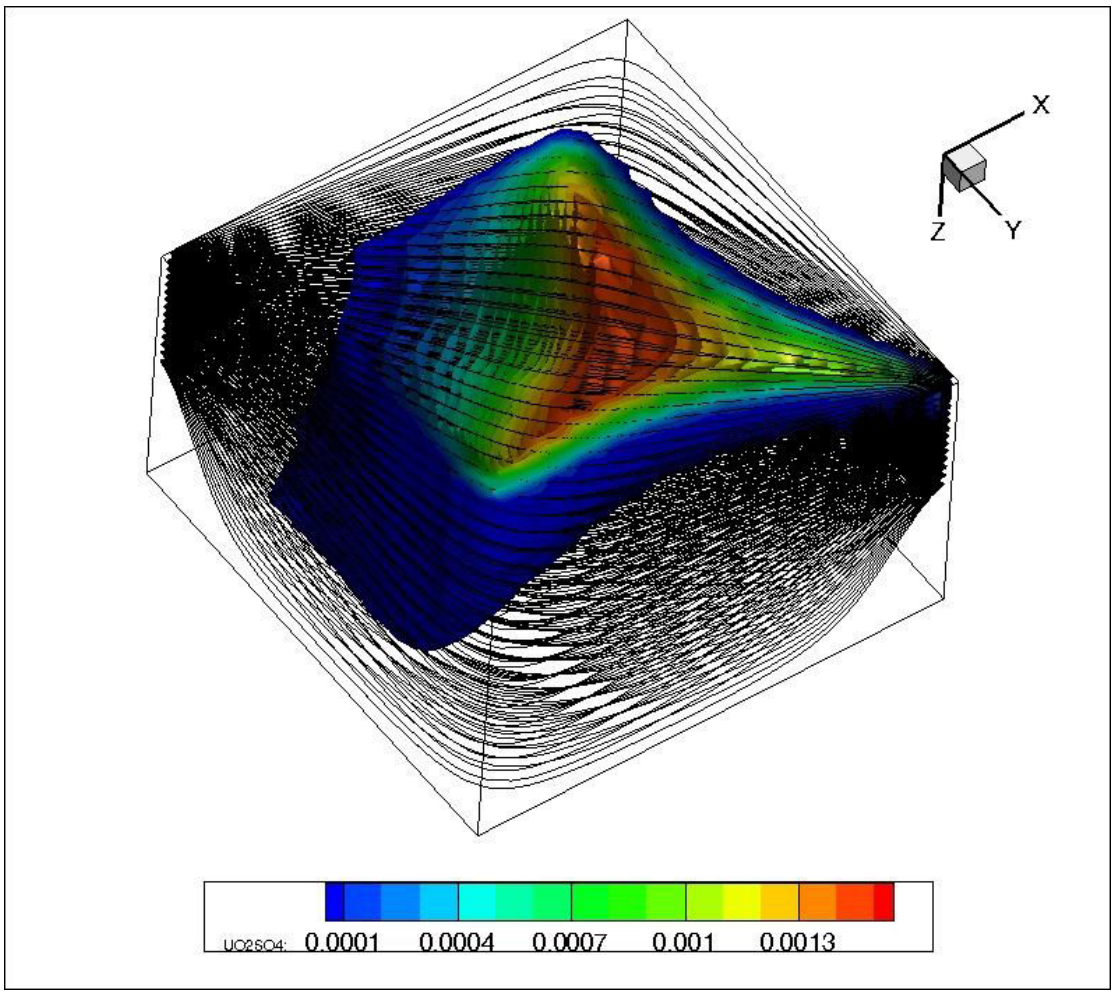

Figure 38 -Distribution of dissolved useful component method for non-uniform initial distribution of solid mineral

The calculations are carried out for a randomly distributed solid mineral concentration. The results are demonstrated on Figure 39. Iso-surface of sulfuric acid (a), solid mineral (b) and dissolved mineral (c) for non-uniform initial distribution of solid mineral are presented on Figure 40.

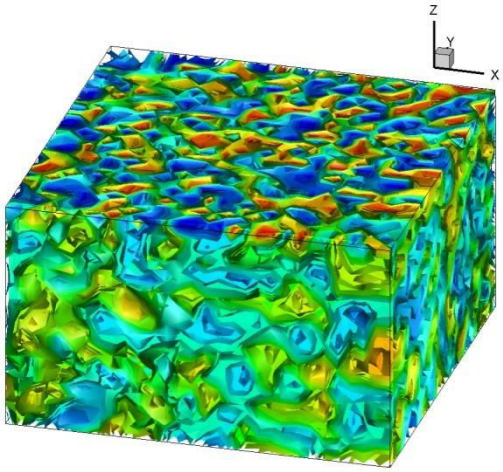

Figure 39 -Non-uniform initial distribution of solid mineral

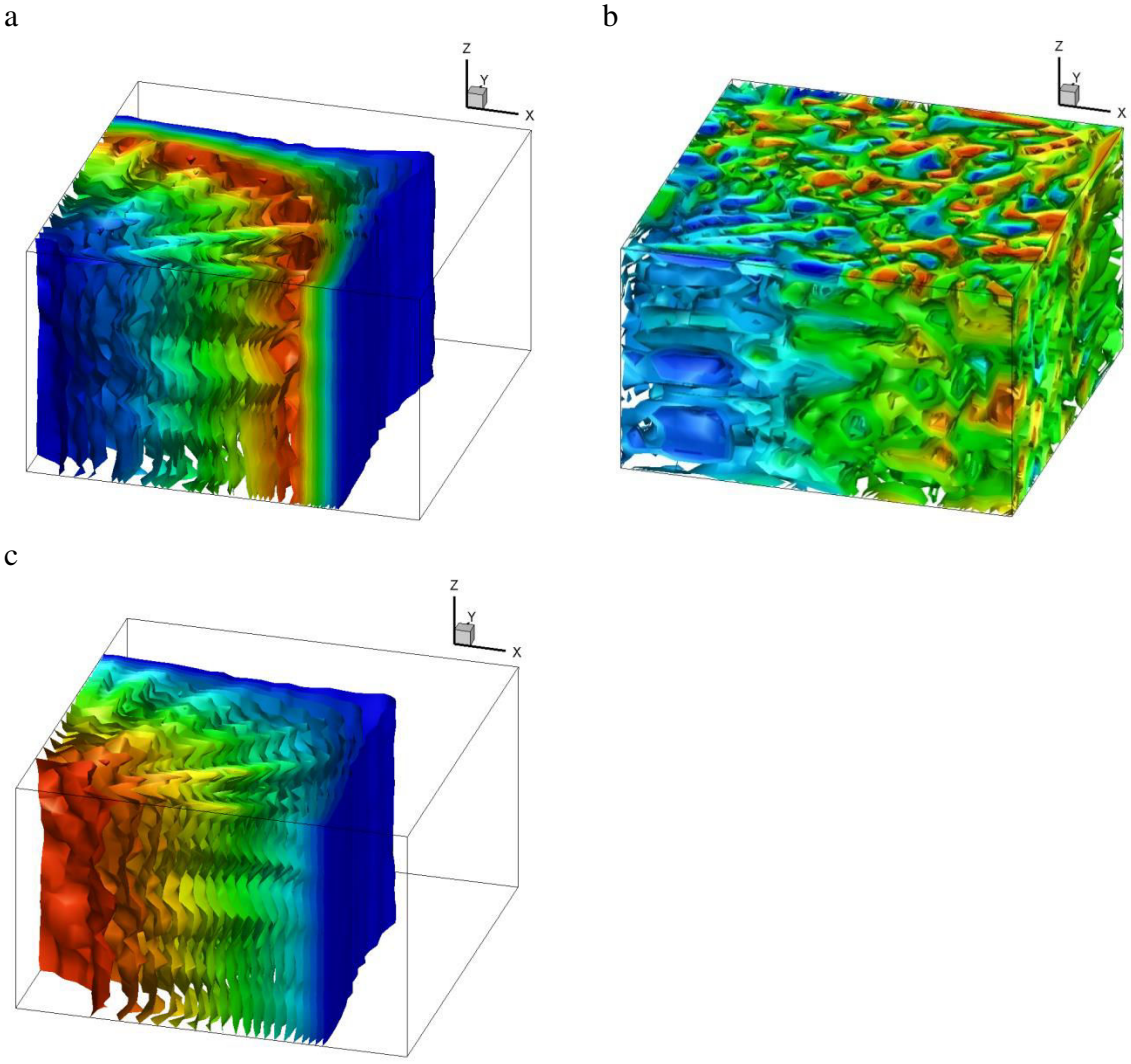

Figure 40- Iso-surface of sulfuric acid (a), solid mineral (b) and dissolved mineral (c) for non-uniform initial distribution of solid mineral

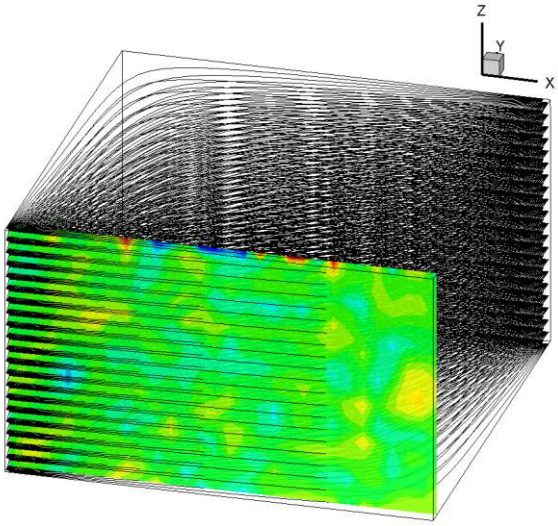

Figure 41- Cross sectional view of non-uniform initial distribution of solid mineral

a

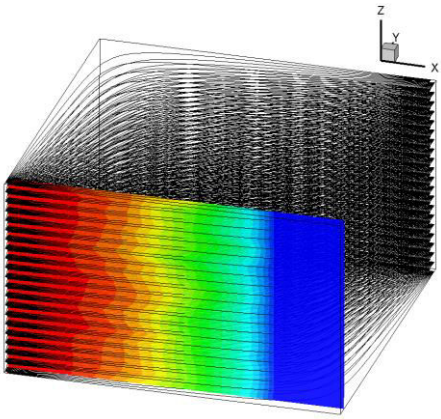

b

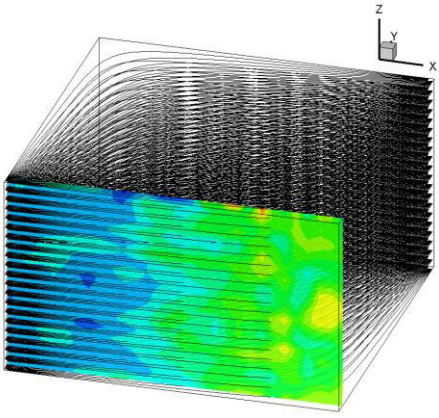

c

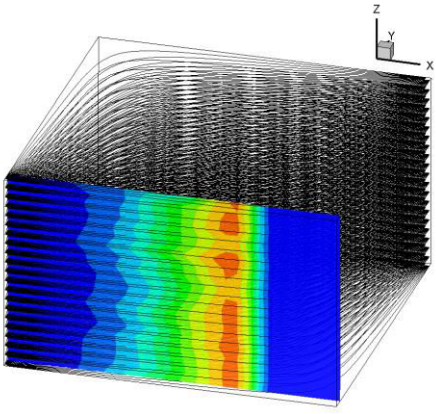

Figure 42- Cross sectional view of non-uniform initial distribution of solid mineral (a), sulfuric acid (b), solid mineral (c) and dissolved mineral (d) non-uniform initial distribution of solid mineral

Influence of passivation rate on extraction degree for isotropic hydraulic conductivity of ore bearing zone with uniform initial distribution is investigated. Evolution of extraction degree without passivation is shown on Figure 43.

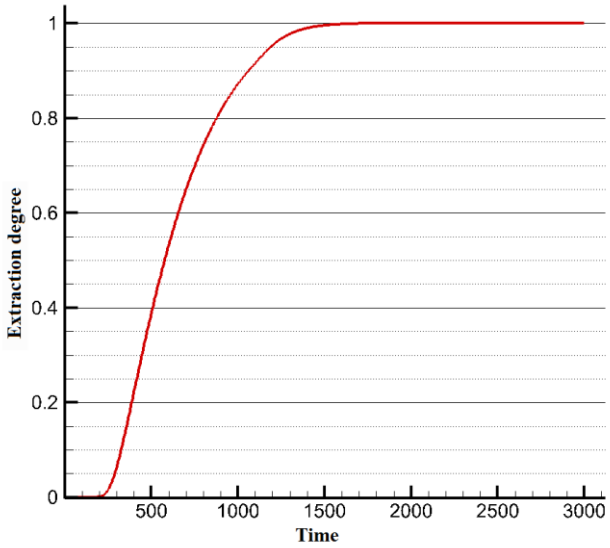

Figure 43- Evolution of extraction degree without passivation

Dependence of extraction degree on passivation rate $\omega = \beta C^{s4,0}$ by time obtained numerically is shown on Figure 44. Numerical (Figure 44) results are in good accordance with analytical (Figure 12).

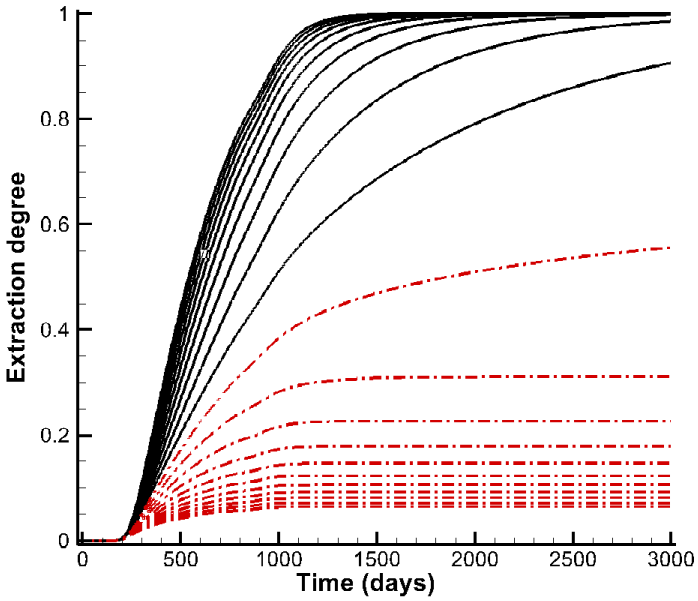

Figure 44- Dependence of extraction degree on passivation rate

$\omega \in [0;1) \quad step = 0.1,$

$\omega \in [1;2] \quad step = 0.1$

5 DISCUSSION

We have discussed the reactive transport results obtained by streamlines. However, there must be a question with regard to advantages or disadvantages of streamline *vs.* Eulerian classical 3D FD resolution. In FDM, the reservoir is represented as a regular gridblock and the time steps are adapted to the problem to be solved, here the resolution of 11 coupled equations describing the solution precipitation of species. The equations are solved on each elementary cell which may take huge computational time, especially for high nonlinear problems.

The main advantages of streamline are the computational time which can be attributed to the following: (i) the transport equation is discretized along streamlines using the time of flight (TOF) instead of the spatial coordinates. TOF is more numerically efficient regarding resolution because it corresponds to irregular spacing in space; (ii) dissolution / precipitation processes may change the porosity and the permeability of the medium, but the change in the velocity field is slower than the chemical reaction, making the necessity of streamline updating less frequent. The same remarks are valid in the case of a transient fluid flow. (iii) lateral diffusion is not accounted for by streamlines while it is inherent in the classical Eulerian approach. However, in convective dominant flow regime, resolution along the streamlines can be performed in a given TOF (i.e time) steps, results being mapped on the gridblocks less frequently to estimate the diffusion component. (iii) in case of homogeneous media, the transport equation along streamlines can often be solved analytically. However, for the case discussed here, it is a very limited situation as the uranium mineralization is rarely constant in space, nor the distribution of mineral species. (iv) solving transport equations using *n* streamlines is a *n-1D* numerical problem, the resolution along one streamlines can be made independently of the other streamlines. Thus, the problem is scalable (i.e. the transport equation can be solve along the *n* streamlines in parallel). This property of streamlines is very interesting as the resolution of the transport equations can be made on the GPU (Graphic Processor Unit) or on CPU clusters, making the resolution quite immediate even with large number of streamlines. It is trickier in the classical gridblock Eulerian approach. The only bottleneck is that in the presence of significant diffusion terms, the streamline results regarding the chemical species must be mapped regularly onto the gridblock, it implies massive data exchange between the GPU and the CPU (and vice versa). (v) as streamline resolution is far much faster than classical 3D gridblocks, it gives the opportunity to calculate several solutions varying parameters (such as uranium grade, the passivation rate, composition of the injected reactant

leaching solution ...)in order to quantify the sensitivity of the recovery curves on the uncertainty of some input parameters.

The most important limitation in using streamlines is the assumption that the fluid transport is made in 1D, and along the streamlines. This is not the case for transient flow regimes (changing well rates) or when the flow is changing, in general, when the flow regime is changing. Another point is that strictly speaking the streamline is not conservative in terms of flow (stream tubes are). In non-steady state regimes the streamlines vary in space introducing a 3D transverse flux to the original flow direction (Datta-Gupta and King 2007 [19]). This can be corrected by re-mapping the solution on the gridblock regularly, or by transferring the results from one streamline to their neighbors.

Regarding the results obtained from the uranium case study, only gypsum has been considered as an inhibitor; other species, such as, titanate and vanadate may also play an important inhibitor effect. However, the general theoretical model developed above can account for additional inhibitor species.

6CONCLUSION

Depending on the rock types present in the geological formation, sulphuric acid also reacts with several other minerals. Among them, the reaction between sulphuric acid and calcium carbonate $CaCO_3$ can have a significant effect on the uranium recovery rate. Indeed, that reaction yields calcium sulfate $CaSO_4$ which is in most conditions insoluble in water and can attach to the pore walls, thus preventing chemical reactions between liquid phase and uraninite to take place.

In case of roll front deposits, the uranium is present as oxide compounds mainly of UO_2, UO_3 and their combination. In a typical leaching operation, a solution containing sulphuric acid H_2SO_4 is injected into the formation. Its role is to react with UO_3 molecules and with ferric hydroxide which is generally present in the rocks. In some cases, iron ions can also be introduced in the initial leaching solution. Both reactions lead to uranyl sulfate complexes, predominantly $UO_2(SO_4)_3^{4-}$, which are soluble in water and can thus be transported by the liquid phase to the production well. The impact of the initial composition of the solute was studied using the analytical approach, and it is observed that in some cases the passivation rate due to the presence of gyps may seriously limits the uranium recovery. Most limiting chemical reactions when uranium leaching by sulfuric acid solution was considered. The precipitation of calcium sulfate in liquid phase may lead to the formation of a crust at the liquid/solid interface. The structure of the crust can be estimated using the Pilling-Bedworth ratio, used in metal oxidation, which compares the molar volume of the product to the molar volume of the reactant.

Reactive transport processes were considered in the special case of in-situ leaching methods applied to the recovery of uranium. After a review of the previous literature concerning in-situ leaching applied in different context, a chemical reactions theory (involving 11 couples equations) for multi-components interacting with solid and liquid phases was developed accounting for possible clogging of reaction surface by secondary precipitated by-products such as gyps. An asymptotic analytical solution is found assuming a homogeneous medium flowed by a reactant solution at a constant velocity. Analytical results are consistent with the results obtained by solving the coupled transport equations numerically. The impact of the reaction passivation rate on the uranium recovery is also obtained analytically for the 1D case.

The analytical solution is applicable when the initial concentration of uranium is assumed to be constant. This is a serious limitation in practice. This is why a numerical method based on streamline was developed to solve the couple transport equations. Streamline results compared

to those obtained by classical 3D FDM are consistent. However, it is observed that the stream line approach is more accurate, faster and stable numerically. Another advantages of the streamline approach is the possibility to parallelize this technique. Case studies including several situations were investigated: (i) whether accounting or not for passivation secondary mineral species; (ii) dissolution of insoluble mineral through oxidation by ferric oxides $FeSO_4$; (iii) non-uniform initial distribution of soluble components of ore bearing zone; (iv) anisotropic hydraulic conductivity. This mathematical model can be applied to real industrial cases as a modeling and prediction tool for calculation of efficient geometrical configuration of well arrangement and/or solute composition. Finally, elaborated model can be used as a tool for improving extraction degree of useful component.

The theory and methodology developed in this work on the roll-front uranium deposits can be easily extended and applied on other type of deposits, in particular, stratiform copper deposits or porphyry coppers deposits.

NOMENCLATURE

$UO_2 \times 2UO_3$	-	uraninite
UO_2,	-	oxide of uranium
$Fe(OH)_3$	-	iron hydroxide
$CaCO_3$,	-	carbonate
$CaSO_4$.	-	gypsum
H_2SO_4	-	the sulfuric acid
UO_2SO_4	-	the sulfate of uranium
H_2O,	-	water
$Fe_2(SO_4)_3$,	-	iron(III) sulfate
$FeSO_4$,	-	iron(II) sulfate
H_2CO_3.	-	carbonic acid
$h = p/\rho g$	-	hydraulic head, *m*
$C^{(s1)}$	-	$UO_2 \times 2UO_3$ concentration of solid components
$C^{(s2)}$	-	UO_2 concentration of solid components
$C^{(s3)}$	-	$Fe(OH)_3$ concentration of solid components
$C^{(s4)}$	-	$CaCO_3$ concentration of solid components
$C^{(s5)}$	-	$CaSO_4$ concentration of solid components
$C^{(1)}$	-	H_2SO_4 concentration of liquid components
$C^{(2)}$	-	UO_2SO_4 concentration of liquid components
$C^{(3)}$	-	H_2O concentration of liquid components
$C^{(4)}$	-	$Fe_2(SO_4)_3$ concentration of liquid components
$C^{(5)}$	-	$FeSO_4$ concentration of liquid components
$C^{(6)}$	-	H_2CO_3 concentration of liquid components
k_I , k_{II} , k_{III} , k_{IV}	-	reaction constant

R	-	Boltzmann constant
T	-	temperature
E_α	-	activation energy
$k_{0\,\mathrm{S}}$	-	pre-exponential factor (also called factor of frequency) which takes into account the collision frequency and steric effects
$\nu_q^{(i)}$	-	stoichiometric coefficients of the component *i* in reaction
h	-	hydraulic head,
$\omega_{s,q}$	-	reaction rate
S	-	solid surface in ERV
ρ_s	-	molar density of the solid (the total number of moles in 1 m^3 of the solid)
ρ_l	-	molar density of the liquid (the total number of moles in 1 m^3 of the liquid);
ϕ	-	porosity
K	-	permeability
$\vec{U} = \vec{V} / \phi$	-	velocity
$D^{(ii)} \equiv D^{(i)}$	-	diffusion coefficient
M_{CaCO_3}	-	molar masses
ρ_{CaSO_4}	-	molar densities
σ	-	reactive surface
σ_0	-	specific surface of porous walls before calcite precipitation
β	-	empirical parameter
$\omega = \beta C^{s4,0}$	-	passivation rate
$Q_{inj}^k,\ Q_{pr}^l$	-	volumetric flow rate per unit volume of aquifer representing fluid sources (positive) and sinks (negative)
t	-	time
δ	-	Dirac delta function
u_{ijk} , v_{ijk} , w_{ijk}	-	discrete components of velocity
v_x, v_y , v_z	-	components of velocity

Abbreviation

ISL	-	In-Situ leaching
SLM	-	Streamline based modeling
FDM	-	Finite-differences methods
REV	-	Representative elementary volume

BIBLIOGRAPHY

1. Abadpour, A., Panfilov, M. - Asymptotic Decomposed Model of Two-Phase Compositional Flow in Porous Media: Analytical Front Tracking Method for Riemann Problem., *Transport in Porous Media*, **82**(3), 2010, 547 – 565.
2. Archie, G.E. - The electrical resistivity log as an aid to determining some reservoir characteristics,- *Trans. of the Amer. Inst. of Mining Eng.,* **146**, 1942, 54–61.
3. Batycky, R. P. - *A three-dimensionnal two-phase two-phase field scale streamline simulator,* PhD Thesis submitted to the department of petroleum engineering, Stanford University, 1997.
4. Bear J. - *Dynamics of Fluids In Porous Media*, Dover Publications, New York, 1972. 764.
5. Bekri, S., Thovert, J.F., Adler, P.M. - Dissolution of porous media. *Chemical Engineering Science*, **50**(17), 1995, 2765- 2791,
6. Beleckij, V.I., Bogatkov, L.K., Volkov, N.I. - *Spravochnik po geotehnologii urana,* Moskva: Energoatomizdat, 1997, 672 (in Russian).
7. Berner, R.A. - Sulfate reduction and the rate of deposition of marine sediments. *Earth Planet Sci. Lett.*, **37**, 1978, 492-498.
8. Blunt, M.J., Lui, K., Thiele, M.R. - A generalized Streamline Method to Predict Reservoir Flow, - *Petroleum Geoscience*, **2**, 1996, 259-269.
9. Bratvedt, F., Gimse, T., Tegnander, C. - Streamline Computation for Porous Media Flow including Gravity*, Transport in Porous Media*, **25**(1), 1996, 63-78.
10. Brovin, K.G., Grabovnikov, V.A. - *Prognoz, poiski, razvedka i promyshlennja ocenka mestorozhdenij urana dlja otrabotki podzemnym vyshhelachivaniem*, – Almaty - Gylym, 1997, 384 (in Russian).
11. Buddhima, I., Punyama, U.P., Rowe, K., Banasiak, L. - Coupled hydro-geochemical modelling of a permeable reactive barrier for treating acidic groundwater, *Computers and Geotechnics*, 55(1), 2014, 429-439 .
12. Carman, P.C. - Fluid through granular beds. *Transactions, - Institution of Chemical Engineers*, 1937, 150 - 166.
13. Charalambous, F.A., Ram, R., McMaster S., Pownceby M.I., Tardio J., Bhargava S.K. - Leaching behavior of natural and heat-treated brannerite-containing uranium ores in sulphate solutions with iron(III)., *Minerals Engineering*, **57**, 2014, 25–35.

14. Chilingarian, G.V., Torabzadeh, J., Rieke, H.H., Metghalchi, M., and Mazzullo, S.J., - Interrelationships among surface area, permeability, porosity, pore size, and residual water saturation, *in G.V. Chilingarian, S.J. Mazzullo, and H.H. Rieke, eds.,* Carbonate Reservoir Characterization: A Geologic-Engineering Analysis, Part I: Elsevier Publ. Co., Amsterdam, *Developments in Petroleum Science*, ***30***, 1992, 379-397.
15. Chung, T.J - *Computational Fluid Dynamics*, Cambridge University Press, 2006, 1012.
16. Connelly D. - Uranium processing, *Int. Mining*, January, 2008, 58-61
17. Costine, A., Nikoloski, A.N., Da Costa, M., Chong, K.F., Hackl, R. - Uranium extraction from a pure natural brannerite mineral by acidic ferric sulphate leaching. *Miner. Eng.*, 53, 2013, 84–90.
18. Danaev, N.T., Korsakova, N.K., Pen'kovskij, V.I. - *Massoperenos v priskvazhinnoj zone i elektromagnitnyj karotazh plasta,* – Almaty, Kazakh University, 2005, - 180 (in Russian).
19. Datta-Gupta, A., King, M.J. - *Streamline Simulation: Theory and Practice,* - SPE Textbook Series, vol. 11, Textbook, 2007, - 394.
20. Deffeyes, K.S., MacGregor, I.D., World uranium resources. *Scientific American*, **242**, 1980, 66-76.
21. Dentz, M., Borgne, T.L., Englert, A., Bijeljic, B. - Mixing, spreading and reaction in heterogeneous media: A brief review*, Journal of Contaminant Hydrology*, 2011, 1-17.
22. Dentz, M., Gouze, P., Carrera, J. - Effective non-local reaction kinetics for transport in physically and chemically heterogeneous media, *Journal of Contaminant Hydrology*, 2012, 222-236.
23. Felder, Ch., Oltean, C., Panfilov, M., Buès, M.A. - Dispersion de Taylor généralisée à un fluide à propriétés physiques variables., *C. R. Acad. Sci. Paris, Ser. Mécanique,* **332**, 2004, 223 – 229.
24. Fetel, E., Voillemont, J. C., Le Carlier de Veslud, C., and Royer, J. J. *,* - Oil-Reservoir Streamline Simulation in gOcad, *Proc. 24th gOcad Meeting, Nancy*, 2004, 1-13.
25. Gogoleva, E. M. - The leaching kinetics of brannerite ore in sulfate solutions with iron(III)*, Radioanal Nucl. Chem.*, 2012, 185-191.
26. Golubev, B.C., Krichevec, G.N. - Matematicheskaja model' diffuzionnogo vyshhelachivanija., *Problemy geotehnologii, Moskva*, 1983, 113-117 (in Russian).
27. Golubev, V.S., Grabovnikov, V.A., Krichevec, G.N. - O dinamike podzemnogo vyshhelachivanija poleznyh iskopaemyh na osnove matematicheskogo i fizicheskogo

modelirovanija., *Matematicheskoe i fizicheskoe modelirovanie rudo-obrazujushhih processov, Moskva, GIGHS,* 1978, 122-142 (in Russian).

28. Grabovnikov, V.A. - *Geotehnologicheskie issledovanija pri razrabotke metallov*, Moskva: Nedra, 1995, 155 (in Russian).
29. http://www.world-nuclear.org/info/Nuclear-Fuel-Cycle/Mining-of-Uranium/World-Uranium-Mining-Production/.
30. IAEA, Sediment K_ds and Concentration Factors for Radionuclides in the Marine Environment, *Technical Reports Series,* Vienna - 1985, **247.**
31. Istomin, A.D., Ladejshhikov, A.V., Laptev, Ju.I., Noskov, M.D., Cheglokov, A.A. - *Praktika primenenija gorno-geologicheskoj informacionnoj sistemy «GNOM» pri razvedke, podgotovke i razrabotke mestorozhdenij urana sposobom podzemnogo skvazhinnogo vyshhelachivanija.* - Sbornik dokladov VII Mezhdunarodnoj nauchno-prakticheskoj konferencii "Aktual'nye problemy uranovoj promyshlennosti", 2014, 84-85.
32. Kalmaz, E.V., Barbieri, J.L. - Mathematical modeling and computer simulation of radioactive and toxic chemical species dispersion in porous media in the vicinty of uranium recovery operations., *Ecol. Modeling*, 1981, 159-181.
33. Kancel A.A., - *Matematicheskoe modelirovanie dinamiki processa podzemnogo vyshhelachivanija v neodnorodnom rudonosnom sloe.,* - Dissertacija na soiskanie uchenoj stepeni kandidat fiziko-matematicheskih*,* Moskva, 2008, 127(in Russian).
34. Kazakhstan tops uranium league. - http://www.world-nuclear-news.org/enf-kazakhstan-tops-uranium-league-2701147.html
35. Kieffer, B., Jové, C.F., Oelkers, E.H., Schott, J. - An experimental study of the reactive surface area of the Fontainebleau sandstone as a function of porosity, permeability, and fluid flow rate. *Radiochimica et Cosmochimica Acta*, **63**, 1999, 63, 3225–3534.
36. Kirkpatrick, R.J., - Crystal growth from the melt: A Review. *Amer. Mineral*, **60**, 1975, 798-814.
37. Konikow L.F., Goode D.J. and Hornberger, G.Z. - *A Three-Dimensional Method-of-Characteristics Solute-Transport Model (MOC3D),* - U.S.G.S., Water-Resources Investigations Report 96-4267, Reston, Virginia, 1996, 99.
38. Lagneau, V. - *Influence des processus géochimiques sur le transport en milieu poreux; application au colmatage de barrières de confinement potentielles dans un stockage en formation géologique*, Ph.D. thesis École des Mines de Paris, 2000, - 181.

39. Lagneau, V., Lee, J. - Operator-splitting-based reactive transport models in strong feedback of porosity change: The contribution of analytical solutions for accuracy validation and estimator improvement, *Journal of Contaminant Hydrology,* **112**, 2010, 118–129

40. Li L., Catherine A.P., Michael A.C. - Upscaling geochemical reaction rates using pore-scale network modeling, *Advances in Water Resources,* 2006, **29**, 1351–1370.

41. Lichtner, P.C. - Time–space continuum description of the fluid/rock interaction in permeable media*. Water Resources Research* , 28, 1992,3135–3155

42. Manual of acid in situ leach uranium mining technology. IAEA, Vienna, 2001, IAEA-TECDOC-1239.

43. Mathieu, J.B., Collon, P., Caumon, G., and Royer, J.J. - GOCAD StreamLab Revisited for Hydrogeology Applications*, 2^{8th} gOcad Meeting, Nancy,* 2008, 1-16*.*

44. Mikhailov, V.V., Petrov, N.N. - Age of exogene uranium deposits in south and south-east Kazakhstan according to the lead-isotope study., *Geology of Kazakhstan,* 1998, **2**(354),63–70.

45. Nesterov, Ju.V., Sultanov, Ju., - *O nekotoryh zakonomernostjah processa podzemnogo vyshhelachivanija urana iz rud*, V kn.: Himija urana., pod. red. Laskorina B.N., Moskva: Nauka, 1983, 91-100 (in Russian).

46. Nierode, D.E., Williams, B.B., - *Characteristics of acid reaction in limestone formations*. SPE, 1973, 3101.

47. Noskov, M.D., Babkin, A.S., Zhiganov, A.N., Istomin, A.D., Kesler, A.D., Laptev, Ju.I., Noskova, S.N. - Primenenie programmnogo kompleksa "Sevmur" dlja optimizacii otrabotki blokov Dalmatovsogo mestorozhdenija urana., *Sbornik dokladov V Mezhdunarodnoj nauchno-prakticheskoj konferencii "Aktual'nye problemy uranovoj promyshlennosti"*, 2008, - 62-67.

48. Oladyshkin, S., Royer, J. J., and Panfilov, M., - Effective solution through the streamline technique and HT-splitting for the 3D dynamic analysis of the compositional flows in oil reservoirs *Transport in Porous Media,* **74**(3), 2008, 311-329.

49. Panfilov, M., - Asymptotic Form of the Solution to the Problem of Multicomponent Mixture flow through a porous medium with a boundary layer., *Fluid Dynamics*, **20**(4), 1986, 574-580.

50. Panfilov, M., Shilovich, N., - Flow of Fluids with Substantially Different Mobilities through a Porous Medium in the Presence of Phase Transitions: Boundary Layer Phenomena, Spatial Phase Structures, and Instability of the Flow., *Fluid Dynamics*, v. **35**, N **2**, 2000, 258-267.

51. Peaceman, D. W. - *Fundamentals of Numerical Reservoir Simulation*, Elsevier Scientific Publishing Co., 2000, - 175 .

52. Pen'kovskij, V.I., Rybakova, S.T. - Chislennoe modelirovanie processov massoperenosa pri podzemnom vyshhelachivanii., *Dinamika sploshnoj sredy*., **90,** 1989, 81-92 (in Russian).

53. Petrov, NN. - Epigenetic stratified-infiltration uranium deposits of Kazakhstan, 1998, *Geology of Kazakhstan* **2**(354): 22–39, (in Russian).

54. Pilling, N.B., Bedworth, R. E., - The Oxidation of Metals at High Temperatures. *J. Inst. Met*, 1923, **29**, 529-591.

55. Poezzhaev, I.P., Abdul'manova, D.M. - Issledovanie gidrodinamiki processa vyshhelachivanija na nekotoryh obektah PSV., *Sbornik dokladov III Mezhdunarodnoj nauchno-prakticheskoj konferencii «Aktual'nye problemy uranovoj promyshlennosti»*. – Almaty, 2004, 163-165 (in Russian).

56. Pollock, D. W. - Semi-analytical Computation of Path Line for Finite Difference Models. *Ground Water*, **26**(6), 1988, 743-750

57. Radioactive riches – the five countries with the biggest uranium reserves. - http://www.mining-technology.com/features/featureradioactive-riches-the-five-biggest-uranium-rich-countries-4274059/.

58. Regnault, O., Fiet, N., Lagneau, V., Mathieu, R., Garnier, V., Selezneva, V., Pouradier, A., Petiteau, S.- 3D reactive transport simulations of uranium in situ leaching. Forecast and process optimization for increasing technological blocks performance, *Sbornik dokladov VII Mezhdunarodnoj nauchno-prakticheskoj konferencii «Aktual'nye problemy uranovoj promyshlennosti*». Almaty, 2014, 65-68.

59. Rogov, E.I., Jazikov, V.G., Rogov, A.E. - Teorija rastekanija rastvorov i opredelenie parametra f(Zh:T) pri podzemnom skvazhinnom vyshhelachivanii urana., *Sbornik dokladov III Mezhdunarodnoj nauchno-prakticheskoj konferencii «Aktual'nye problemy uranovoj promyshlennosti»*. – Almaty, 2004. - S.169-173 (in Russian)

60. Rubin, J. - Transport of reacting solutions in porousmedia: relation between mathematical nature of problem formulation and chemical nature of reactions , *Wat. Resour. Res.*, **19**, 1983, 1231-1252.

61. Sagatov, E., *Nuclear Power in Kazakhstan, coursework*, Stanford Univ., **210**, 2010, 2p.

62. Schechter, R. S., Gidley, J. L. - The change in poresize distribution from surface reaction in porous media. A.I.Ch.E.J., **15**, 1969, 339-350.

63. Shafer, J.M - Reverse Pathline Calculation of time-related Capture Zones in Nonuniform Flows, *Ground Water*, **25**(3), 283-289.

64. Uranium mining. http://www.kazatomprom.kz/en/#!/industry/uranium/uranium_mining

65. Voillemont, J C, and Royer, J.J. - StreamLine-based reservoir characterization: Latest advances., *Proc. 23rd gOcad Meeting*, Nancy, 2003, 1-11

66. Voillemont, J.C., and Royer, J.J. - *Streamline-based reservoir characterization using tracer and two phase fluid flow,* Proc. 22nd gOcad Meeting, Nancy, 2002, 1-15,

67. Zheng, B.C., Wang, P.P. - MT3DMS*: A Modular Three-Dimensional Multispecies Transport Model for Simulation of Advection, Dispersion, and Chemical Reaction of Contaminants in Groundwater Systems. - Documentation and User's Guide*, Dept. of Geological Sciences, University of Alabama, 1999,160.

Analytical and numerical models of chemical leaching with gypsum precipitation in porous media

Abstract: In the present thesis we develop the optimized phenomenological model of in-situ chemical leaching (ISL) of uranium by the injection of sulfuric acid, with special account for the precipitation of non-soluble species as gypsum, which reduces the uranium recovery. The suggested model describes the mass transport with heterogeneous chemical reactions between liquid and solid rocks, leading to dissolve uranium oxides and recover uranium in liquid form. This model is optimized, i.e., it contains the minimum number of chemical reactions, at the same time ensuring the sufficient degree of consistency with the real systems. It includes both useful reactions, describing the dissolution of various kinds of uranium oxides, and detrimental reactions, leading to the precipitation of solid sediments (gypsum), whose flakes cover the surface of porous channels and reduce the efficiency of useful reactions.

We developed the efficient asymptotic method of analysis based on the approximation of the true multicomponent system by a pseudo-binary mixture, which enables us to separate nonlinear and compositional effects: all nonlinear effects are captured in the zero approximation which corresponds to a two-component mixture, whilst all the multi-compositional effects, including the reactions, are kept in the first approximation which is linear. We showed that the real systems perfectly correspond to the pseudo-binary approximation. In 1D case we obtained the analytical solution of the strongly nonlinear problem for the fluid-solid chemically interacting system consisted of 11 chemical components described by 11 nonlinear partial differential equations.

For 3D flow, we developed the numerical code, based on the streamline approach, which enables us to transform any three-dimensional problem into the system of mono-dimensional problems of chemical transport. At the first step we calculate the system of streamlines by solving the simplified 3D problem of flow of a homogeneous fluid. At the second step we solve the 1D problem of species transport along each streamline. The correctness of the simulations was validated by performing several numerical tests and comparing the results obtained with other numerical methods.

Among the qualitative results we revealed the existence of a critical rate of gypsum sedimentation, below which the ultimate uranium recovery is complete. In contrast, it tends to a limit value lower than 100% when the sedimentation rate is higher than the critical value. This limit recovery depends on various parameters of the process.

The theory and the methodology developed in this work can be easily extended and applied on other type of ores that are recovered by in-situ leaching method and other types of solvents.

Keywords: reactive transport, heterogeneous chemical reactions, flow in heterogeneous media, streamlines, roll-front uranium deposits.

Les modèles analytique et numérique du lessivage in-situ avec la précipitation du gypse en milieux poreux

Résumé: Dans cette thèse, nous développons le modèle phénoménologique optimisé de lessivage chimique in situ (ISL) de l'uranium par l'injection d'acide sulfurique, en prenant en compte la précipitation des espèces non-solubles telles que le gypse, qui réduisent la récupération de l'uranium. Le modèle proposé décrit le transport de masse avec des réactions chimiques hétérogènes entre le liquide et les roches solides, qui mènent à la dissolution des oxydes d'uranium et à la récupération de l'uranium sous forme liquide. Ce modèle est optimisé, c'est-à-dire, il contient le nombre minimal de réactions chimiques, en assurant en même temps le degré suffisant d'adéquation avec les systèmes réels. Ce modèle comprend à la fois des réactions utiles, qui décrivent la dissolution de divers types d'oxydes d'uranium, et les réactions néfastes qui conduisent à la précipitation des sédiments solides (gypse), dont les flocons couvrent la surface de canaux poreux et réduisent l'efficacité des réactions utiles.

Nous avons développé la méthode asymptotique efficace d'analyse basée sur l'approximation du système réel multi-composant par un mélange pseudo-binaire, ce qui nous permet de séparer les effets non linéaires et les effets compositionnels : tous les effets non linéaires sont capturés dans l'approximation d'ordre zéro, ce qui correspond à un mélange à deux composants, tandis que tous les effets multi-compositionnels, y compris les réactions chimiques, sont maintenus dans l'approximation d'ordre 1 qui est linéaire. Nous avons montré que les systèmes réels correspondent parfaitement à l'approximation pseudo-binaire. Dans le cas 1D, nous avons obtenu la solution analytique du problème fortement non linéaire pour un système fluide-solide chimiquement actif et composé de 11 espèces chimiques décrites par 11 équations aux dérivées partielles non linéaires.

Pour un écoulement 3D, nous avons développé un code numérique, basée sur l'approche de ligne de courant, ce qui nous permet de transformer tout problème en trois dimensions en un système de problèmes mono-dimensionnels de transport d'espèces chimiques. Lors de la première étape, on calcule le système de lignes de courant en résolvant le problème simplifié 3D de l'écoulement d'un fluide homogène. Lors de la deuxième étape, nous résolvons le problème 1D du transport d'espèces le long de chaque ligne de courant. Les résultats de simulation ont été validés en effectuant plusieurs essais numériques et en les comparant avec ceux obtenus par d'autres méthodes numériques.

Parmi les résultats qualitatifs, nous avons révélé l'existence d'un taux critique de sédimentation de gypse, en dessous duquel la récupération ultime de l'uranium est complète. En revanche, elle tend à une valeur limite inférieure à 100% lorsque le taux de sédimentation est supérieur à la valeur critique. Ce taux de récupération limite dépend de divers paramètres du processus. La théorie et la méthodologie développées dans ce travail peuvent être facilement étendues et appliquées aux autres types de minerais qui sont récupérés par la méthode de lessivage in situ, et autres types de solvant.

Mots-clés: transport réactif, réactions chimiques hétérogènes, écoulements en milieu poreux hétérogènes, lignes de courant, des gisements d'uranium de type roll front.